CONSTRUCTION MATERIALS CONSULTANTS, INC.

Laboratory Analyses of Three Masonry Mortars From The Historic Old Lehigh County Courthouse In Allentown, Pennsylvania

Old Lehigh County Courthouse
455 Hamilton Street
Allentown, PA

September 23, 2021
CMC 0821157

TABLE OF CONTENTS

LABORATORY ANALYSES OF THREE MASONRY MORTARS FROM THE HISTORIC OLD LEHIGH COUNTY COURTHOUSE IN ALLENTOWN, PA

EXECUTIVE SUMMARY

As part of renovation of the historic Old Lehigh County Courthouse in Allentown, Pennsylvania, three masonry mortar samples (#1, 3, and 4) were provided for detailed laboratory studies to determine: (a) the compositions and conditions of the mortars, and (b) assessment of suitable replacement mortars for the examined ones to be used for future restorations.

The samples were examined by following the procedures of ASTM C 1324, "Standard Test Method for Examination and Analysis of Hardened Masonry Mortar," and the RILEM Test Methods, which include a comprehensive array of tests, including: (1) detailed optical microscopical examinations of as-received, lapped, and thin sectioned pieces of mortars with stereo-zoom microscope and petrographic microscope to determine the types, conditions, and compositions of sands, binders, and overall compositions and microstructures of mortars used; (2) scanning electron microscopy and energy-dispersive X-ray microanalyses of interstitial paste fractions of mortars to ascertain the binder compositions determined from optical microscopy; (3) extraction of siliceous sands by acid digestion, followed by sieve analyses of extracted sands to determine grain-size distribution of sands; (4) chemical (gravimetric) analyses to determine soluble silica contents from cold-acid digestion of mortars followed by hot-alkali digestion of residues; (5) siliceous sand contents from hydrochloric-acid insoluble residue contents, (6) free and combined water and carbonate contents from loss on ignition at 110°C, 550°C, and 950°C, respectively, (7) X-ray fluorescence spectroscopy (XRF) to determine chemical (oxide) compositions of mortars, (8) X-ray diffraction (XRD) to determine mineralogical compositions, (9) thermal analyses (TGA, DSC, DTG) to determine the hydrate, carbonate, and sulfate phases in the mortars and proportion of silica sand, and, (10) ion chromatography to determine water-soluble chloride, sulfate and other anion contents in the mortars. Based on all these comprehensive analyses, the overall conditions, extent of deterioration, and compositions of the mortars can be assessed, from which suitable replacement mortars for the examined ones can be best evaluated.

Based on optical microscopy and SEM-EDS studies, all three mortars are determined to contain: (a) Portland cement as the major binder component, (b) variable proportions of dolomitic lime, which is mostly detected from high magnesia contents of pastes in SEM-EDS studies mainly in Mortars 3 and 4, and (c) siliceous sand. Overall hydraulicities of paste show higher values of cementation indices in Mortar #1 (mostly close to 1) compared to #3 (mean around 0.75), which, in turn, has overall higher values than the paste in Mortar #4 (mean around 0.5) indicating a progressively higher proportion of Portland cement added from Mortar #4 to 3 to 1. Consistent with magnesian composition of paste in the Mortars 3 and 4 detected in SEM-EDS studies, thermal analysis also detected brucite but only in Mortar #3 thus confirming the dolomitic lime addition at least in Mortar #3.

Sand showed variations in grain size, shape, angularity, and gradation from sample-to-sample, indicating their potentially different sources. Sand is noticeably finer in Mortar #1 with a fineness modulus of only 0.87 as opposed to fineness modulus of 2.09 and 2.02 in Mortars 3 and 4, respectively. Sand content is 59% in Mortar #1 compared to 66% sand detected from acid digestion in Mortars 3 and 4. Sand in all three mortars are compositionally similar variably crushed natural siliceous sands consisting of major amount of variably strained quartz, and subordinate amounts of quartzite,

quartz siltstone, feldspar, and other siliceous and minor ferruginous components. Particles are subangular to subrounded in Mortar #1, whereas subrounded to well-rounded in Mortar #3 and 4. In all samples, particles are mostly equidimensional to a few elongated, dense, hard, well-graded, well-distributed, nominal 0.5 to 0.6-mm in size in Mortar #1, 1 mm in Mortar #3 and 0.8 mm in Mortar #4, and present in sound conditions without any evidence of potentially deleterious reactions. Grain size distribution of extracted sands are compared with the ASTM C 144 specification of natural sand for unit masonry, which showed that for all size fractions, sands from Mortar #1 are higher than the upper limit of ASTM C 144 size gradation for natural sand indicating a noticeably finer particle size than C 144 masonry sand, which is also consistent with its very low fineness modulus of only 0.87. By contrast, size distribution of sands from Mortar #3 and 4 are within the upper and lower limits of ASTM C 144 natural sand, at least in the coarser fractions, indicating their possible replacement in a repointing event with modern ASTM C 144 masonry sand.

Based on: (i) the determined binder compositions of mortars from optical microscopy; (ii) sand compositions from optical microscopy; (iii) chemical (XRF and gravimetric) analysis of loss on ignition, and soluble silica contents; and (iv) XRD studies of mineralogical compositions, the volumetric proportions of replacement mortars suitable for the mortars examined are judged to be ***ASTM C 270 Type S cement-lime mortar or Type N cement-lime mortar depending on the types of masonry units and exposure conditions***. Overall appearance of the final mortars would depend on a match on sand that constitutes the dominant proportion of the mortars.

Sands to be used should be: (1) siliceous, (2) match in color to the color of sand in the examined mortars, (3) preferably be from similar sources, (4) be free of any debris, unsound, clay particles, or any potentially deleterious constituents, (5) conform to the size requirements of ASTM C 144 for masonry sand, (6) not exceed maximum 3 times the sum of separate volumes of cement, and lime, and (7) be durable. Since sand constitutes the dominant constituent of mortar, a match in appearance and properties of sand in the pointing mortar to the original one is important.

As an alternate to the proposed ASTM C 270 Type N cement-lime, which is indeed a common repointing mortar used for many restoration work for original lime mortars, similar ASTM C 270 Type S or N masonry cement-sand mortar can also be tried depending on the host masonry unit and performance of the masonry wall. A small test area should be tried with mock-up batches before large scale repointing. No pigment should be added to the pointing mortar. Use of Portland cement or Portland cement-based blended cement especially at amounts approaching that of lime should preferably be avoided. Initial rate of absorption (suction), and compressive strength of host masonry units are also important to determine the suitable mortar type, e.g., high-lime mortars (i.e., having high water retention properties) should be considered with masonry units having high suction properties. Due to atmospheric weathering and alterations, an exact match in color to the existing mortars may not be possible, which, even if possible, could alter in future due to continued atmospheric weathering in the presence of oxygen, moisture, and other environmental elements.

INTRODUCTION

As part of renovation of the historic Old Lehigh County Courthouse in Allentown, Pennsylvania, three masonry mortar samples were provided for detailed laboratory studies to determine: (a) the compositions and conditions of the mortars, and (b) assessment of suitable replacement mortars for the examined ones during future restorations. The samples were examined by following the procedures of ASTM C 1324, "Standard Test Method for Examination and Analysis of Hardened Masonry Mortar." Many details of the analytical procedures of ASTM C 1324 as well as of the relevant European (RILEM) methods of mortar testing followed in this present investigation are provided in Appendix 1.

BACKGROUND

Old Lehigh County Courthouse is a historic county courthouse located in Allentown, Lehigh County, Pennsylvania. The original section was built between 1814 and 1819, and was a $2^1/_2$-story, stone building with a hipped roof. It was remodeled and enlarged in 1864 in the Italianate style. An addition on the west was added in 1880–1881, and the addition to the north was built in 1914–1916 in the Beaux-Arts style. It was added to the National Register of Historic Places in 1981.

Figure 1: Old Lehigh County Courthouse in Allentown, Pennsylvania.

SAMPLES

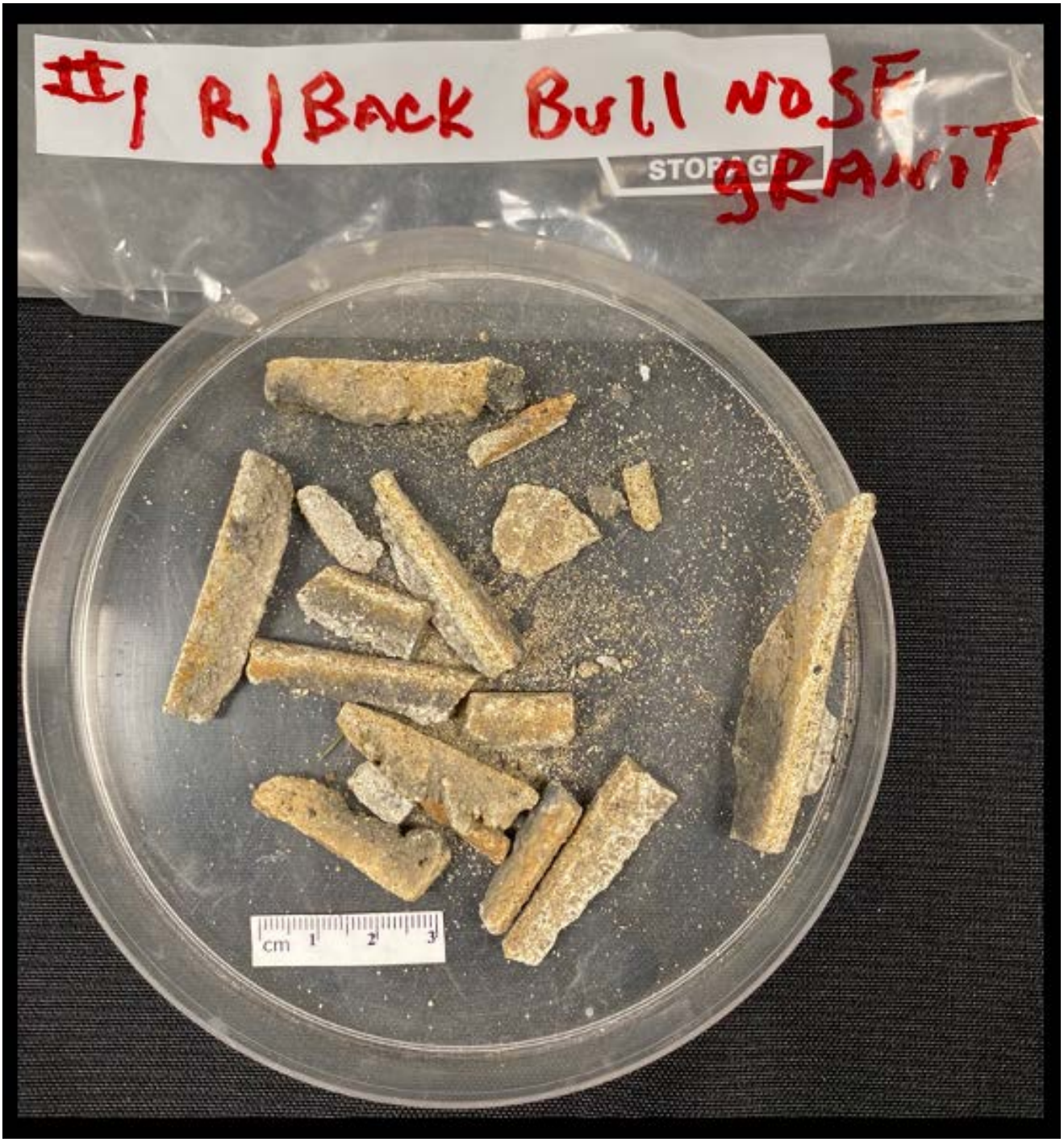

Figure 2: Mortar fragments #1 marked as 'R/Back Bull Nose Granite' (hereafter described throughout the report as Mortar #1). The sample consists of several elongated pieces from the mortar joint that are mostly weathered brown to dark gray with sand-textured exposed faces. Overall integrity of the pieces are hard, in fact noticeably harder than typical historic lime mortar suggesting the potential presence of a Portland cement based component in the binder, which is responsible for the dense, hard, medium gray nature of fresh fractured surfaces of pieces.

Figure 3: Mortar fragments #3 marked as 'Blue/Gray Stone Street side '(hereafter described throughout the report as Mortar #3). The sample consists of several rectangular pieces from the mortar joint that are mostly weathered brown to dark gray with excessively sand-textured exposed faces. Overall integrity of the pieces is moderately hard, in fact noticeably harder than typical historic lime mortar suggesting the potential presence of a Portland cement based component in the binder, which is responsible for the dense hard medium gray nature of fresh fractured surfaces of pieces. Notice loose sand particles on the faces that have been plucked out from the fragments during recovery.

Figure 4: Mortar fragments #4 marked as 'Blue-Gray Black Stone Front' (hereafter described throughout the report as Mortar #4). The sample consists of numerous elongated pieces from the mortar joint that are mostly weathered brown to dark gray with sand-textured exposed faces. Overall integrity of the pieces are hard, in fact noticeably harder than typical historic lime mortar suggesting the potential presence of a Portland cement based component in the binder, which is responsible for the dense, hard, medium gray nature of fresh fractured surfaces of pieces.

Figure 5: Comparison of three mortar samples received all showing more or less similar medium gray, dense, hard, sand-textured appearances indicating potential presence of similar binder and sand components in the samples. Grain size, shape, and gradation (sorting) of sand particles, however, appeared to differ from sample-to-sample indicating their derivation from different sources and/or times.

RESULTS

Grain-size Distribution & Micrographs of Sands Extracted From Mortars

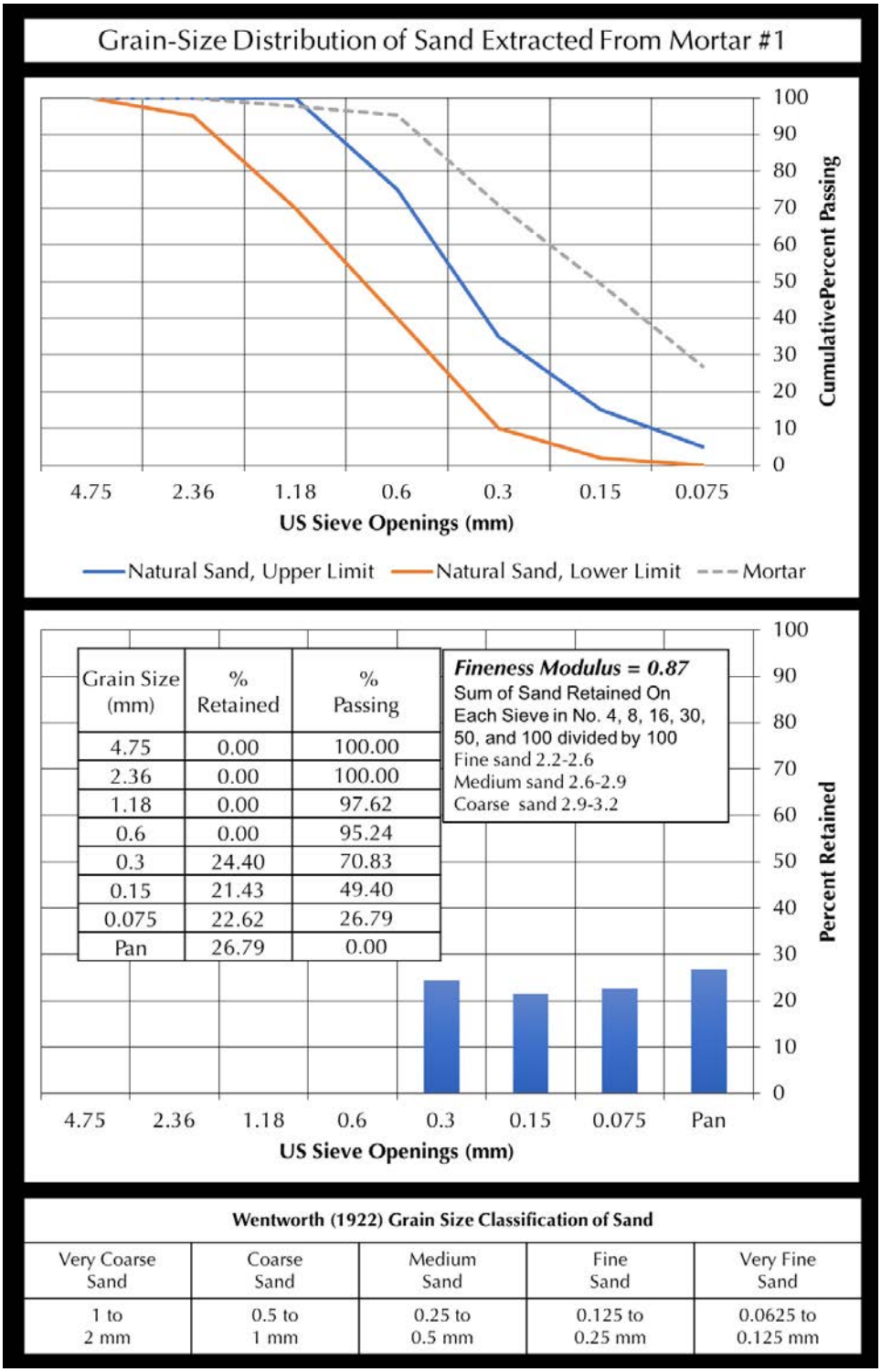

Grain Size (mm)	% Retained	% Passing
4.75	0.00	100.00
2.36	0.00	100.00
1.18	0.00	97.62
0.6	0.00	95.24
0.3	24.40	70.83
0.15	21.43	49.40
0.075	22.62	26.79
Pan	26.79	0.00

Fineness Modulus = 0.87
Sum of Sand Retained On Each Sieve in No. 4, 8, 16, 30, 50, and 100 divided by 100
Fine sand 2.2-2.6
Medium sand 2.6-2.9
Coarse sand 2.9-3.2

Wentworth (1922) Grain Size Classification of Sand

Very Coarse Sand	Coarse Sand	Medium Sand	Fine Sand	Very Fine Sand
1 to 2 mm	0.5 to 1 mm	0.25 to 0.5 mm	0.125 to 0.25 mm	0.0625 to 0.125 mm

Figure 6: Grain-size distribution of sand extracted from Mortar #1 after acid digestion.

In the top plot, grain size distribution of sand is compared with the upper and lower limits of natural sand in ASTM C 144 (blue and red lines, respectively) showing use of noticeably finer sand than the modern ASTM C 144 masonry sand.

The bottom plot shows distribution of sand, which is again showing overall very fine size of sand.

Inset Table shows percent retained, and cumulative percent passing through each sieve.

Fineness modulus of sand is calculated from sum of cumulative percent retained on Sieves 4, 8, 16, 30, 50, and 100 divided by 100 where very fine sand size is again depicted from very low fineness modulus.

Fineness modulus of only 0.87 indicates use of very fine sand.

Next Figure shows stereo-micrographs of sand particles retained on various sieves.

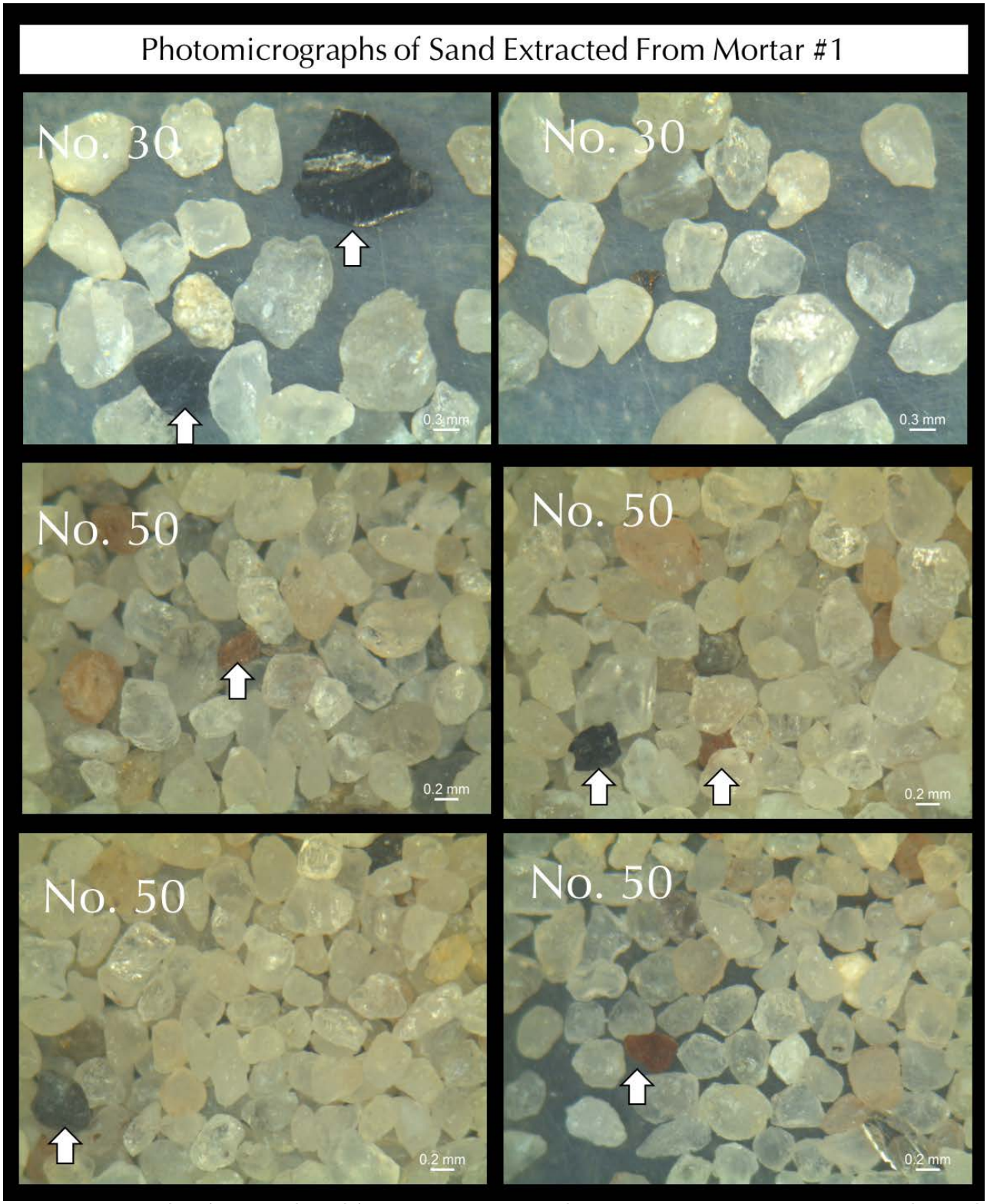

Figure 7: Micrographs of extracted sand from Mortar #1 retained on various sieves. Sieves containing the modal amounts of sand are shown. Arrows show a few black or colored particles in sand.

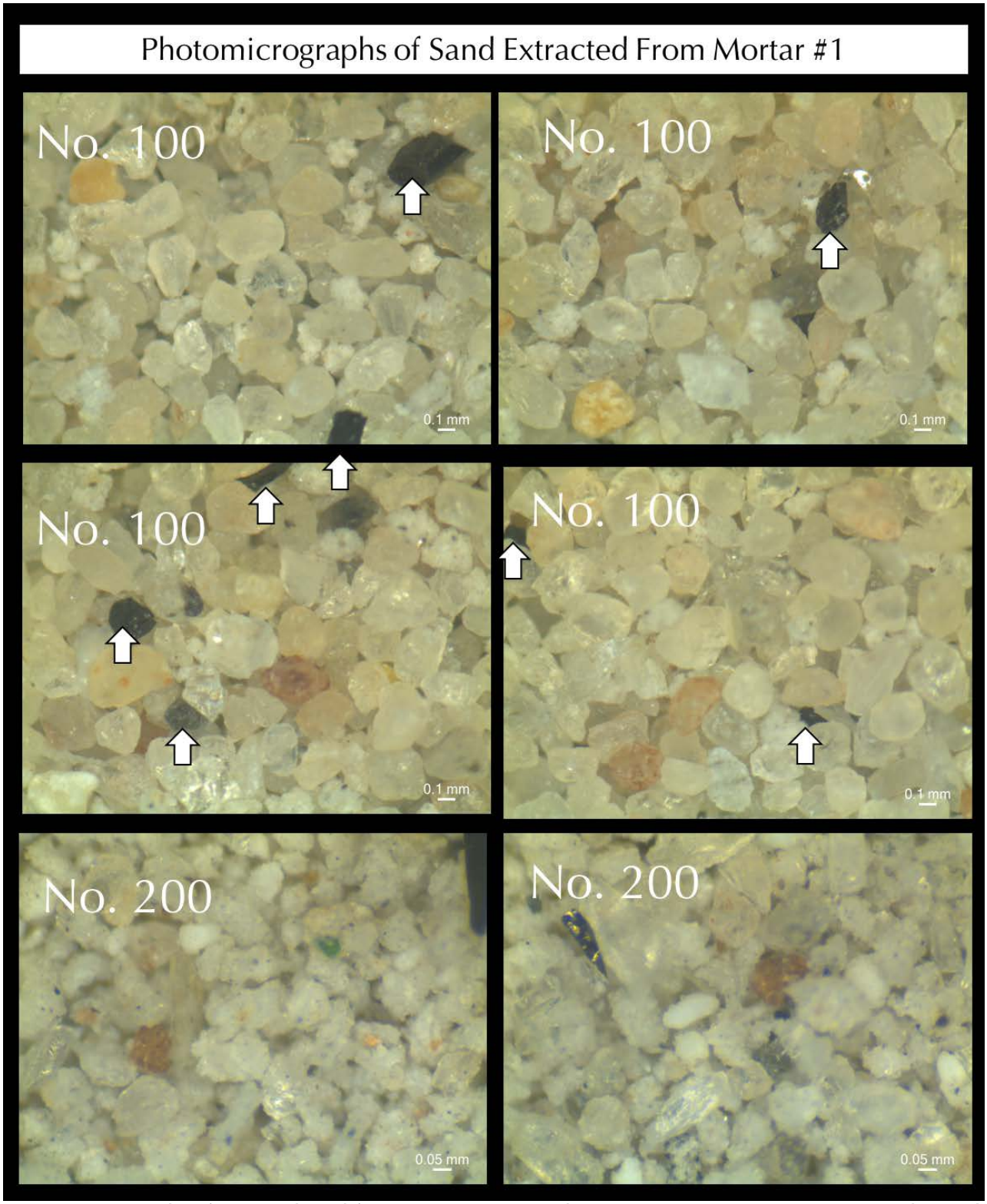

Figure 8: Micrographs of extracted sand from Mortar #1 retained on various sieves. Sieves containing the modal amounts of sand are shown. Arrows show a few black or colored particles in sand. Sieve 200 retained lumps of undigested mortar fragments, which didn't dissociate despite week-long acid digestion.

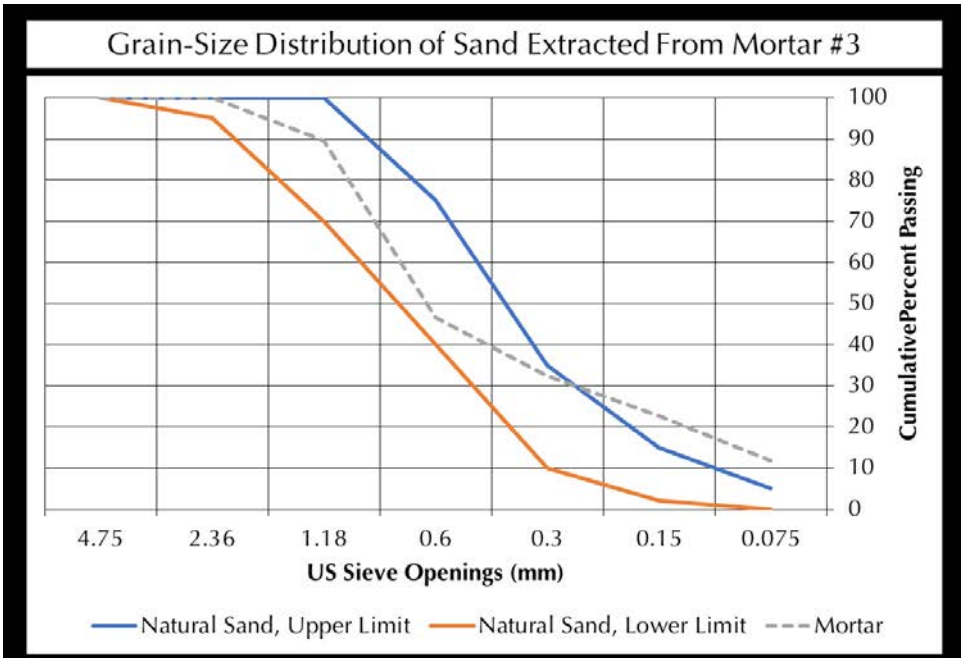

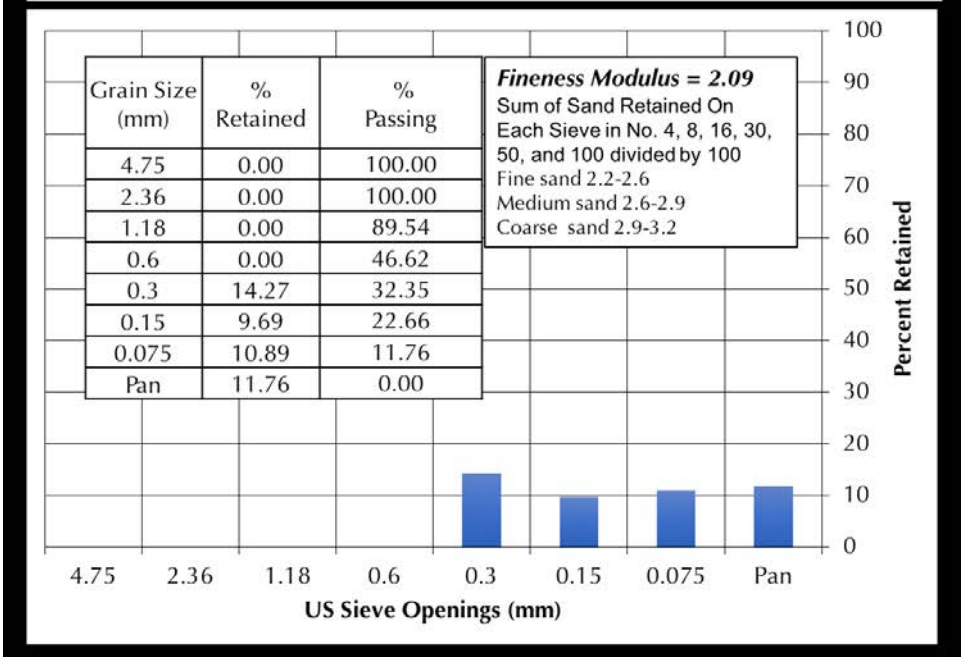

Wentworth (1922) Grain Size Classification of Sand

Very Coarse Sand	Coarse Sand	Medium Sand	Fine Sand	Very Fine Sand
1 to 2 mm	0.5 to 1 mm	0.25 to 0.5 mm	0.125 to 0.25 mm	0.0625 to 0.125 mm

Figure 9: Grain-size distribution of sand extracted from Mortar #3 after acid digestion.

In the top plot, grain size distribution of sand is compared with the upper and lower limits of natural sand in ASTM C 144 (blue and red lines, respectively) showing use of noticeably finer sand than the modern ASTM C 144 masonry sand.

The bottom plot shows distribution of sand, which is again showing overall very fine size of sand.

Inset Table shows percent retained, and cumulative percent passing through each sieve.

Fineness modulus of sand is calculated from sum of cumulative percent retained on Sieves 4, 8, 16, 30, 50, and 100 divided by 100 where very fine sand size is again depicted from very low fineness modulus.

Fineness modulus of 2.09 indicates use of fine sand, which, however, is coarser than the sand in Mortar #1 with FM of only 0.87.

Next Figure shows stereo-micrographs of sand particles retained on various sieves.

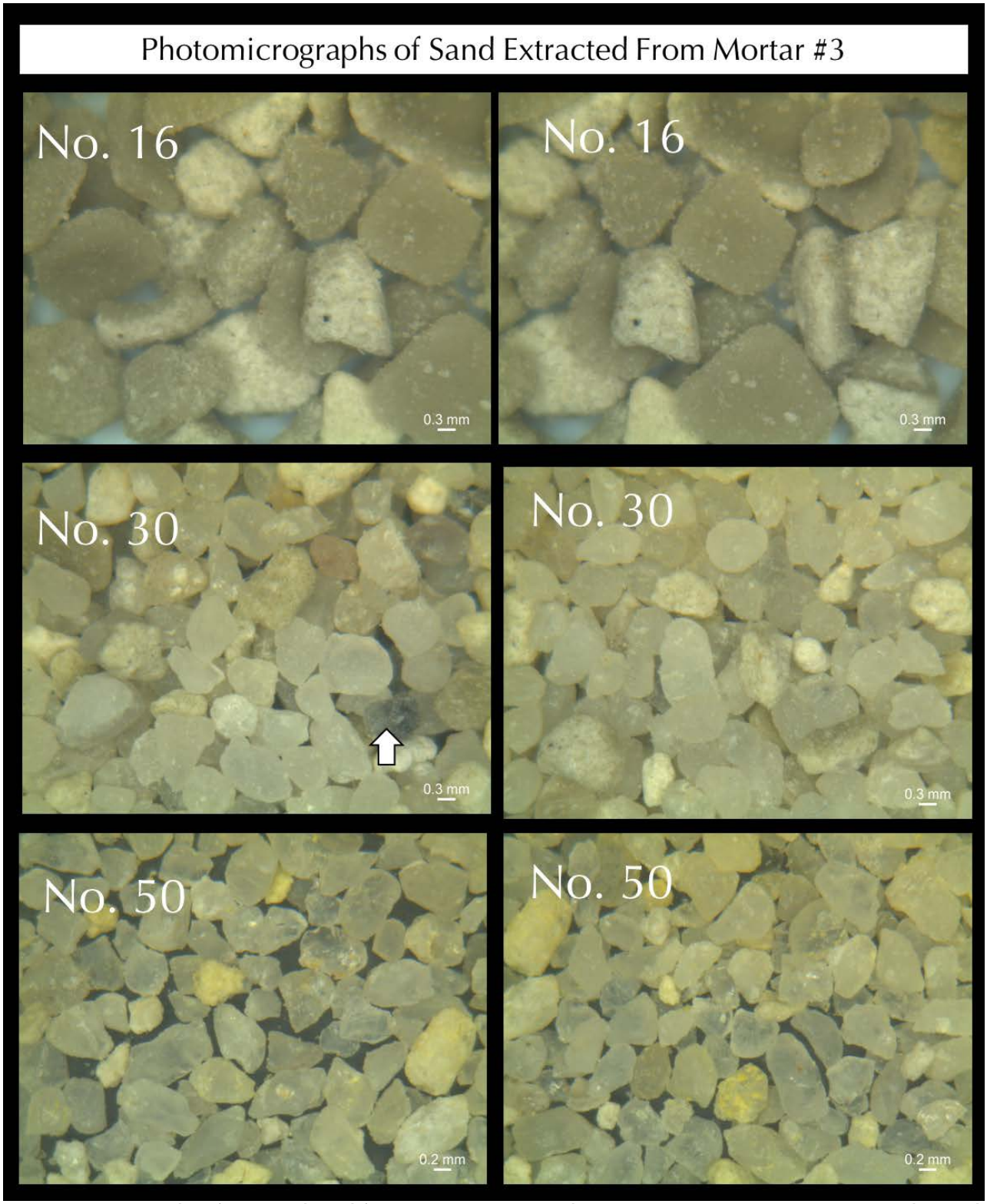

Figure 10: Micrographs of extracted sand from Mortar #3 retained on various sieves. Sieves containing the modal amounts of sand are shown. Arrows show a few black or colored particles in sand.

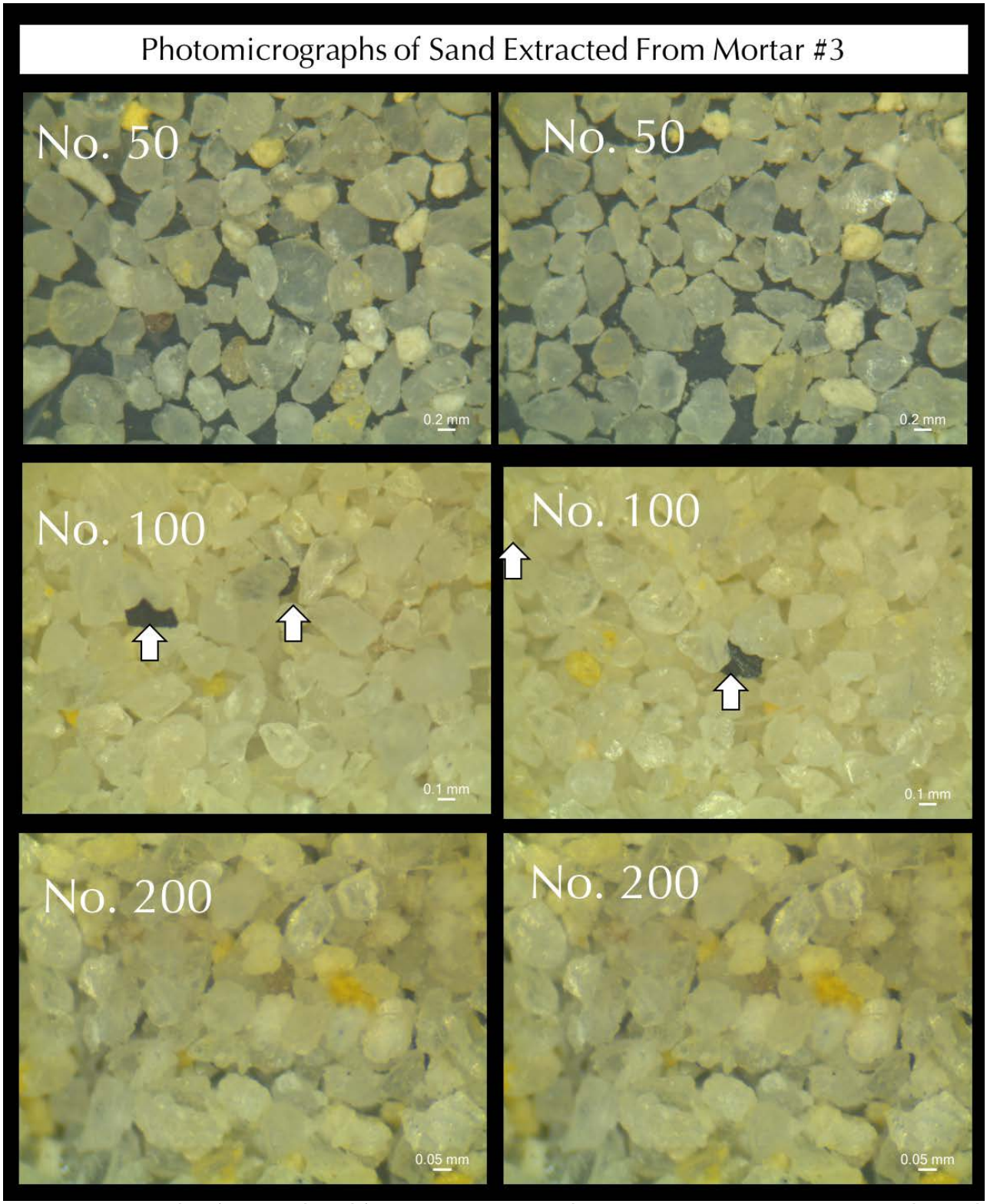

Figure 11: Micrographs of extracted sand from Mortar #3 retained on various sieves. Sieves containing the modal amounts of sand are shown. Arrows show a few black or colored particles in sand.

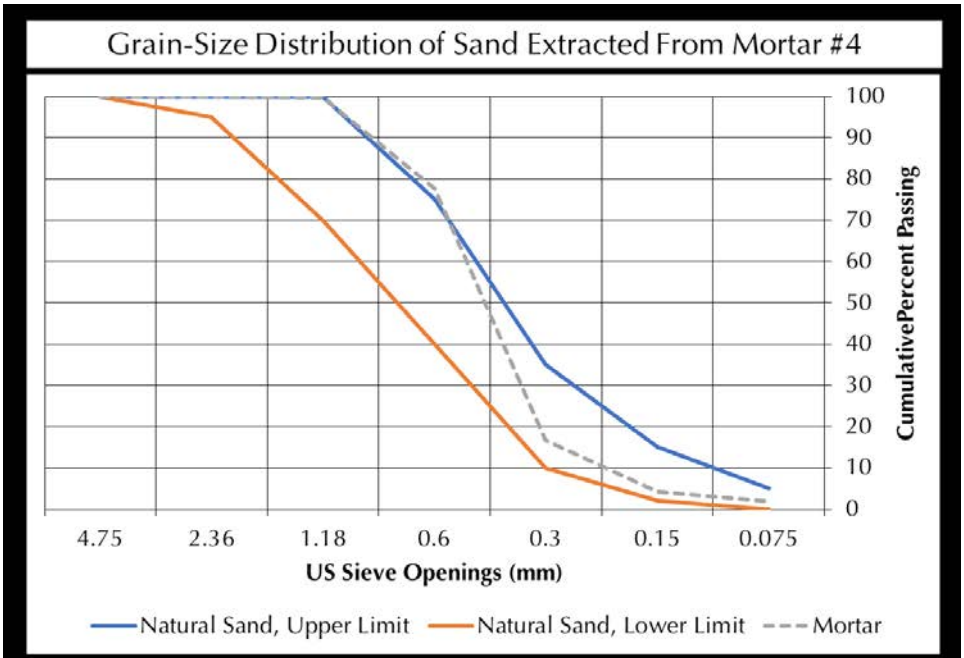

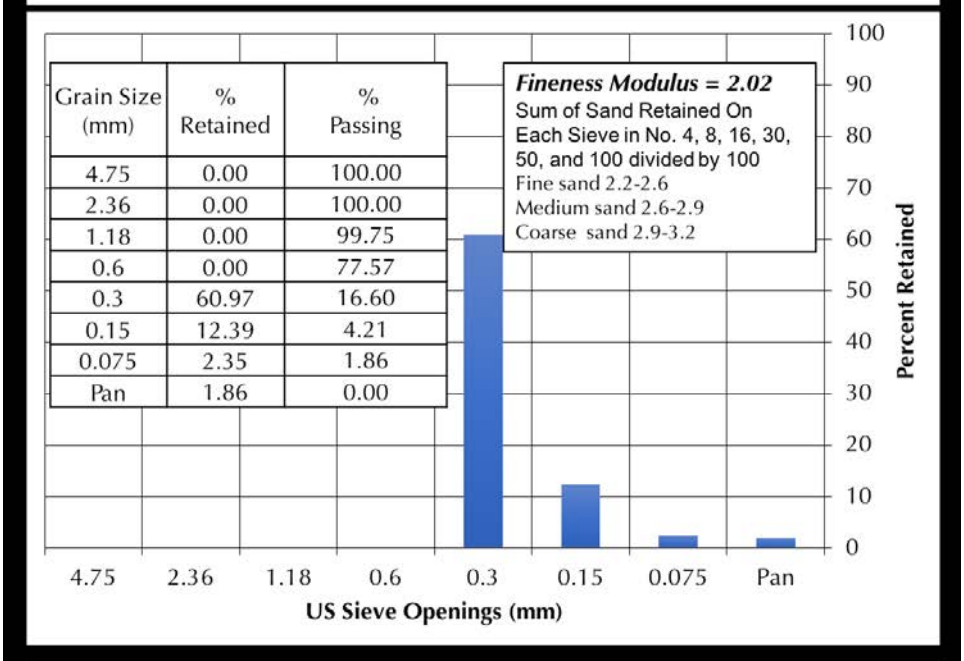

Wentworth (1922) Grain Size Classification of Sand

Very Coarse Sand	Coarse Sand	Medium Sand	Fine Sand	Very Fine Sand
1 to 2 mm	0.5 to 1 mm	0.25 to 0.5 mm	0.125 to 0.25 mm	0.0625 to 0.125 mm

Figure 12: Grain-size distribution of sand extracted from Mortar #4 after acid digestion.

In the top plot, grain size distribution of sand is compared with the upper and lower limits of natural sand in ASTM C 144 (blue and red lines, respectively) showing use of noticeably finer sand than the modern ASTM C 144 masonry sand.

The bottom plot shows distribution of sand, which is again showing overall very fine size of sand.

Inset Table shows percent retained, and cumulative percent passing through each sieve.

Fineness modulus of sand is calculated from sum of cumulative percent retained on Sieves 4, 8, 16, 30, 50, and 100 divided by 100 where very fine sand size is again depicted from very low fineness modulus.

Fineness modulus of 2.02 indicates use of fine sand, which is similar to the sand in Mortar #3 but coarser than the sand in Mortar #1 with FM of only 0.87.

Next Figure shows stereo-micrographs of sand particles retained on various sieves.

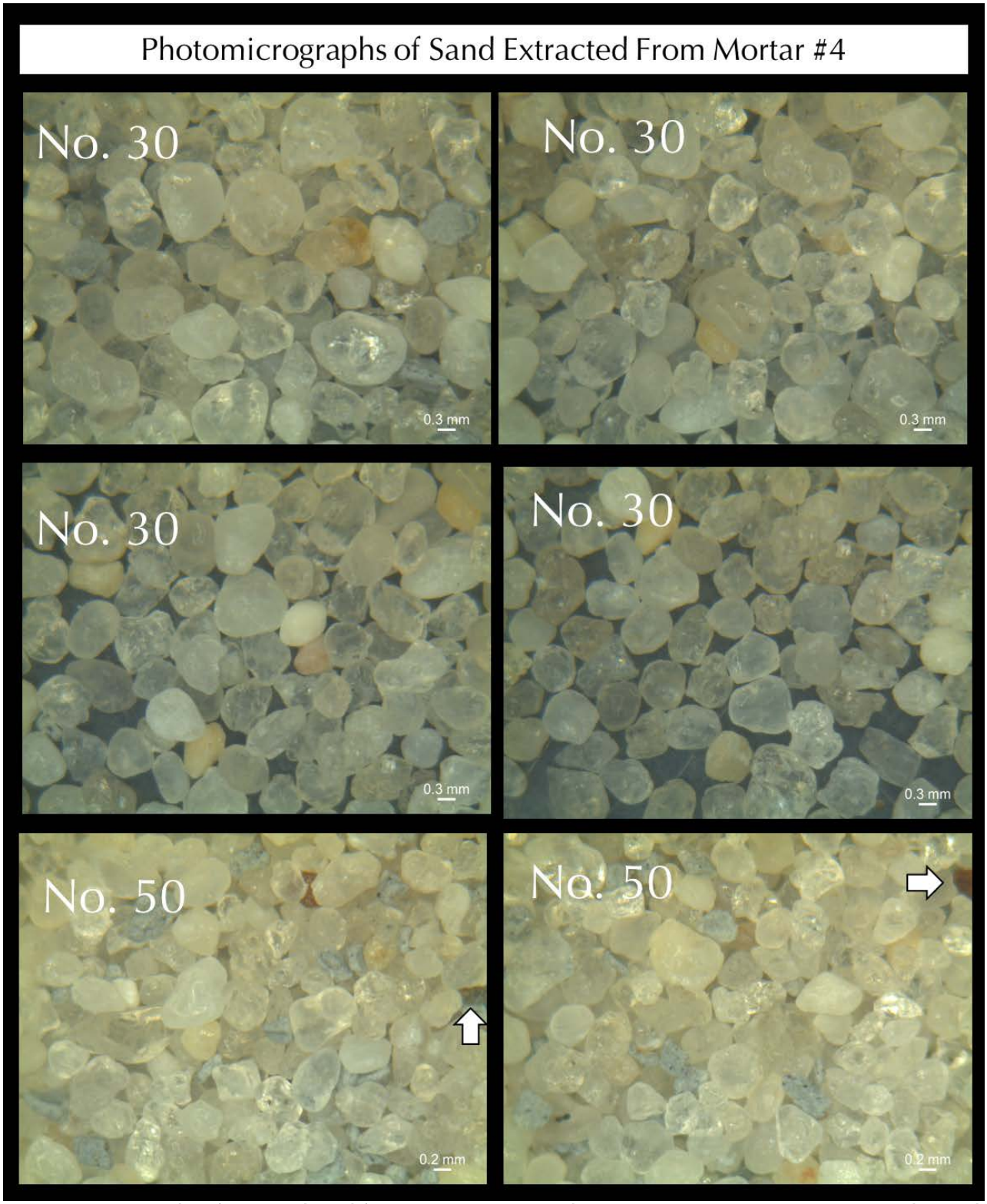

Figure 13: Micrographs of extracted sand from Mortar #4 retained on various sieves. Sieves containing the modal amounts of sand are shown. Arrows show a few black or colored particles in sand.

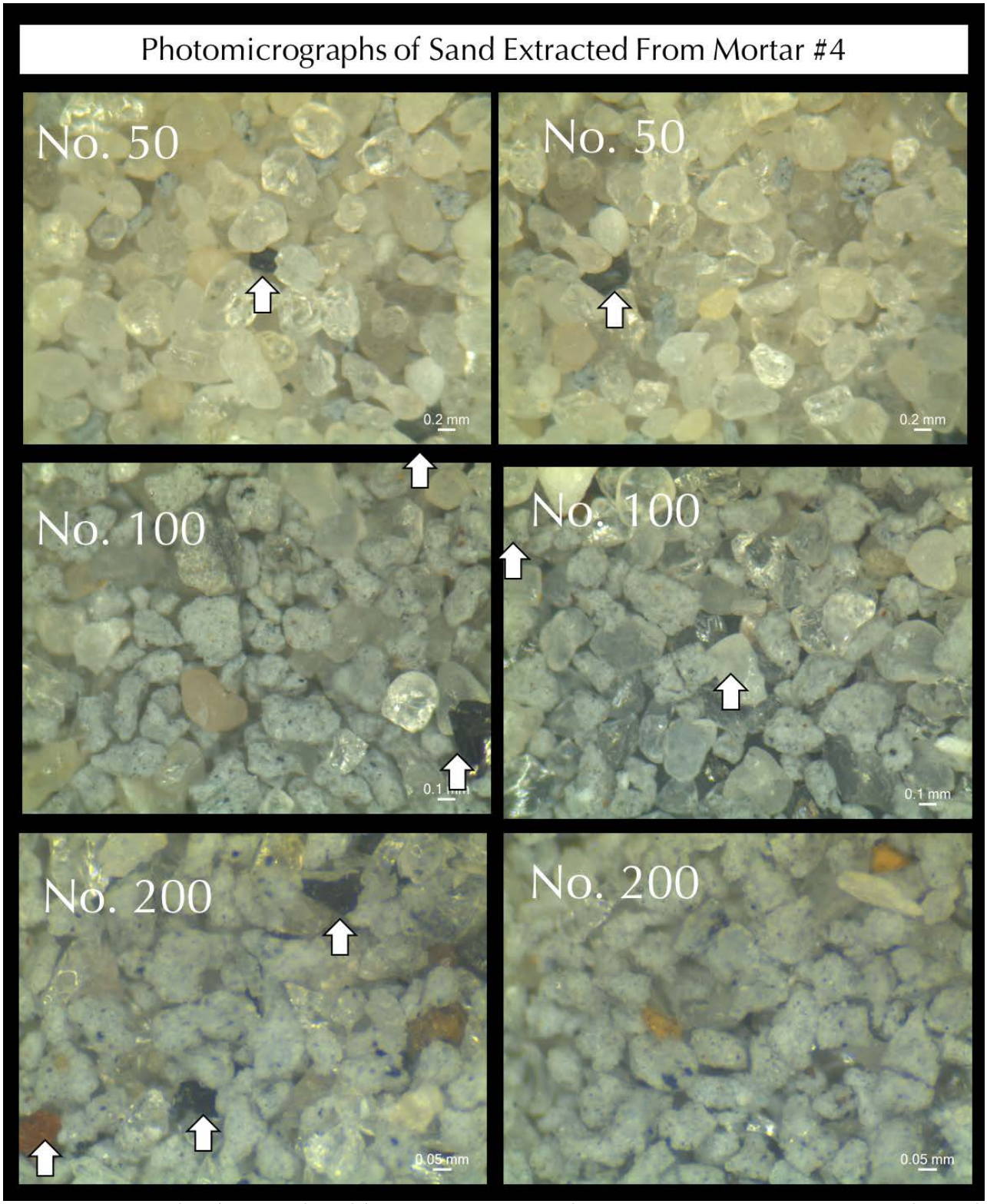

Figure 14: Micrographs of extracted sand from Mortar #4 retained on various sieves. Sieves containing the modal amounts of sand are shown. Arrows show a few black or colored particles in sand. Sieves 100 and 200 retained lumps of undigested mortar fragments, which didn't dissociate despite week-long acid digestion.

Figures 6 through 14 show: (a) grain-size distribution of sands extracted after digestion of mortar in dilute (1+3) hydrochloric acid, and (b) micrographs of extracted sand particles taken with a stereomicroscope, retained on various sieves including size, shape, angularity, and color variations of sand particles.

Note noticeably clear colorless to light gray to brown to off-white color tones of majority of sand particles that are compositionally similar siliceous sand across all three mortars. However, grain-size distribution of sands showed a fineness modulus of only 0.87 for sand from Mortar #1 as opposed 2.09 and 2.02 for sands from Mortar #3 and 4, respectively indicating use of a noticeably finer sand in Mortar #1 as opposed to the other two samples.

Sand particles in all three samples are dense, hard, subangular to subrounded, and mostly equidimensional to a few elongated. A few particles in the finer sieve fractions are still agglomerated due to incomplete separation of binder from sand despite repeated acid digestion for 7 days.

It is important to remember that argillaceous sand particles, if any, have broken down during acid digestion and hence are present mostly in the finest fractions instead of intact grains; and calcareous particles, if present, are mostly dissolved out in acid. Hence, photos of particles retained on each sieve are mostly from the siliceous component of sand.

Grain size distribution of extracted sands are compared with the ASTM C 144 specification of natural sand for unit masonry, which shows that for all size fractions, sands from Mortar #1 are higher than the upper limit of ASTM C 144 size gradation for natural sand indicating a noticeably finer particle size than C 144 masonry sand, which is also consistent with its very low fineness modulus of only 0.87.

By contrast, size distribution of sands from Mortar #3 and 4 are within the upper and low limits of ASTM C 144 natural sand, at least in the coarser fractions, indicating their possible replacement in a repointing event with modern ASTM C 144 masonry sand. The 'percent retained' histogram plots also show enrichment of fines compared to the 'normal' distribution.

Subsequent optical microscopical examinations of sands determined dominantly **siliceous composition** for mortars, consisting of major amounts of quartz and subordinate amounts of quartzite, feldspar, quartz siltstone, and ferruginous particles, which are all insoluble in acid.

Lapped Section

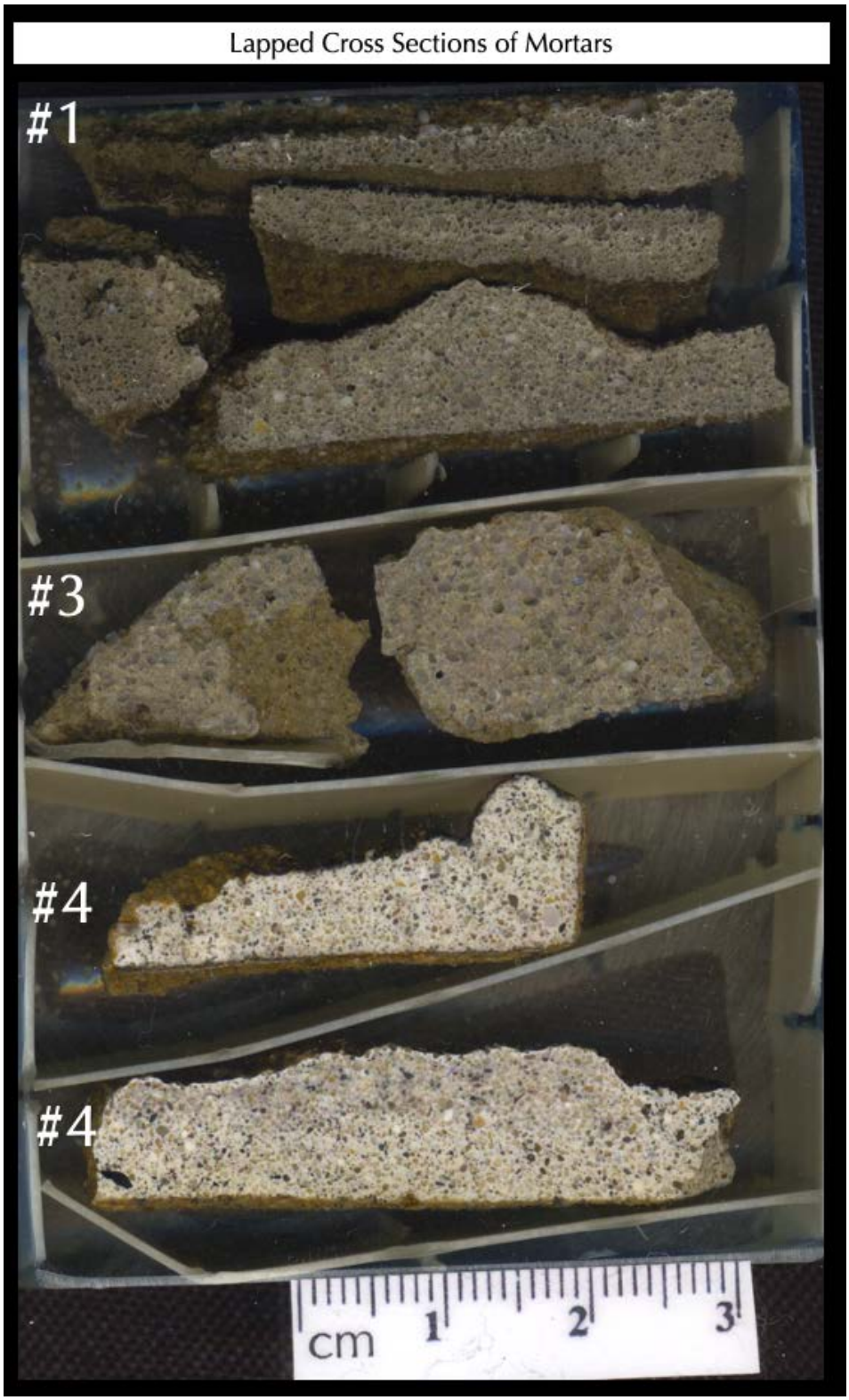

Figure 15: Polished cross section of fragments of three mortar samples showing overall difference in color, appearance, and grain size of sand in the mortars. Sand is noticeably finer in Mortar #1 as opposed to other two samples whereas Mortar #4 shows an overall lighter gray color tone as opposed to medium gray color tones of other two mortars.

Figures 16 through 18 show micrographs of this polished cross section of three mortars where size, shape, angularity, gradation, sorting, and distribution of sand particles are shown in vivid detail.

The fragments were placed inside a flexible silicone mold and encapsulated with a low-viscosity clear epoxy under vacuum to penetrate deep inside the pores and void spaces in the mortars thereby improving the overall integrity of the fragments.

Micrographs of Lapped Section

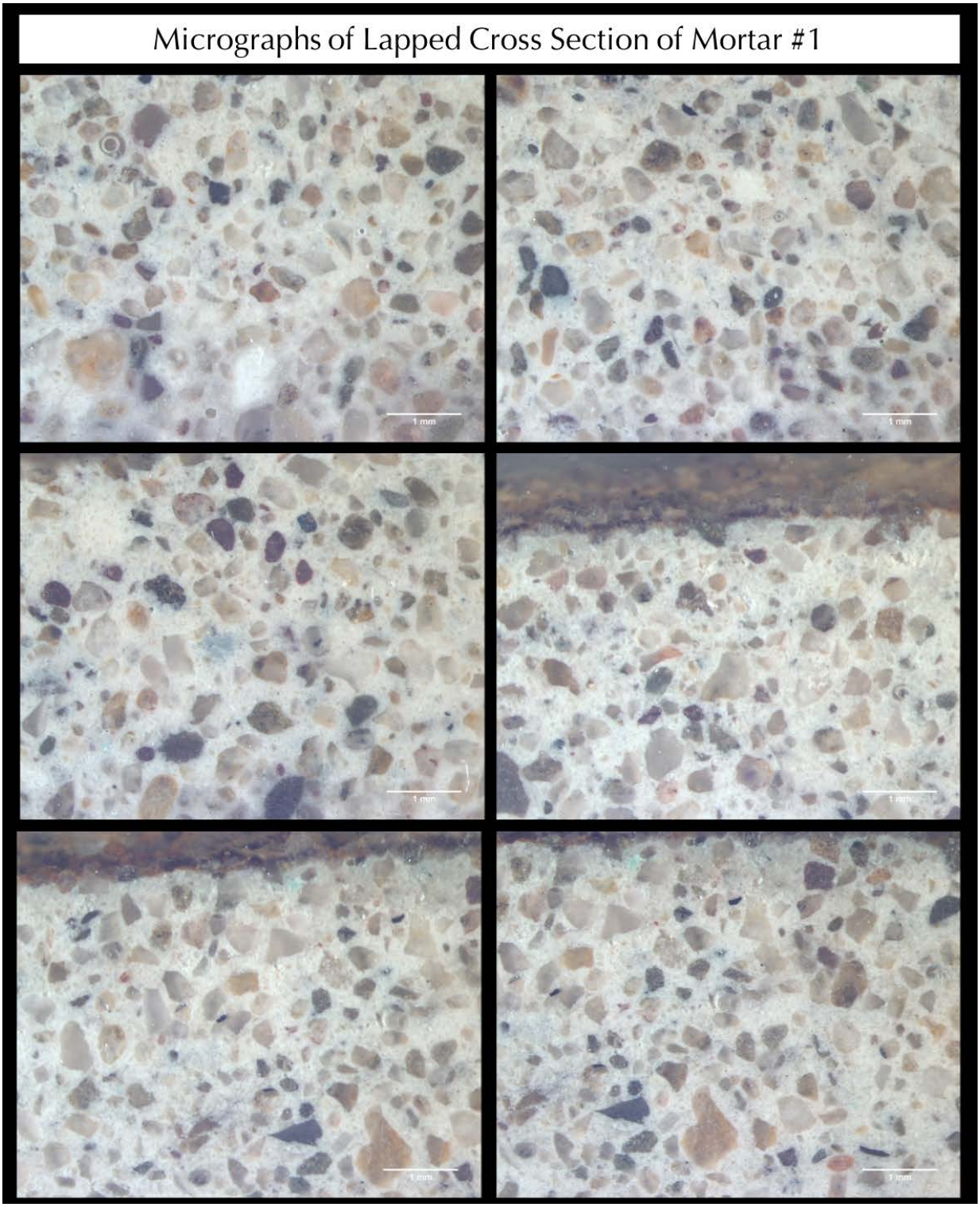

Figure 16: Micrographs of polished cross section of Mortar #1 showing size, shape, angularity, gradation, sorting, and distribution of sand particles across the sample. Sand particles are nominal 0.5 to 0.7 mm in size, well-graded, well-distributed, subangular to subrounded, and multi-colored from clear to light gray to light brown with occasional darker gray, brown, and black particles. Interstitial paste fraction is medium gray. Notice lack of any air bubbles or air entrainment in the mortar.

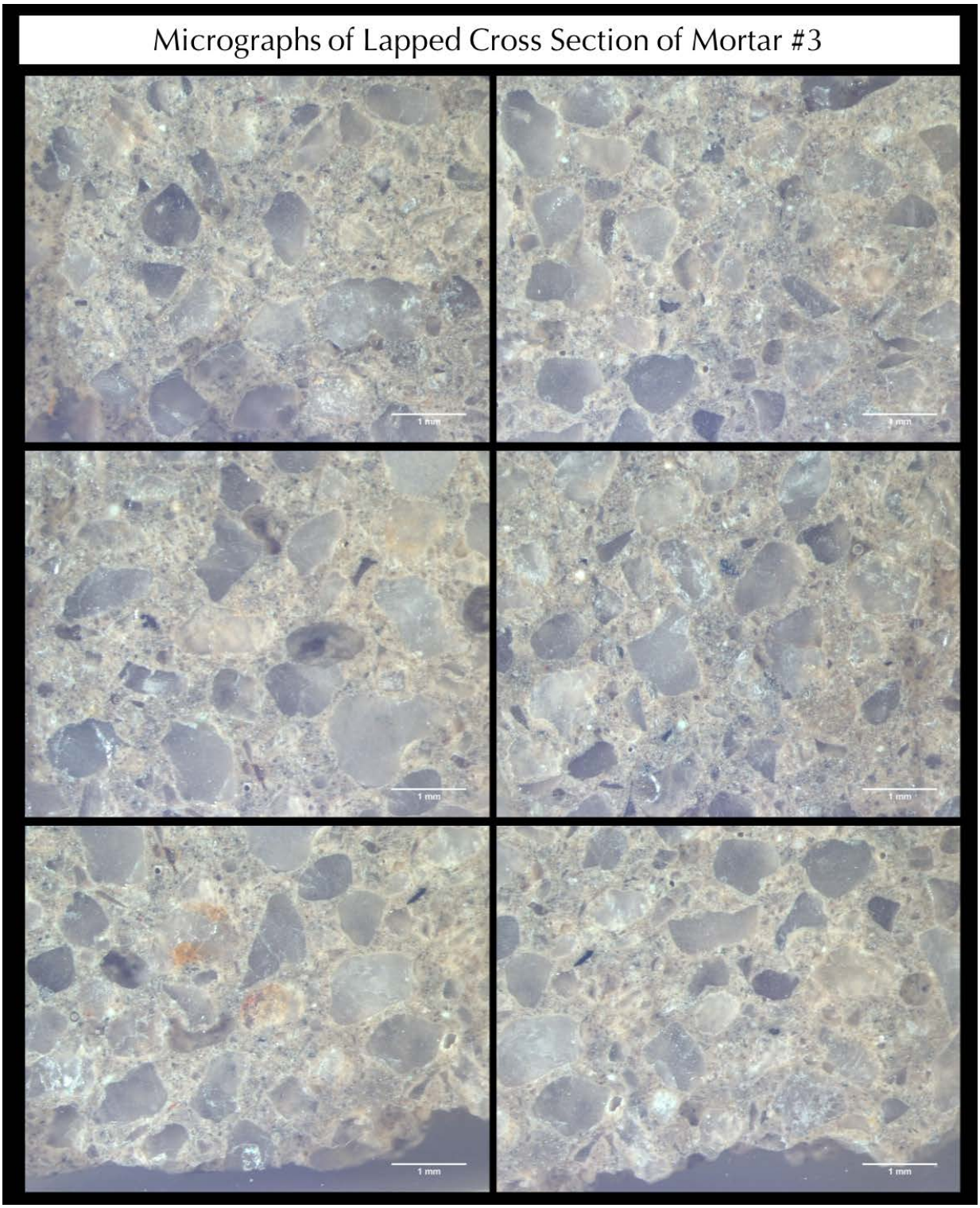

Figure 17: Micrographs of polished cross section of Mortar #3 showing size, shape, angularity, gradation, sorting, and distribution of sand particles across the sample. Sand particles are nominal 1 mm in size, well-graded, well-distributed, subrounded to well-rounded, and mostly uniform in color tones of lighter to medium gray (as opposed to subangular sand fragments and more variation in sand color tones in Mortar #1). Interstitial paste fraction is medium gray, slightly darker than the paste in Mortar #1. Notice lack of any air bubbles or air entrainment in the mortar.

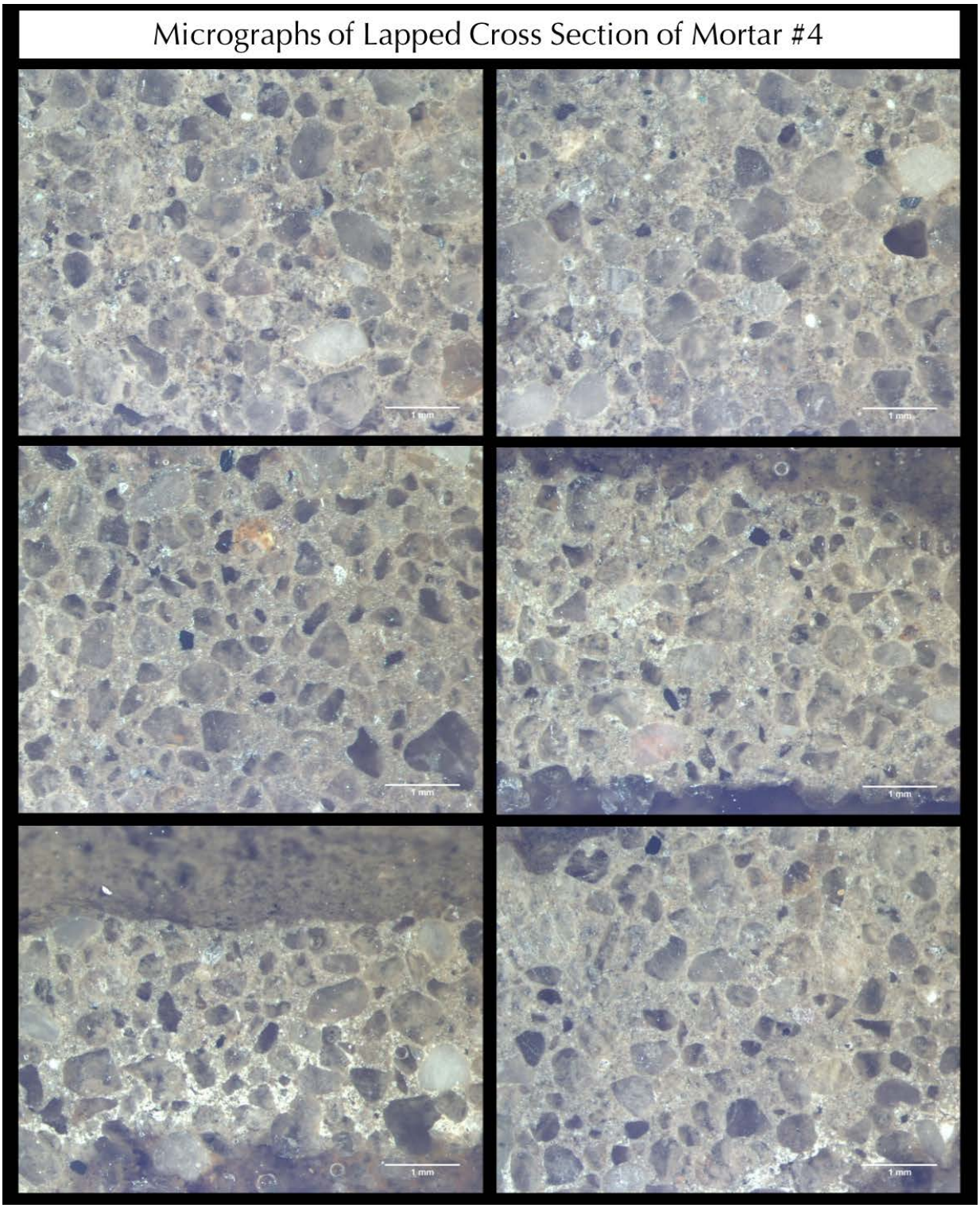

Figure 18: Micrographs of polished cross section of Mortar #4 showing size, shape, angularity, gradation, sorting, and distribution of sand particles across the sample. Sand particles are nominal 0.8 mm in size, well-graded, well-distributed, subrounded to well-rounded, and mostly uniform in color tones of lighter to medium gray (as opposed to subangular sand fragments and more variation in sand color tones in Mortar #1). Interstitial paste fraction is medium gray similar to that in Mortar #3 but slightly darker than the paste in Mortar #1. Notice lack of any air bubbles or air entrainment in the mortar.

Thin Section

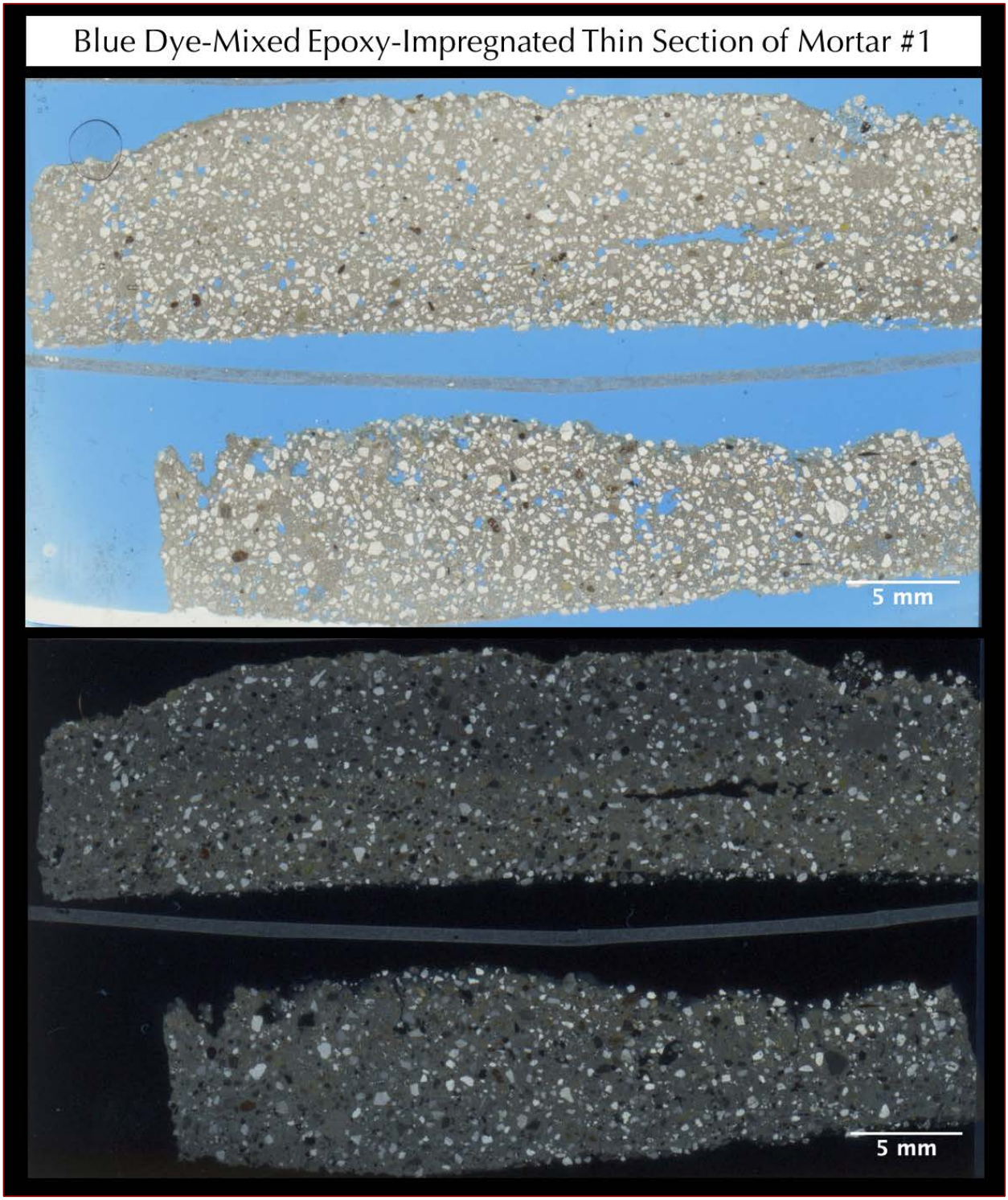

Figure 19: Blue dye-mixed epoxy-encapsulated thin section of Mortar #1 taken by using a flatbed film scanner, where thin section was scanned with a polarizing filter to recreate plane polarized light view of sample (top) to show sand grain size, shape, angularity, and distribution, and pore and void spaces in mortar from blue epoxy, as well as with two perpendicular polarizing filters to recreate crossed polarized light image (bottom) to show the siliceous composition of sand and variably carbonated paste. Notice overall very fine grain size of sand.

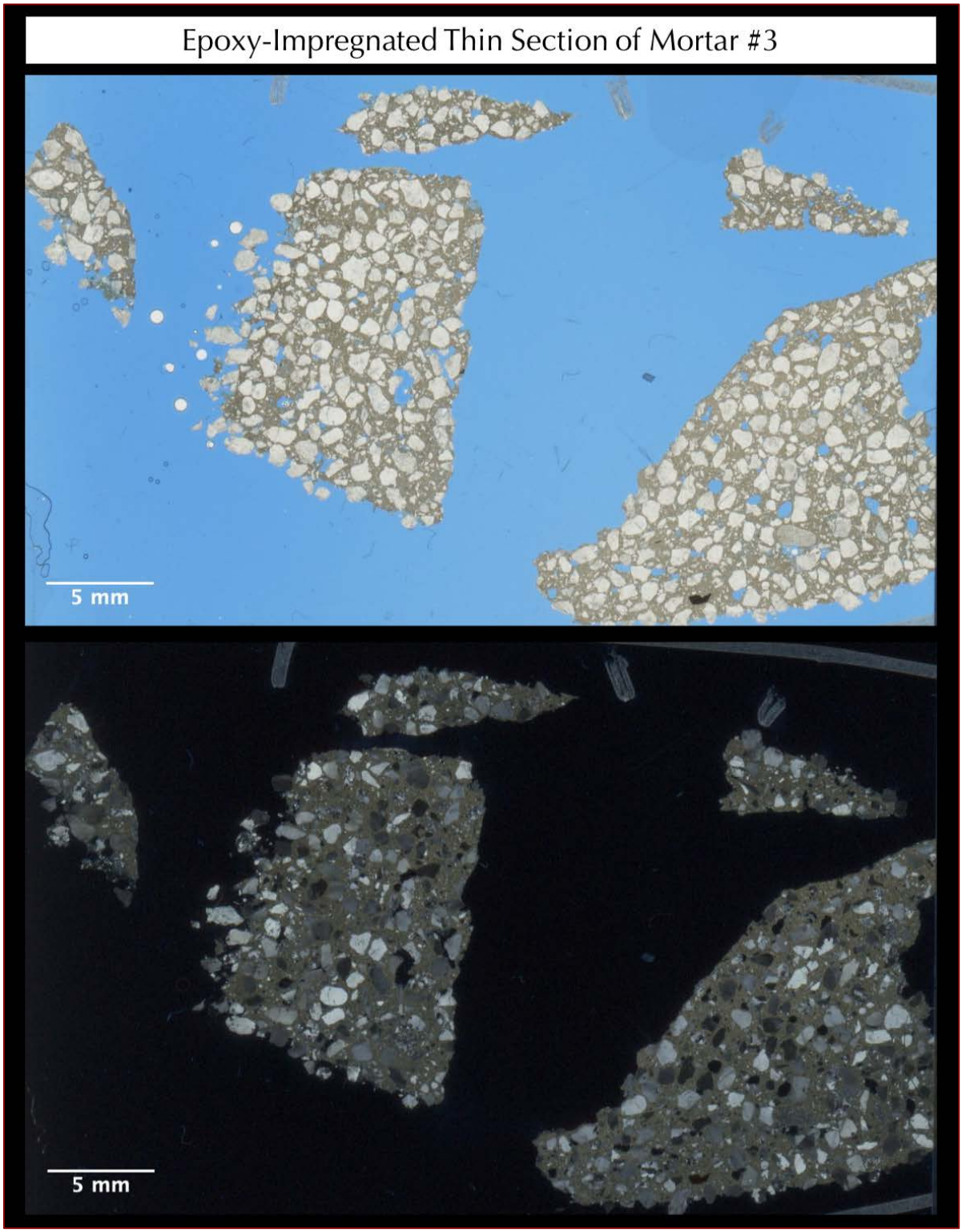

Figure 20: Blue dye-mixed epoxy-encapsulated thin section of Mortar #3 taken by using a flatbed film scanner, where thin section was scanned with a polarizing filter to recreate plane polarized light view of sample (top) to show sand grain size, shape, angularity, and distribution, and pore and void spaces in mortar from blue epoxy, as well as with two perpendicular polarizing filters to recreate crossed polarized light image (bottom) to show the siliceous composition of sand and variably carbonated paste. Notice overall coarser and more rounded grain size of sand compared to finer and more angular sand in Mortar #1.

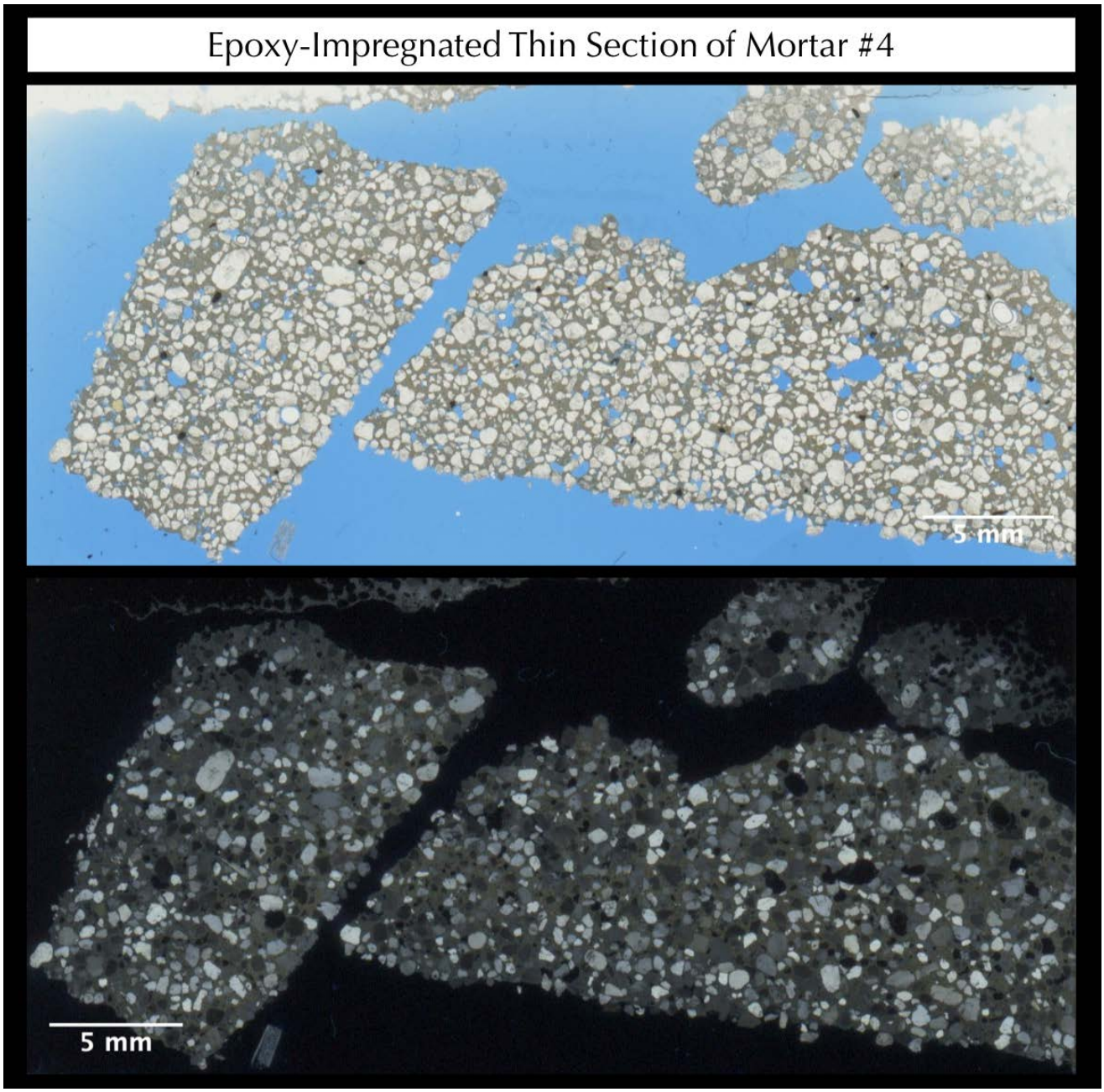

Figure 21: Blue dye-mixed epoxy-encapsulated thin section of Mortar #4 taken by using a flatbed film scanner, where thin section was scanned with a polarizing filter to recreate plane polarized light view of sample (top) to show sand grain size, shape, angularity, and distribution, and pore and void spaces in mortar from blue epoxy, as well as with two perpendicular polarizing filters to recreate crossed polarized light image (bottom) to show the siliceous composition of sand and variably carbonated paste. Notice overall coarser and more subrounded to rounded grain size of sand compared to finer and more angular sand in Mortar #1.

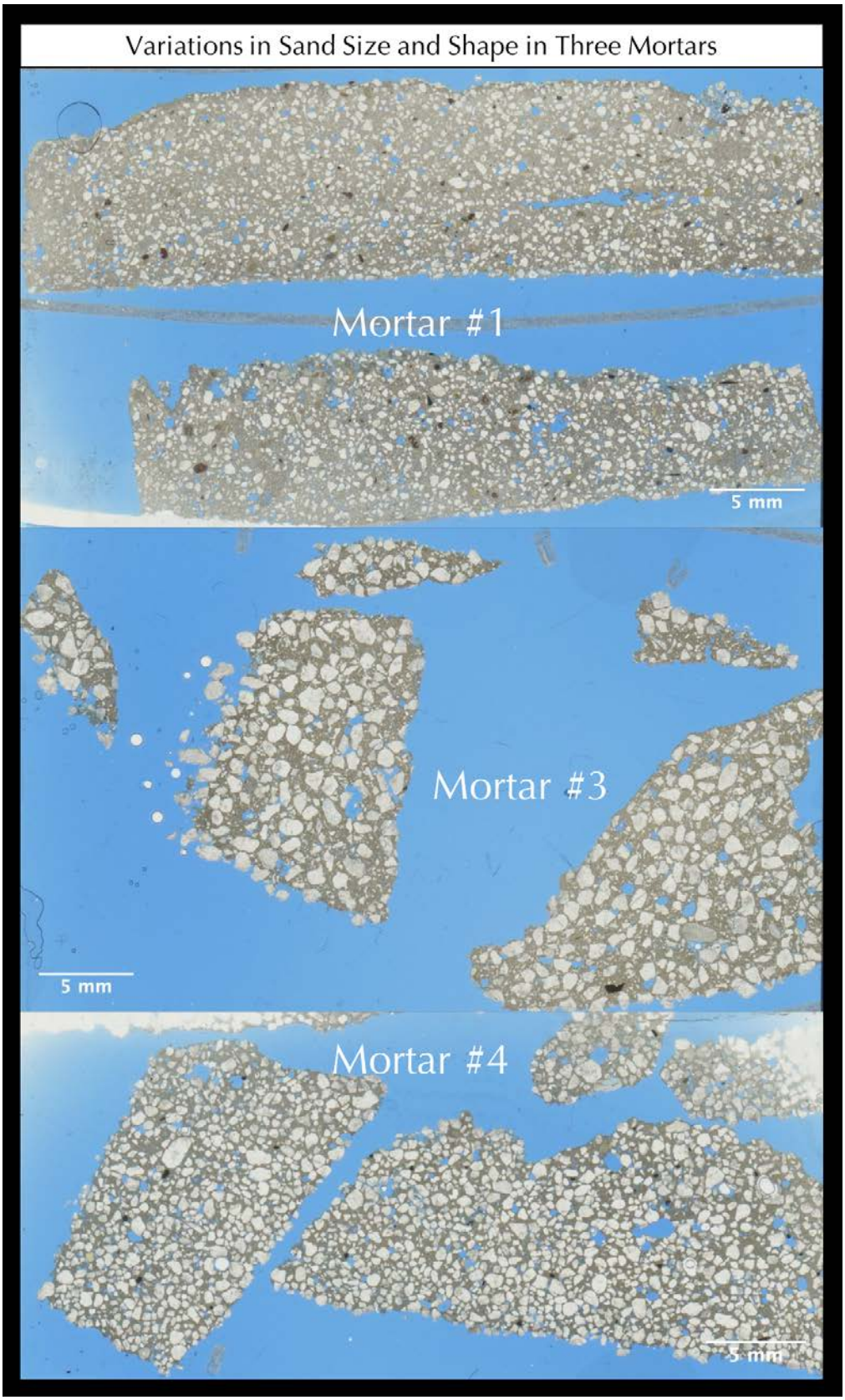

Figure 22: Comparison of size, shape, angularity, gradation, and distribution of sand in three samples, which are best seen in these plane polarized light images of thin sections where sand is clearly noticeably finer and well-graded in Mortar #1 whereas coarser and more rounded well-graded, but better sorted in Mortar #3 compared to #1, and slightly finer in Mortar #4 than that in Mortar #3, well-graded and well-distributed. Such variations in grain size, shape, angularity, and gradation of sand, despite use of siliceous sand across three samples indicate their derivations from three different sources.

Micrographs of Thin Section

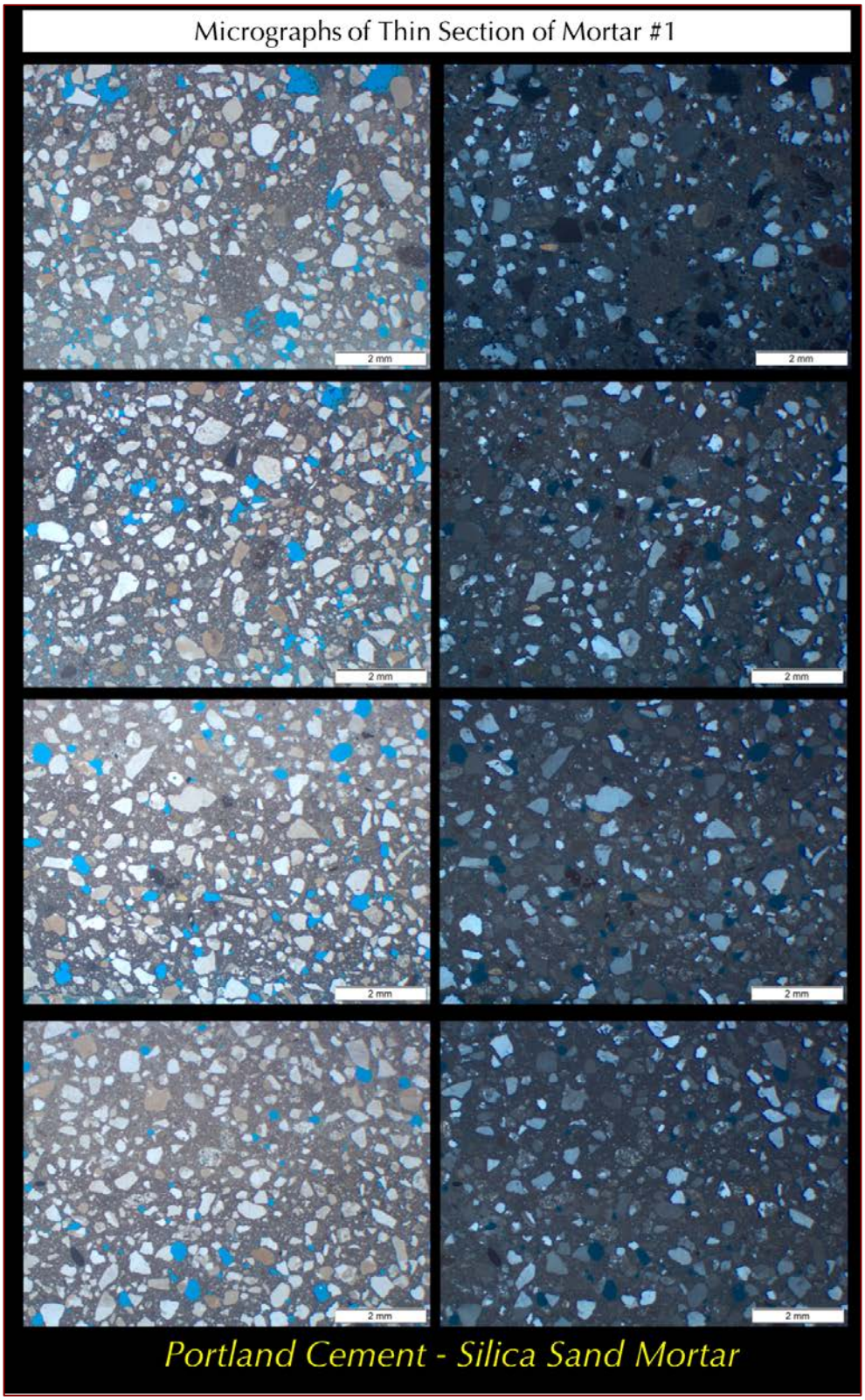

Figure 23: Micrographs of thin section of Mortar #1 showing: (a) non-air-entrained nature of mortar; (b) subangular to subrounded, mostly equidimensional siliceous sand particles that are nominal 0.5-0.6 mm in size, well-graded, well-distributed, consisting of major amount of variably strained quartz and subordinate amounts of quartzite, feldspar, quartz siltstone, and other siliceous particles; and (c) variably dense and carbonated paste.

Left column shows the plane polarized view to highlight sand particles and voids, whereas right column shows corresponding crossed polarized light images to show siliceous composition of sand and carbonated paste.

Notice the paste fraction is significantly denser and harder than a traditional historic lime or even cement-lime mortar, indicating use of Portland cement as the main binder component, which is responsible for the medium gray, dense, and hard nature of the mortar fragments when received.

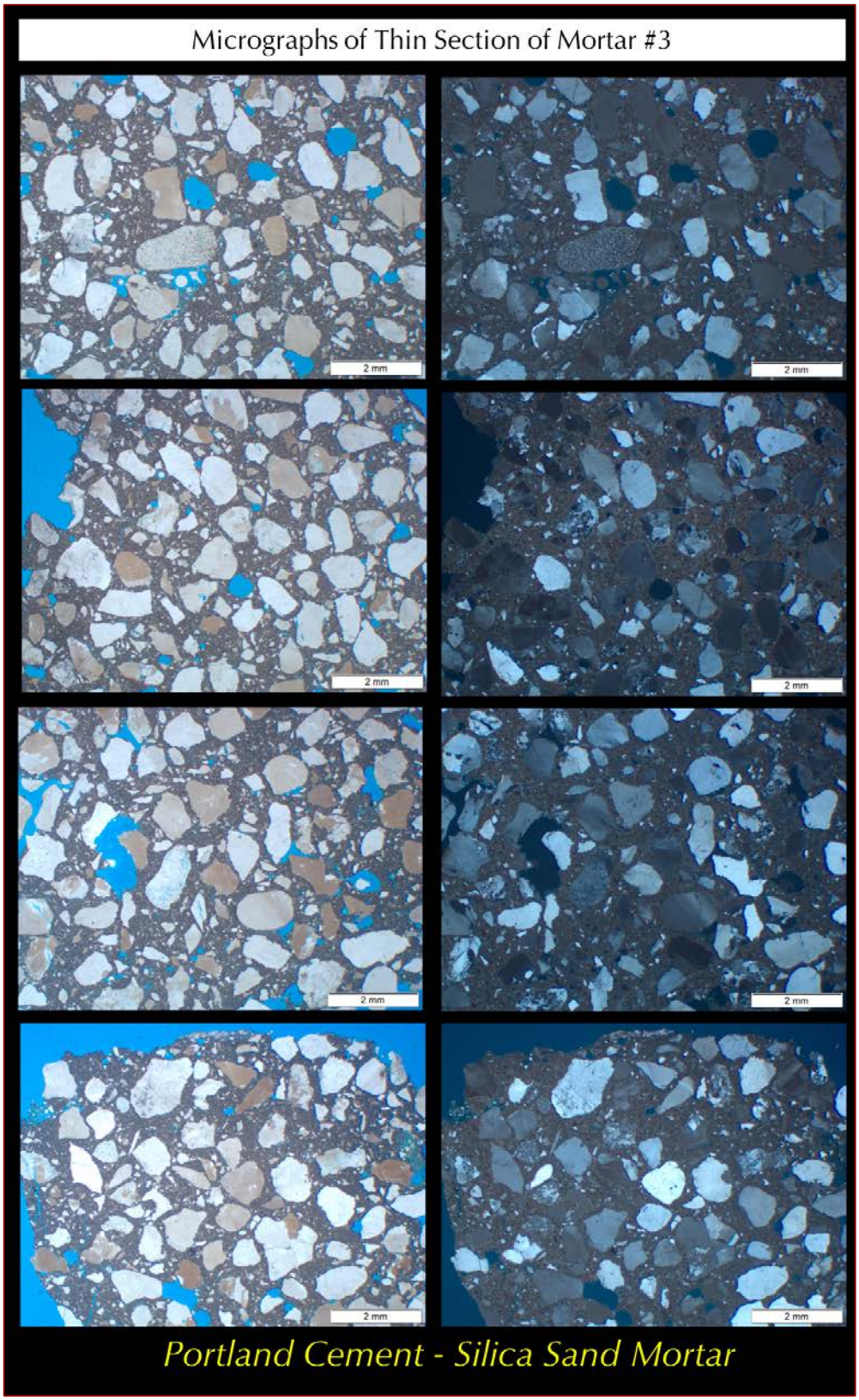

Figure 24: Micrographs of thin section of Mortar #3 showing: (a) non-air-entrained nature of mortar; (b) subangular to subrounded, mostly equidimensional siliceous sand particles that are nominal 1 mm in size, well-graded, well-distributed, consisting of major amount of variably strained quartz and subordinate amounts of quartzite, feldspar, quartz siltstone, and other siliceous particles; and (c) variably dense and carbonated paste.

Left column shows the plane polarized view to highlight sand particles and voids, whereas right column shows corresponding crossed polarized light images to show siliceous composition of sand.

Notice the paste fraction is significantly denser and hard than a traditional historic lime or even cement-lime mortar, indicating use of Portland cement as the main binder component, which is responsible for the medium gray, dense, and hard nature of the mortar fragments when received.

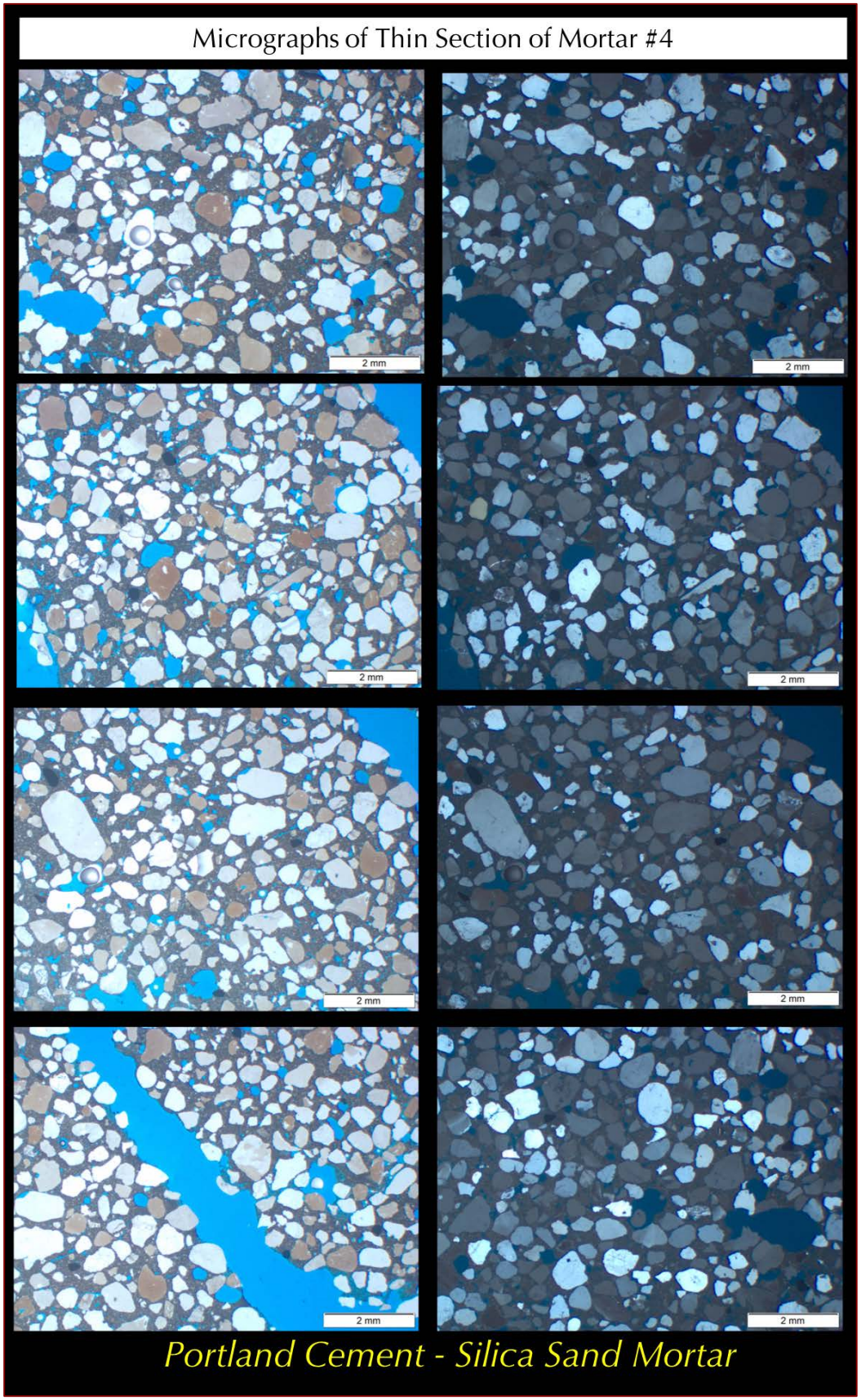

Figure 25: Micrographs of thin section of Mortar #4 showing: (a) non-air-entrained nature of mortar; (b) subangular to subrounded, mostly equidimensional siliceous sand particles that are nominal 0.8 mm in size, well-graded, well-distributed, consisting of major amount of variably strained quartz and subordinate amounts of quartzite, feldspar, quartz siltstone, and other siliceous particles; and (c) variably dense and carbonated paste.

Left column shows the plane polarized view to highlight sand particles and voids, whereas right column shows corresponding crossed polarized light images to show siliceous composition of sand.

Notice the paste fraction is significantly denser and harder than a traditional historic lime or even cement-lime mortar, indicating use of Portland cement as the main binder component, which is responsible for the medium gray, dense, and hard nature of the mortar fragments when received.

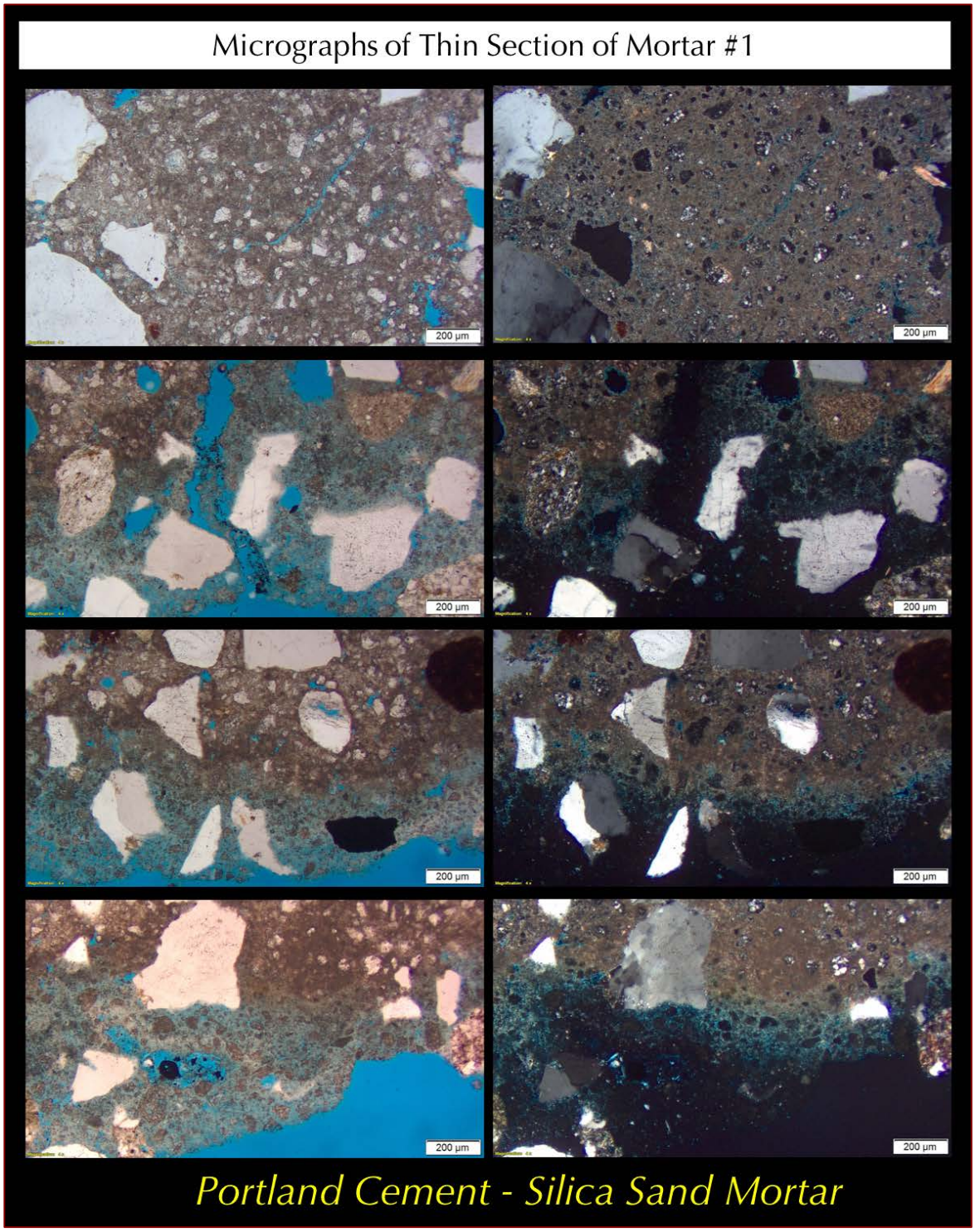

Figure 26: Micrographs of thin section of Mortar #1 in plane (left column) and corresponding cross polarized light (right column) showing very dense nature of paste containing abundant residual Portland cement particles. The exposed edge of the fragment shows some leaching of lime and carbonation, but the interior paste is significantly denser, harder, and shows less carbonated nature. Carbonation has increased the paste porosity at the edge where paste is leached, whereas increased the density and decreased paste porosity in the interior due to overall dense nature of paste in the body. A few fine hair-line shrinkage microcracks are seen in paste, which are common features of Portland cement paste.

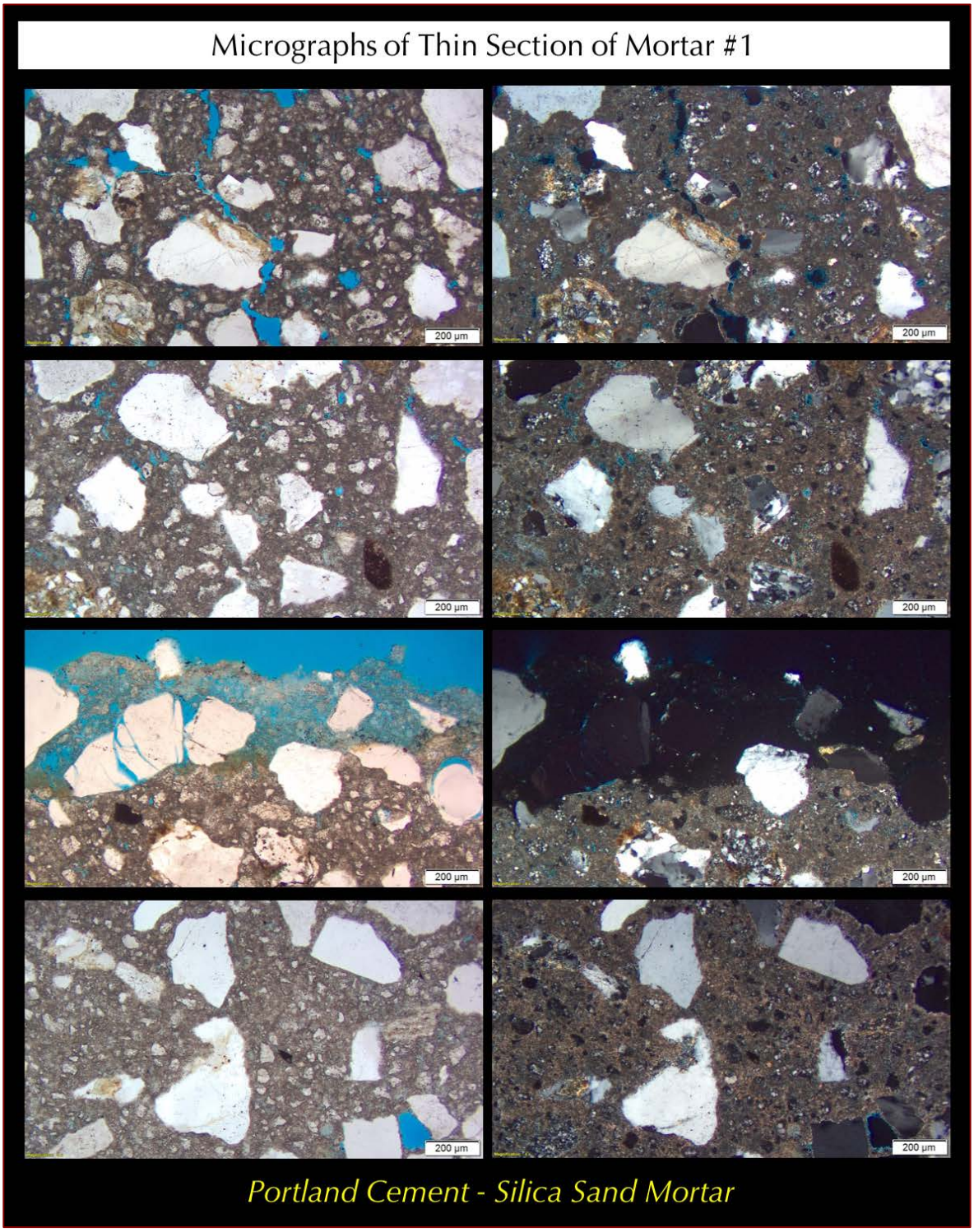

Figure 27: Micrographs of thin section of Mortar #1 in plane (left column) and corresponding cross polarized light (right column) showing very dense nature of paste containing abundant residual Portland cement particles. The exposed edge of the fragment shows some leaching of lime and carbonation, but the interior paste is significantly denser, harder, and shows less carbonated nature. Carbonation has increased the paste porosity at the edge where paste is leached whereas increased the density and decreased paste porosity in the interior due to overall dense nature of paste in the body. A few fine hair-line shrinkage microcracks are seen in paste, which are common features of Portland cement paste. The third row photos show significant leaching of exposed edge of fragment to a depth of 0.2-0.4 mm leaving a soft, porous paste rich in silica gel residue.

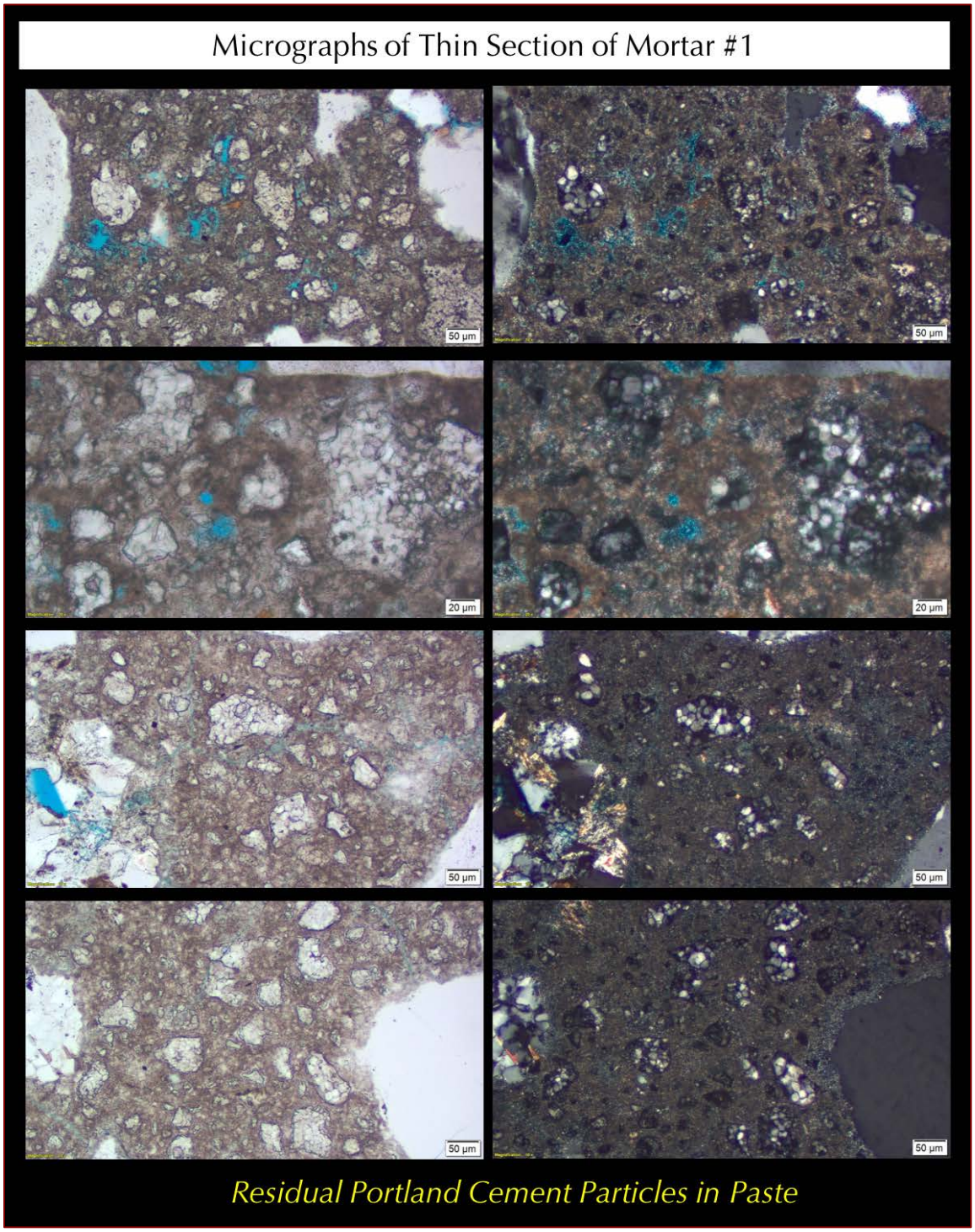

Figure 28: Micrographs of thin section of Mortar #1 in plane (left column) and corresponding cross polarized light (right column) showing very dense nature of paste containing abundant residual Portland cement particles consisting of subhedral alite, anhedral spherical belite, and interstitial dark brown ferrite phases in the residual Portland cement. Notice the absence of lime lump or carbonated lime components that are common in historic lime or even in modern cement-lime mortars indicating use of Portland cement as the main binder with minimum or no lime component, which is commonly added for improved workability and water retention properties of mortar. This Portland cement only composition though makes the mortar denser, harder, stronger and, in fact, less desirable for increased elastic modulus and hence potential to crack as opposed to accommodate masonry wall movement from the beneficial flexibility of masonry that the lime component in binder offers.

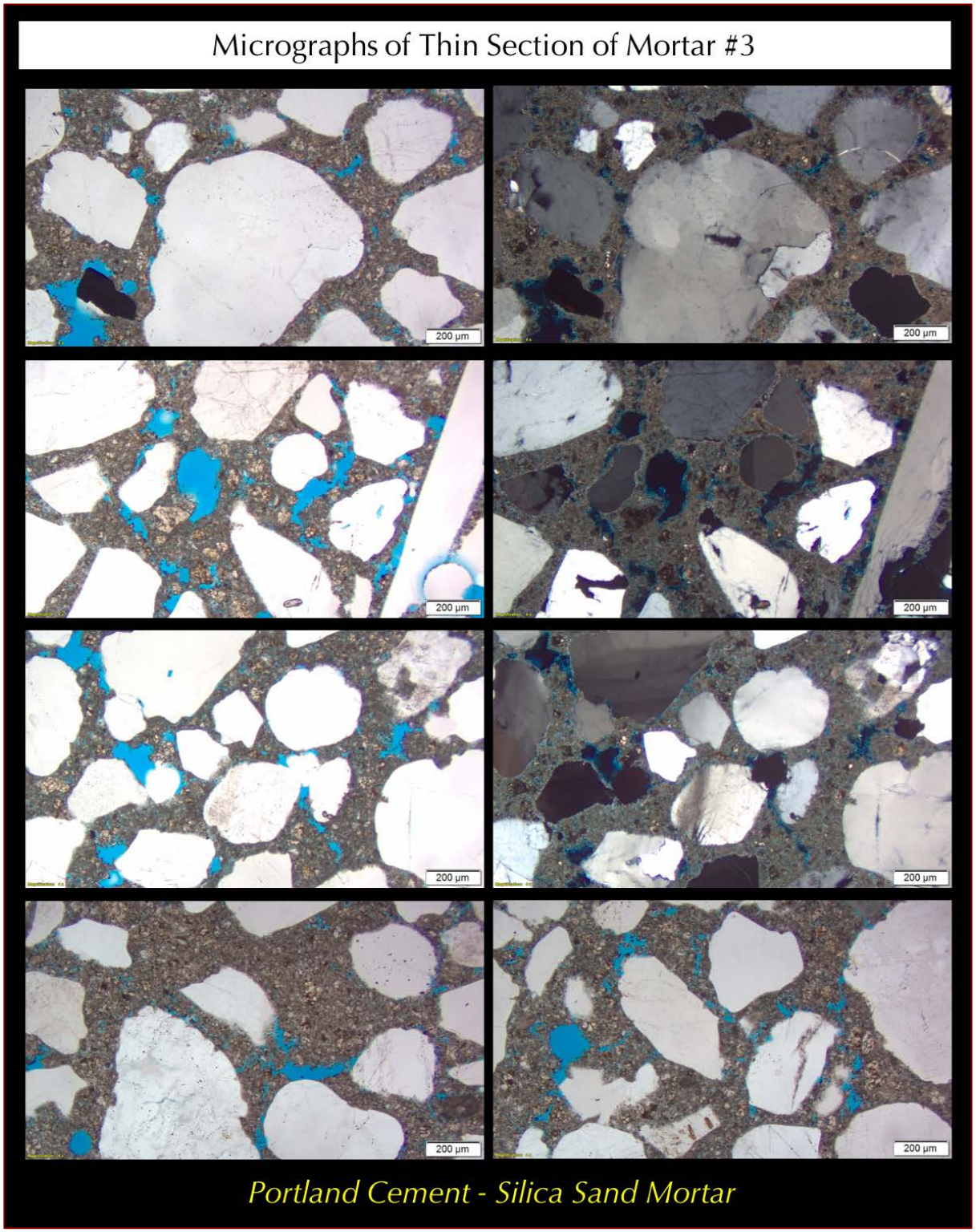

Figure 29: Micrographs of thin section of Mortar #3 in plane (left column) and corresponding cross polarized light (right column) showing very dense nature of paste containing abundant residual Portland cement particles. A few short elongated shrinkage microcracks are seen in paste, which are common features of Portland cement paste. Paste also shows carbonation from interaction with atmospheric carbon dioxide.

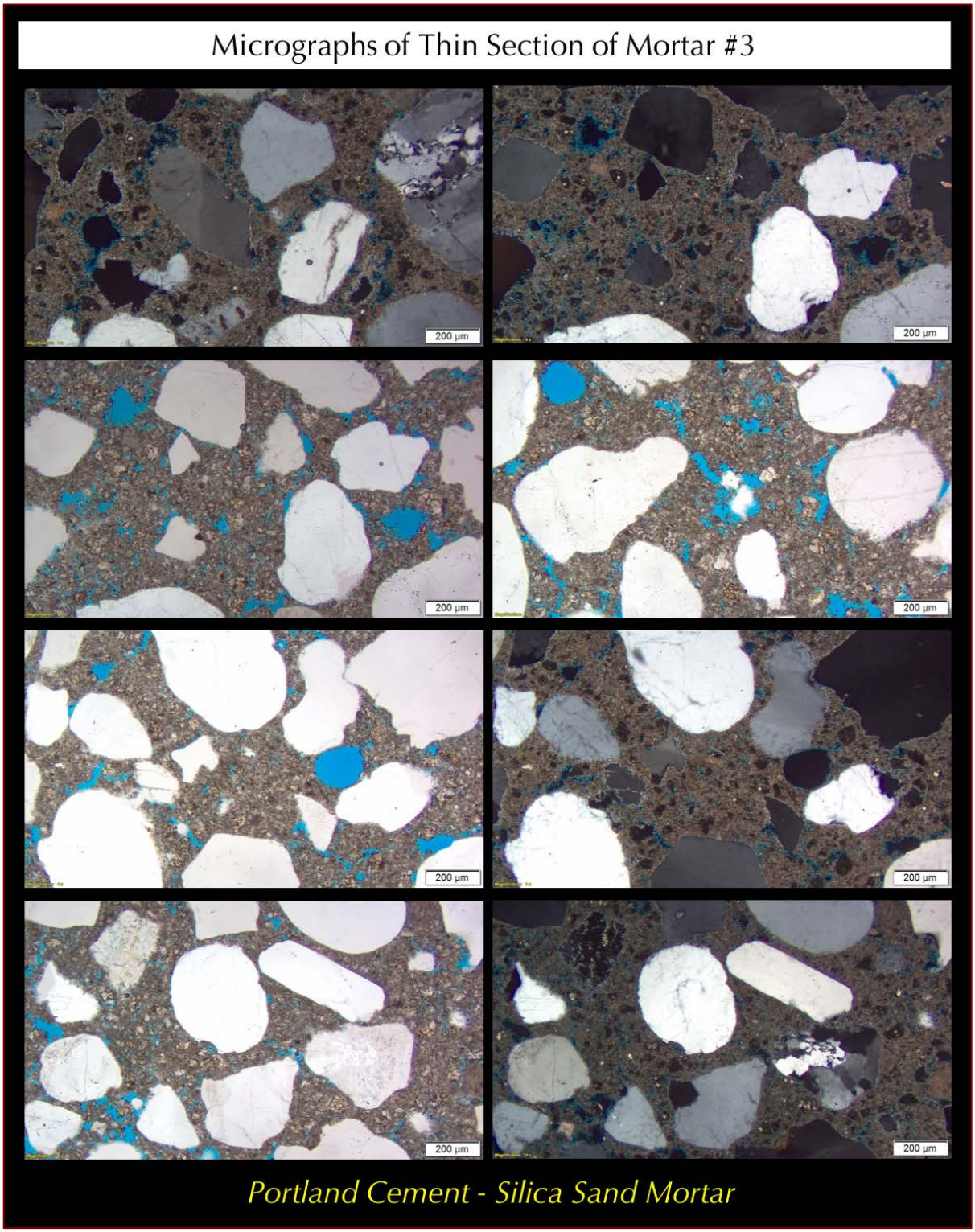

Figure 30: Micrographs of thin section of Mortar #3 in plane (left column) and corresponding cross polarized light (right column) showing very dense nature of paste containing abundant residual Portland cement particles. A few short elongated shrinkage microcracks are seen in paste, which are common features of Portland cement paste. Paste also shows carbonation from interaction with atmospheric carbon dioxide.

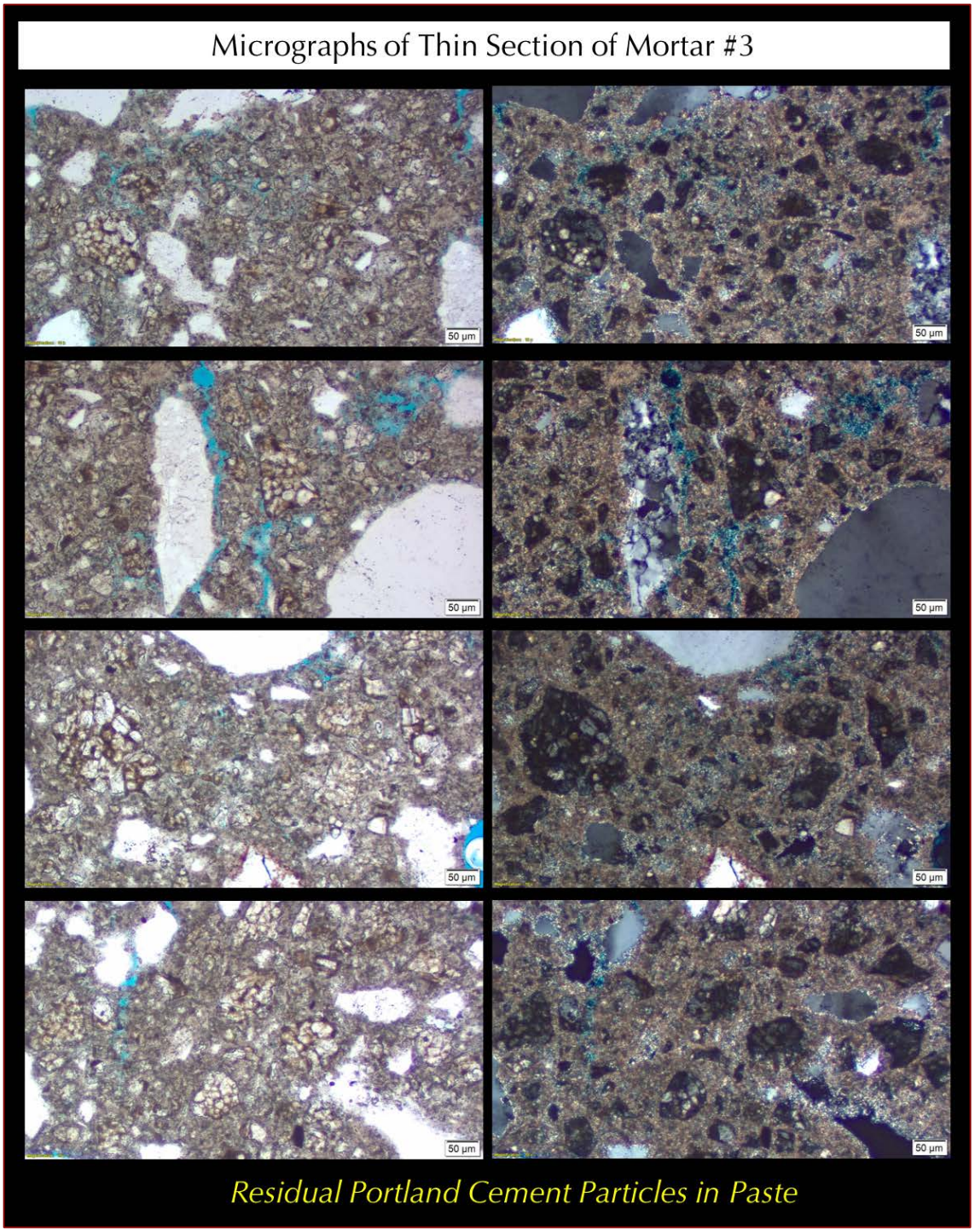

Figure 31: Micrographs of thin section of Mortar #3 in plane (left column) and corresponding cross polarized light (right column) showing very dense nature of paste containing abundant residual Portland cement particles consisting of subhedral alite, anhedral spherical belite, and interstitial dark brown ferrite phases in the residual Portland cement. Notice the absence of lime lump or carbonated lime components that are common in historic lime or even in modern cement-lime mortars indicating use of Portland cement as the main binder with minimum or no lime component, which is commonly added for improved workability and water retention properties of mortar. This Portland cement only composition though makes the mortar denser, harder, stronger and are, in fact, less desirable for increased elastic modulus and hence potential to crack as opposed to accommodate masonry wall movement from the beneficial flexibility of masonry that the lime component in binder offers.

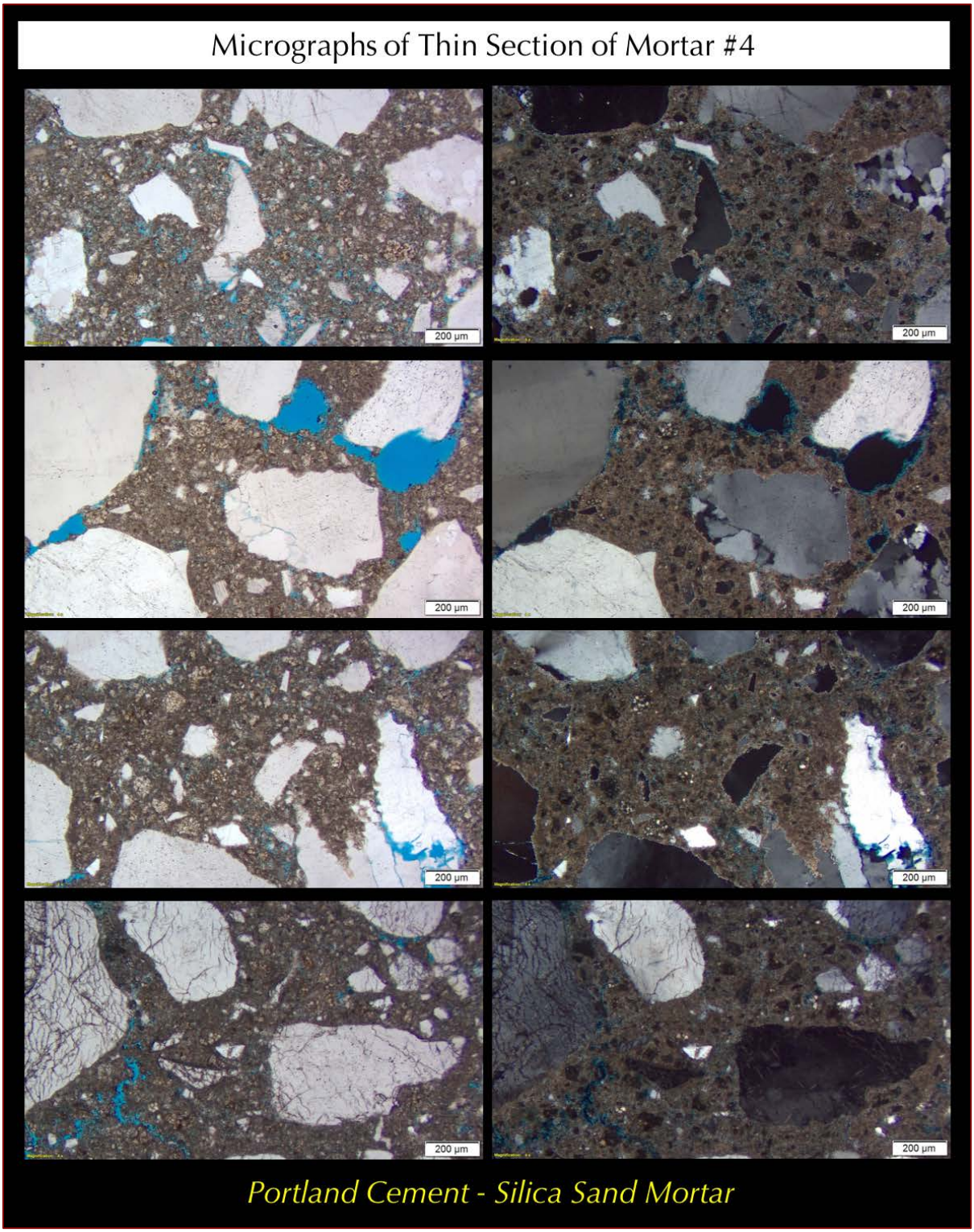

Figure 32: Micrographs of thin section of Mortar #4 in plane (left column) and corresponding cross polarized light (right column) showing very dense nature of paste containing abundant residual Portland cement particles. A few short elongated shrinkage microcracks are seen in paste, which are common features of Portland cement paste. Paste also shows carbonation from interaction with atmospheric carbon dioxide.

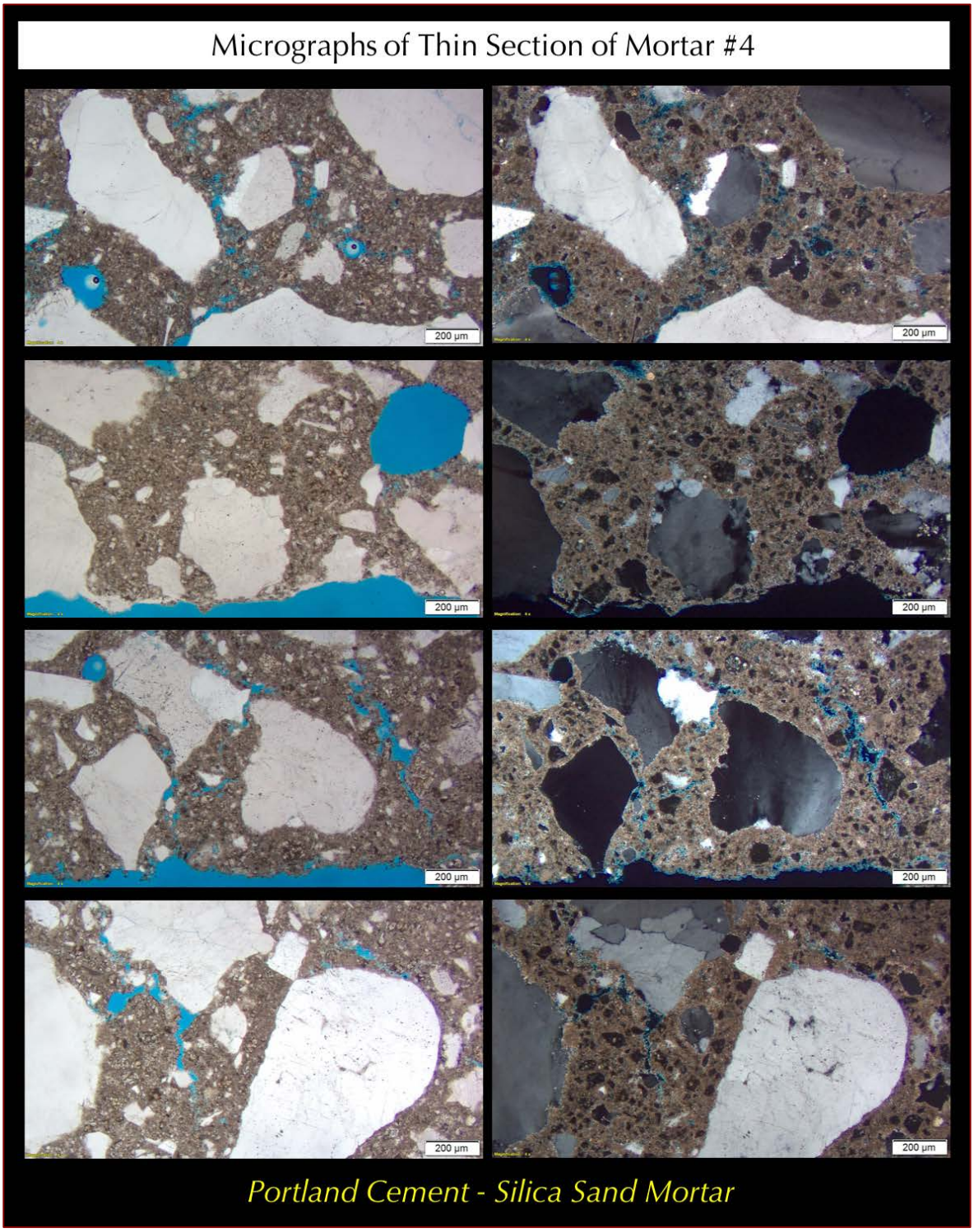

Figure 33: Micrographs of thin section of Mortar #4 in plane (left column) and corresponding cross polarized light (right column) showing very dense nature of paste containing abundant residual Portland cement particles. A few short elongated shrinkage microcracks are seen in paste, which are common features of Portland cement paste. Paste also shows carbonation from interaction with atmospheric carbon dioxide.

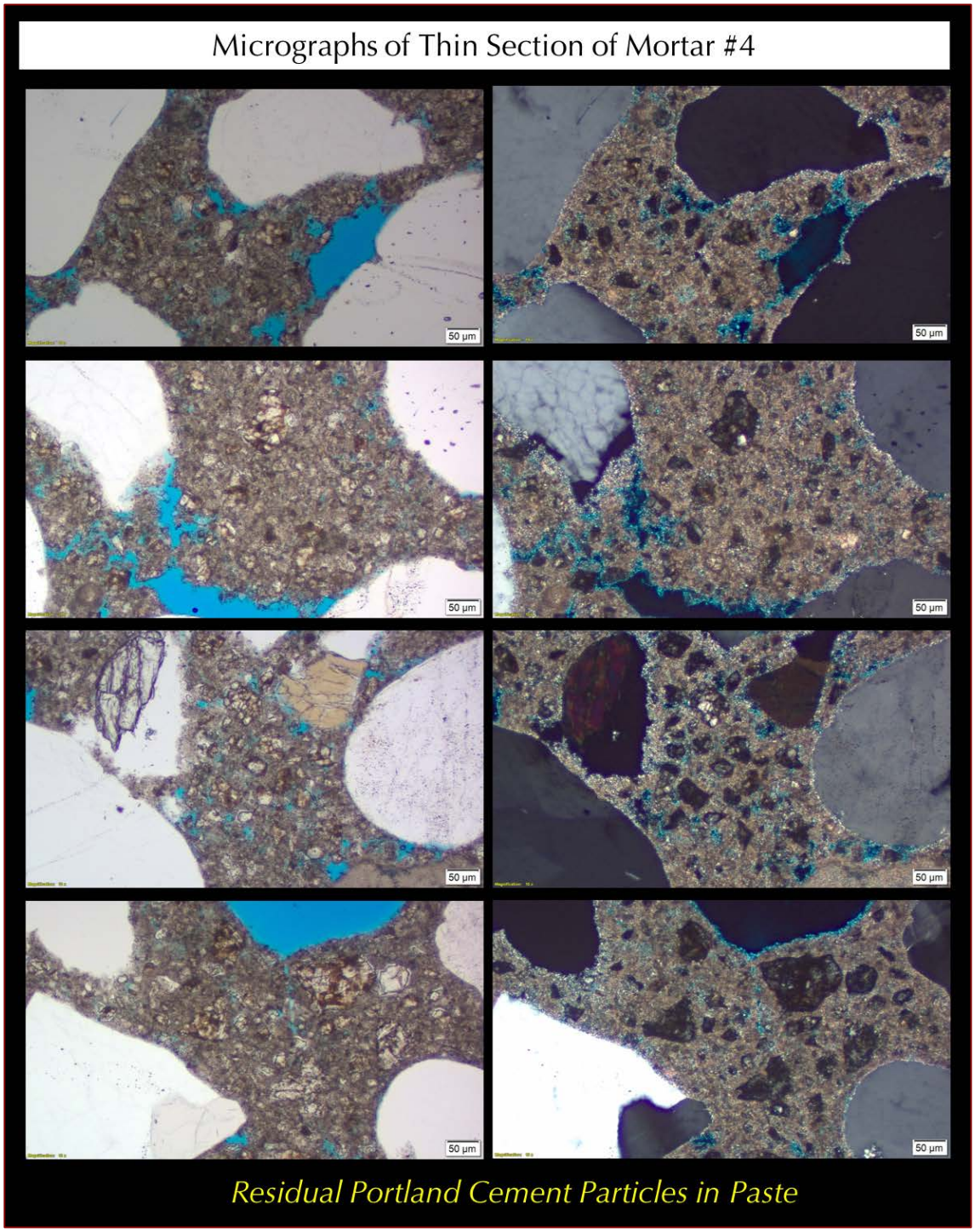

Figure 34: Micrographs of thin section of Mortar #4 in plane (left column) and corresponding cross polarized light (right column) showing very dense nature of paste containing abundant residual Portland cement particles consisting of subhedral alite, anhedral spherical belite, and interstitial dark brown ferrite phases in the residual Portland cement. Notice the absence of lime lump or carbonated lime components that are common in historic lime or even in modern cement-lime mortars indicating use of Portland cement as the main binder with minimum or no lime component which is commonly added for improved workability and water retention properties of mortar. This Portland cement only composition though makes the mortar denser, harder, stronger and are, in fact, less desirable for increased elastic modulus and hence potential to crack as opposed to accommodate masonry wall movement from the beneficial flexibility of masonry that the lime component in binder offers.

Optical Microscopy

Sand

Sand in all three mortars are compositionally similar ***natural siliceous sands*** consisting of major amount of variably strained quartz, and subordinate amounts of quartzite, quartz siltstone, feldspar, and other siliceous and minor ferruginous components. Particles are subangular to subrounded in Mortar #1, whereas subrounded to well-rounded in Mortar #3 and 4. In all samples, particles are mostly equidimensional to a few elongated, dense, hard, well-graded, well-distributed, nominal 0.5 to 0.6-mm in size in Mortar #1, 1 mm in Mortar #3 and 0.8 mm in Mortar #4, and present in sound conditions without any evidence of potentially deleterious reactions. Figures 16 to 18 show size, shape, angularity, gradation, and distribution of sands in polished sections, whereas Figures 19 to 25 show similar features of sands in thin sections of mortars.

Grain size distribution of extracted sands in Figures 6, 9, and 12 are compared with the ASTM C 144 specification of natural sand for unit masonry, which shows that for all size fractions, sands from Mortar #1 are higher than the upper limit of ASTM C 144 size gradation for natural sand indicating a noticeably finer particle size than C 144 masonry sand, which is also consistent with its very lower fineness modulus of only 0.87. By contrast, size distribution of sands from Mortar #3 and 4 are within the upper and low limits of ASTM C 144 natural sand at least in the coarser fractions indicating their possible replacement in a repointing event with modern ASTM C 144 masonry sand.

Binders

Binders in all three mortars are compositionally similar, which are all determined to be ***Portland cement*** with a minor lime component added. Contrary to lime lumps in historic mortars or carbonated fine-grained porous lime paste even in modern cement-lime mortars, paste in all three samples show very dense nature consisting of abundant scattered residual Portland cement particles distributed over the typical hydration products of Portland cement (calcium silicate hydrate, calcium hydroxide, and calcium sulfoaluminate hydrate phase). Figures 26 through 34 show detailed compositions and properties of sands used in the mortars.

Air

All three mortars are ***non-air-entrained*** with no evidence of addition of any air entraining agents. Air contents are similar and estimated to be 3 to 4 percent. Figures 16 to 18 show micrographs of polished cross sections of mortars where lack of air entrainment is seen. Thin section micrographs in Figures 19 to 25 also show the similar absence.

Mortar Types

Based on optical microscopical examinations, all three mortars are determined to be ***Portland cement and silica sand based mortars***, which are not representative of historic mortars, nor are they representative of modern masonry mortars where lime component is added in appreciable amounts for added workability and water retention properties without which use of Portland cement at appreciable or sole amounts, as in the presence case, can introduce significant mismatch with the adjacent masonry and can introduce cracking from shrinkage or excessive brittleness of mortars. Subsequent compositional analyses of pastes in SEM-EDS shown below detected a dolomitic lime component from high magnesia contents in paste, which was added at a subordinate amount compared to Portland cement mainly in Mortar #3 and 4.

Scanning Electron Microscopy and X-ray Microanalyses

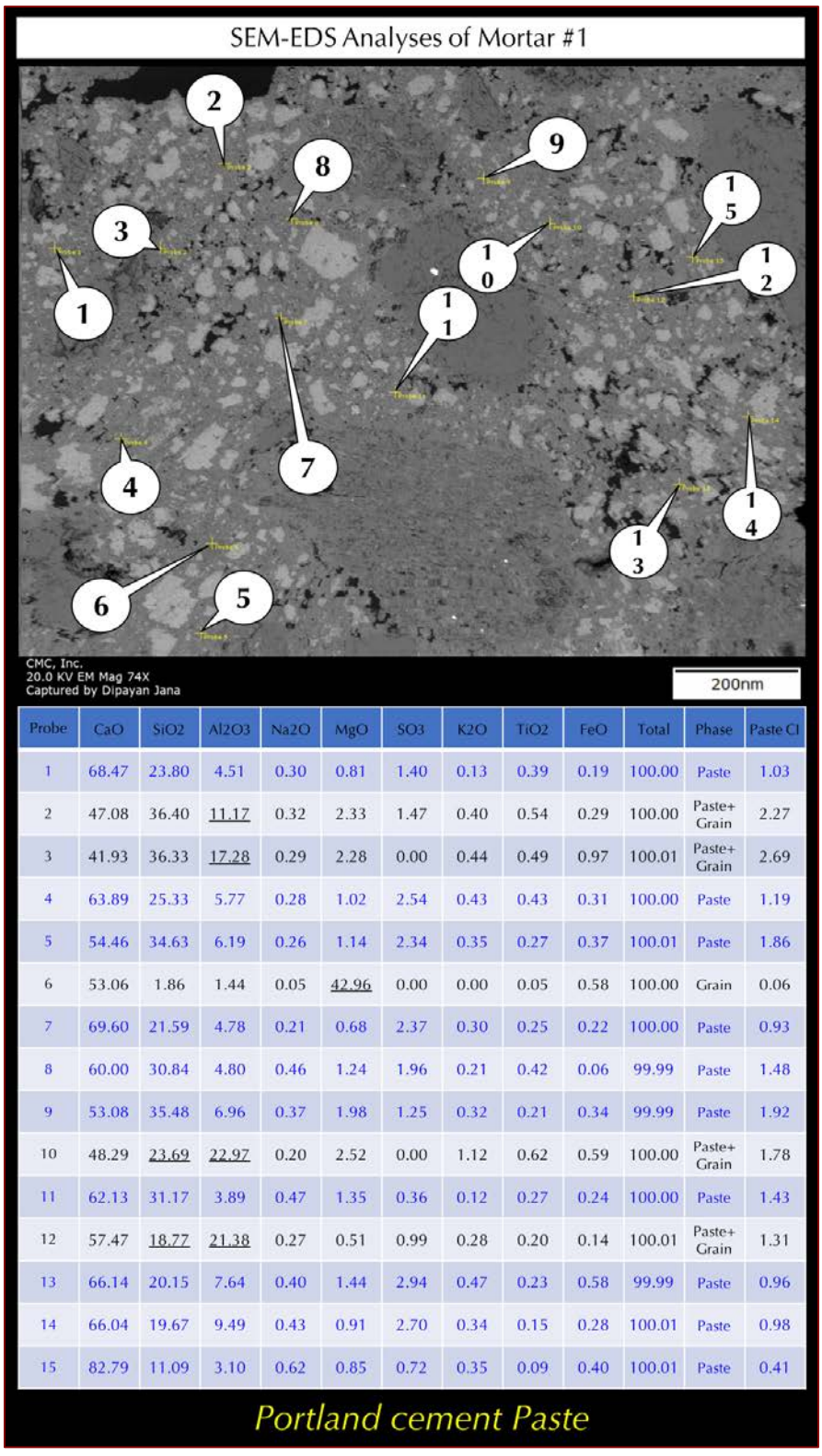

Probe	CaO	SiO2	Al2O3	Na2O	MgO	SO3	K2O	TiO2	FeO	Total	Phase	Paste CI
1	68.47	23.80	4.51	0.30	0.81	1.40	0.13	0.39	0.19	100.00	Paste	1.03
2	47.08	36.40	11.17	0.32	2.33	1.47	0.40	0.54	0.29	100.00	Paste+ Grain	2.27
3	41.93	36.33	17.28	0.29	2.28	0.00	0.44	0.49	0.97	100.01	Paste+ Grain	2.69
4	63.89	25.33	5.77	0.28	1.02	2.54	0.43	0.43	0.31	100.00	Paste	1.19
5	54.46	34.63	6.19	0.26	1.14	2.34	0.35	0.27	0.37	100.01	Paste	1.86
6	53.06	1.86	1.44	0.05	42.96	0.00	0.00	0.05	0.58	100.00	Grain	0.06
7	69.60	21.59	4.78	0.21	0.68	2.37	0.30	0.25	0.22	100.00	Paste	0.93
8	60.00	30.84	4.80	0.46	1.24	1.96	0.21	0.42	0.06	99.99	Paste	1.48
9	53.08	35.48	6.96	0.37	1.98	1.25	0.32	0.21	0.34	99.99	Paste	1.92
10	48.29	23.69	22.97	0.20	2.52	0.00	1.12	0.62	0.59	100.00	Paste+ Grain	1.78
11	62.13	31.17	3.89	0.47	1.35	0.36	0.12	0.27	0.24	100.00	Paste	1.43
12	57.47	18.77	21.38	0.27	0.51	0.99	0.28	0.20	0.14	100.01	Paste+ Grain	1.31
13	66.14	20.15	7.64	0.40	1.44	2.94	0.47	0.23	0.58	99.99	Paste	0.96
14	66.04	19.67	9.49	0.43	0.91	2.70	0.34	0.15	0.28	100.01	Paste	0.98
15	82.79	11.09	3.10	0.62	0.85	0.72	0.35	0.09	0.40	100.01	Paste	0.41

Portland cement Paste

Figure 35: Backscatter electron image (top), and X-ray microanalyses at the tips of callouts in Probes 1 through 15 detecting compositional variations of paste in Mortar #1.

Paste compositions are presented (bottom) as oxide variations of all detected peaks normalized to 100% except carbon (from epoxy) and gold (from coating).

Paste cementation indices, CI (after Eckel 1922) measure relative hydraulicity of paste e.g., non-hydraulic lime pastes have very low CI (< 0.50) compared to Portland cement pastes (CI is >1).

Paste (shown in blue rows) shows very high CIs from use of Portland cement as the main cementitious binder with minor lime component to reduce the overall CIs close to 1 which was not detected in optical microscopical examinations. Variable CI values of paste is due to variable degrees of carbonation which usually reduces the CI.

In all Figures, the cementation indices (CI) of paste are calculated after Eckel (1922) as CI = $[(2.8*SiO_2)+(1.1*Al_2O_3)+(0.7*Fe_2O_3)]/[(CaO)+(1.4*MgO)]$.

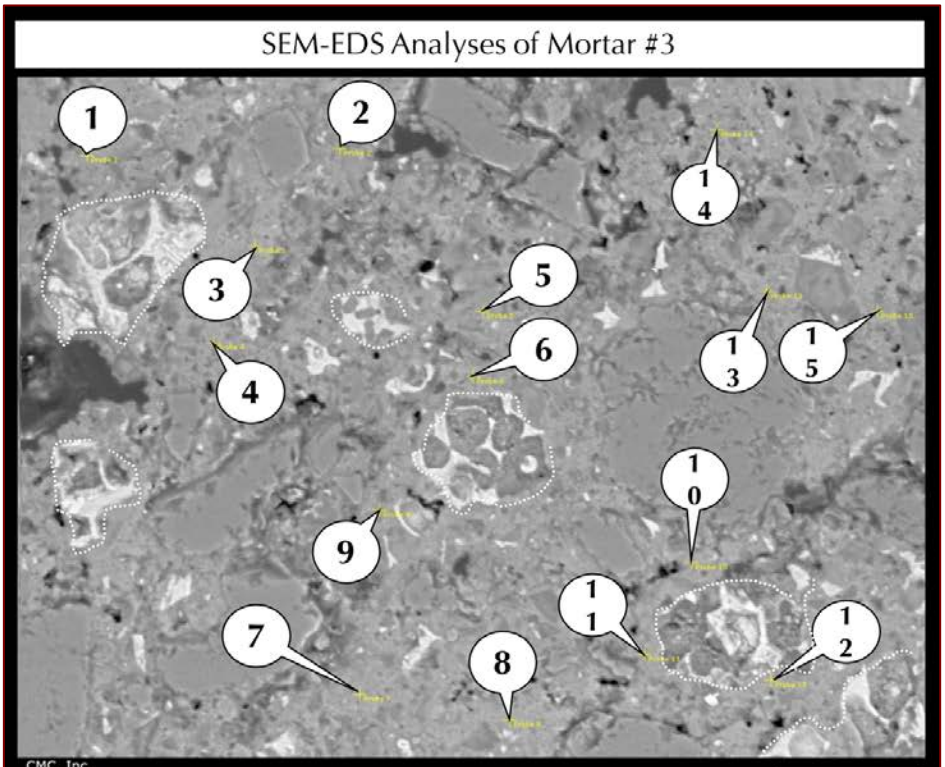

Probe	CaO	SiO2	Al2O3	Na2O	MgO	SO3	K2O	TiO2	FeO	Total	Phase	Paste CI
1	60.17	17.85	6.58	0.03	14.55	0.00	0.01	0.15	0.67	100.0	Paste	0.72
2	64.60	18.65	5.21	0.05	10.68	0.00	0.04	0.00	0.77	100.0	Paste	0.74
3	74.57	13.29	2.90	0.00	8.84	0.00	0.02	0.00	0.38	100.0	Paste	0.47
4	63.84	18.80	8.94	0.09	7.34	0.00	0.03	0.15	0.82	100.0	Paste	0.85
5	66.83	19.47	4.21	0.01	8.06	0.00	0.06	0.27	1.09	100.0	Paste	0.77
6	54.30	19.45	3.83	0.00	22.00	0.00	0.01	0.00	0.40	100.0	Paste	0.69
7	70.01	10.69	1.50	0.00	17.54	0.00	0.01	0.00	0.25	100.0	Paste	0.34
8	61.10	17.97	14.43	0.40	4.36	0.00	0.07	0.15	1.51	100.0	Paste	1.00
9	45.27	32.41	17.96	0.21	3.67	0.00	0.00	0.00	0.48	100.0	Paste	2.20
10	61.41	26.28	5.15	0.14	5.40	0.00	0.01	0.11	1.50	100.0	Paste	1.16
11	56.14	19.70	4.51	0.00	19.22	0.00	0.00	0.06	0.37	100.0	Paste	0.73
12	68.57	16.44	5.03	0.08	9.37	0.00	0.01	0.13	0.35	100.0	Paste	0.63
13	68.02	19.00	3.41	0.17	8.81	0.00	0.01	0.04	0.55	100.0	Paste	0.71
14	64.02	20.43	7.46	0.11	6.78	0.00	0.00	0.16	1.04	100.0	Paste	0.90
15	69.41	15.60	5.72	0.21	6.40	0.00	0.32	0.00	2.34	100.0	Paste	0.66

Portland cement –- Dolomitic Lime Binders

Figure 36: Backscatter electron image (top), and X-ray microanalyses at the tips of callouts in Probes 1 through 15 detecting compositional variations of paste in Mortar #3.

Paste compositions are presented (bottom) as oxide variations of all detected peaks normalized to 100% except carbon (from epoxy) and gold (from coating).

Paste cementation indices, CI (after Eckel 1922) measure relative hydraulicity of paste e.g., non-hydraulic lime pastes have very low CI (< 0.50) compared to Portland cement pastes (CI is >1).

Paste (shown in blue rows) shows very high CIs from use of Portland cement as the main cementitious binder with minor lime component to reduce the overall CIs close to 1 which was not detected in optical microscopical examinations. Variable CI values of paste is due to variable degrees of carbonation which usually reduces the CI. Notice values are overall lower than the values seen in Mortar #1 indicating perhaps a higher proportion of lime than in Mortar #1 and/or higher degree of carbonation.

Some residual Portland cement particles in paste are marked with white dashed lines, which show subhedral alite, anhedral belite, and interstitial ferrite phases.

Notice magnesia contents in paste are significantly higher than that in the paste in Mortar #1 confirming use of a dolomitic lime binder at minor proportion with Portland cement.

SEM-EDS Analyses of Mortar #4

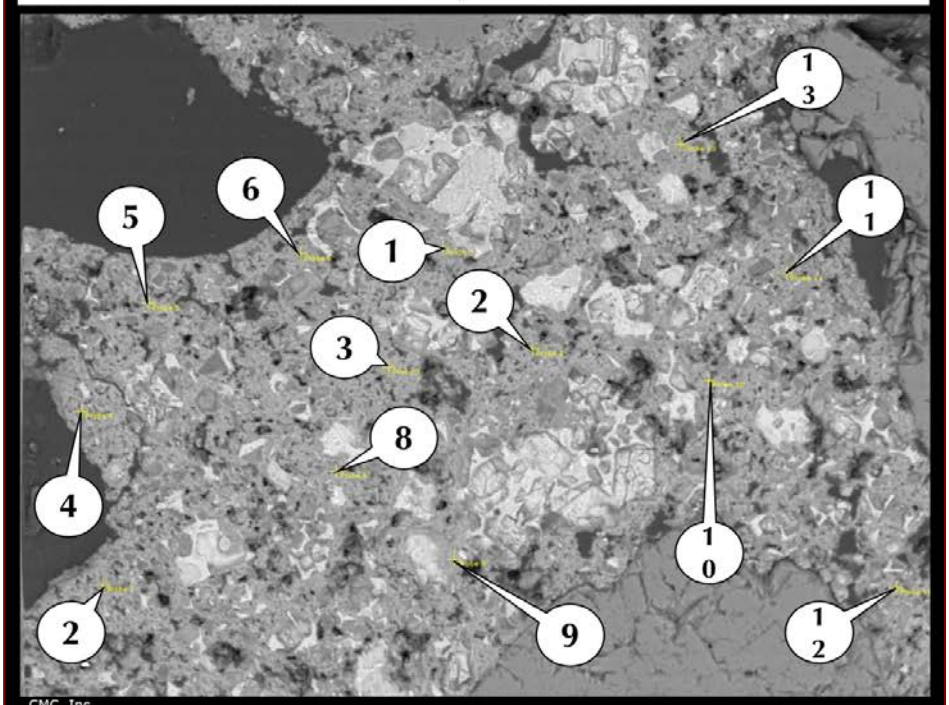

Probe	CaO	SiO2	Al2O3	Na2O	MgO	SO3	K2O	TiO2	FeO	Total	Phase	Paste CI
1	73.81	9.46	2.57	0.13	12.82	0.55	0.06	0.15	0.46	100.0	Paste	0.32
2	62.63	13.36	3.91	0.13	16.42	2.55	0.01	0.12	0.87	100.0	Paste	0.49
3	81.13	6.59	2.34	0.49	8.67	0.25	0.03	0.07	0.41	100.0	Paste	0.23
4	64.14	21.15	2.86	0.48	9.58	0.79	0.01	0.06	0.93	100.0	Paste	0.81
5	73.43	7.24	0.93	0.39	16.70	0.97	0.00	0.00	0.34	100.0	Paste	0.22
6	76.82	8.65	2.99	0.09	9.94	1.13	0.00	0.02	0.36	100.0	Paste	0.31
7	76.26	12.72	1.98	0.36	7.12	1.07	0.05	0.00	0.43	100.0	Paste	0.44
8	67.08	12.19	1.59	0.11	17.03	1.53	0.00	0.08	0.39	100.0	Paste	0.40
9	67.82	16.54	2.82	0.32	9.75	1.90	0.09	0.11	0.65	100.0	Paste	0.61
10	69.22	16.15	3.72	0.27	9.06	0.74	0.00	0.11	0.73	100.0	Paste	0.61
11	75.94	10.96	1.96	0.25	9.28	0.77	0.00	0.11	0.72	100.0	Paste	0.37
12	82.11	5.81	1.35	0.13	9.87	0.05	0.00	0.35	0.34	100.0	Paste	0.19
13	76.88	10.00	1.73	0.31	9.57	0.98	0.00	0.11	0.41	100.0	Paste	0.33

Portland cement –- Dolomitic Lime Binders

Figure 37: Backscatter electron image (top), and X-ray microanalyses at the tips of callouts in Probes 1 through 15 detecting compositional variations of paste in Mortar #4.

Paste compositions are presented (bottom) as oxide variations of all detected peaks normalized to 100% except carbon (from epoxy) and gold (from coating).

Paste cementation indices, CI (after Eckel 1922) measure relative hydraulicity of paste e.g., non-hydraulic lime pastes have very low CI (< 0.50) compared to Portland cement pastes (CI is >1).

Paste (shown in blue rows) shows very high CIs from use of Portland cement as the main cementitious binder with minor lime component to reduce the overall CIs close to 1, which was not detected in optical microscopical examinations. Variable CI values of paste is due to variable degrees of carbonation which usually reduces the CI. Notice values are overall lower than the values seen in Mortar #1 or even in 3 indicating perhaps a still higher proportion of lime than in Mortar #1 and 3 and/or higher degree of carbonation.

Some residual Portland cement particles in paste are marked with white dashed lines which shows subhedral alite, anhedral belite, and interstitial ferrite phases.

Notice magnesia contents in paste are significantly higher than that in the paste in Mortar #1 and similar to Mortar #3 confirming use of a dolomitic lime binder at minor proportion with Portland cement (though at higher amount than that added in Mortar #3).

	CaO	SiO_2	Al_2O_3	Na_2O	MgO	SO_3	K_2O	TiO_2	FeO	Sum	Paste CI
Mortar #1	68.47	23.80	4.51	0.30	0.81	1.40	0.13	0.39	0.19	100	1.03
	63.89	25.33	5.77	0.28	1.02	2.54	0.43	0.43	0.31	100	1.19
	54.46	34.63	6.19	0.26	1.14	2.34	0.35	0.27	0.37	100.01	1.86
	69.60	21.59	4.78	0.21	0.68	2.37	0.30	0.25	0.22	100	0.93
	60.00	30.84	4.80	0.46	1.24	1.96	0.21	0.42	0.06	99.99	1.48
	53.08	35.48	6.96	0.37	1.98	1.25	0.32	0.21	0.34	99.99	1.92
	62.13	31.17	3.89	0.47	1.35	0.36	0.12	0.27	0.24	100	1.43
	66.14	20.15	7.64	0.40	1.44	2.94	0.47	0.23	0.58	99.99	0.96
	66.04	19.67	9.49	0.43	0.91	2.70	0.34	0.15	0.28	100.01	0.98
	82.79	11.09	3.10	0.62	0.85	0.72	0.35	0.09	0.40	100.01	0.41
Mortar #3	60.17	17.85	6.58	0.03	14.55	0.00	0.01	0.15	0.67	100	0.72
	64.60	18.65	5.21	0.05	10.68	0.00	0.04	0.00	0.77	100	0.74
	74.57	13.29	2.90	0.00	8.84	0.00	0.02	0.00	0.38	100	0.47
	63.84	18.80	8.94	0.09	7.34	0.00	0.03	0.15	0.82	100	0.85
	66.83	19.47	4.21	0.01	8.06	0.00	0.06	0.27	1.09	100	0.77
	54.30	19.45	3.83	0.00	22.00	0.00	0.01	0.00	0.40	100	0.69
	70.01	10.69	1.50	0.00	17.54	0.00	0.01	0.00	0.25	100	0.34
	61.10	17.97	14.43	0.40	4.36	0.00	0.07	0.15	1.51	100	1.00
	45.27	32.41	17.96	0.21	3.67	0.00	0.00	0.00	0.48	100	2.20
	61.41	26.28	5.15	0.14	5.40	0.00	0.01	0.11	1.50	100	1.16
	56.14	19.70	4.51	0.00	19.22	0.00	0.00	0.06	0.37	100	0.73
	68.57	16.44	5.03	0.08	9.37	0.00	0.01	0.13	0.35	100	0.63
	68.02	19.00	3.41	0.17	8.81	0.00	0.01	0.04	0.55	100	0.71
	64.02	20.43	7.46	0.11	6.78	0.00	0.00	0.16	1.04	100	0.90
	69.41	15.60	5.72	0.21	6.40	0.00	0.32	0.00	2.34	100	0.66
Mortar #4	73.81	9.46	2.57	0.13	12.82	0.55	0.06	0.15	0.46	100	0.32
	62.63	13.36	3.91	0.13	16.42	2.55	0.01	0.12	0.87	100	0.49
	81.13	6.59	2.34	0.49	8.67	0.25	0.03	0.07	0.41	100	0.23
	64.14	21.15	2.86	0.48	9.58	0.79	0.01	0.06	0.93	100	0.81
	73.43	7.24	0.93	0.39	16.70	0.97	0.00	0.00	0.34	100	0.22
	76.82	8.65	2.99	0.09	9.94	1.13	0.00	0.02	0.36	100	0.31
	76.26	12.72	1.98	0.36	7.12	1.07	0.05	0.00	0.43	100	0.44
	67.08	12.19	1.59	0.11	17.03	1.53	0.00	0.08	0.39	100	0.40
	67.82	16.54	2.82	0.32	9.75	1.90	0.09	0.11	0.65	100	0.61
	69.22	16.15	3.72	0.27	9.06	0.74	0.00	0.11	0.73	100	0.61
	75.94	10.96	1.96	0.25	9.28	0.77	0.00	0.11	0.72	100	0.37
	82.11	5.81	1.35	0.13	9.87	0.05	0.00	0.35	0.34	100	0.19
	76.88	10.00	1.73	0.31	9.57	0.98	0.00	0.11	0.41	100	0.33

Figure 38: Oxide compositional variations of paste in three mortars determined from SEM-EDS studies. Paste compositions determine the type of binder used. Three mortars show some noticeable differences in compositions that are best depicted in the following two oxide variation diagrams plotted against paste-CIs depicting variations in lime, silica, magnesia, and iron oxide contents across the paste with corresponding CIs. Paste in Mortar #1 clearly shows noticeably lower magnesia and iron oxide contents than the values in other two mortars which indicates use of a dolomitic lime component in the binder in Mortars 3 and 4, which were not possible to detect from optical microscopy. The systematic compositional variations of lime and silica with paste-CIs are due to variations in proportions of lime added in minor amounts compared to Portland cement as well as variations in degree of carbonation of paste.

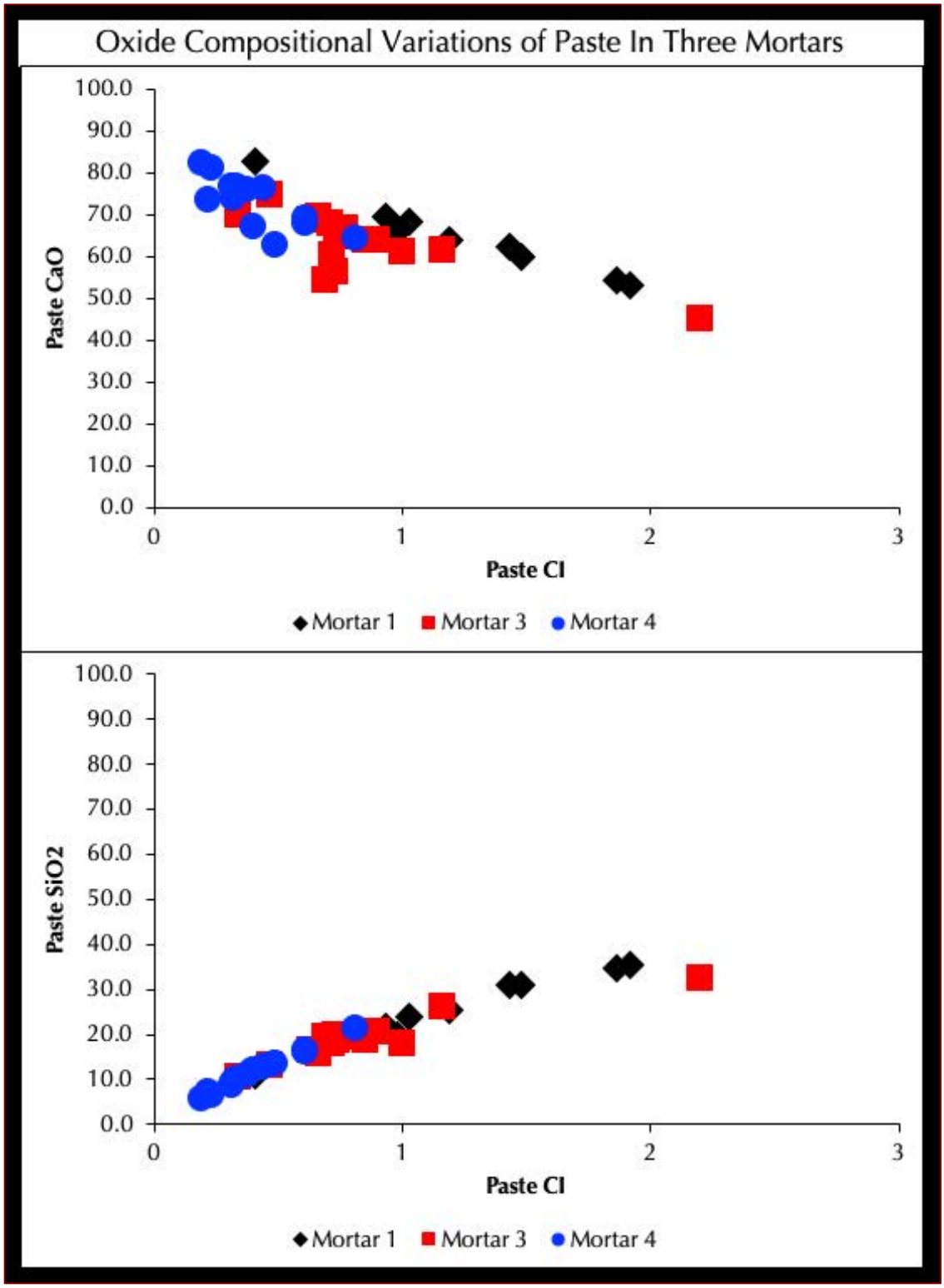

Figure 39: Systematic linear compositional variations of decreasing lime and increasing silica contents in all three mortars with increasing paste-CIs, which is a characteristic compositional variation of paste in various historic lime mortars of variable hydraulicities as well as modern cement-lime mortars of variable proportions of Portland cement and lime components. The present three mortars showed similar linear trends due to variations in lime proportions within and between the samples, which was added at minor (in Mortar #1) to subordinate (in Mortar #3 and 4) amounts compared to Portland cement. Mortar #1 has overall higher paste-CI values than the other two.

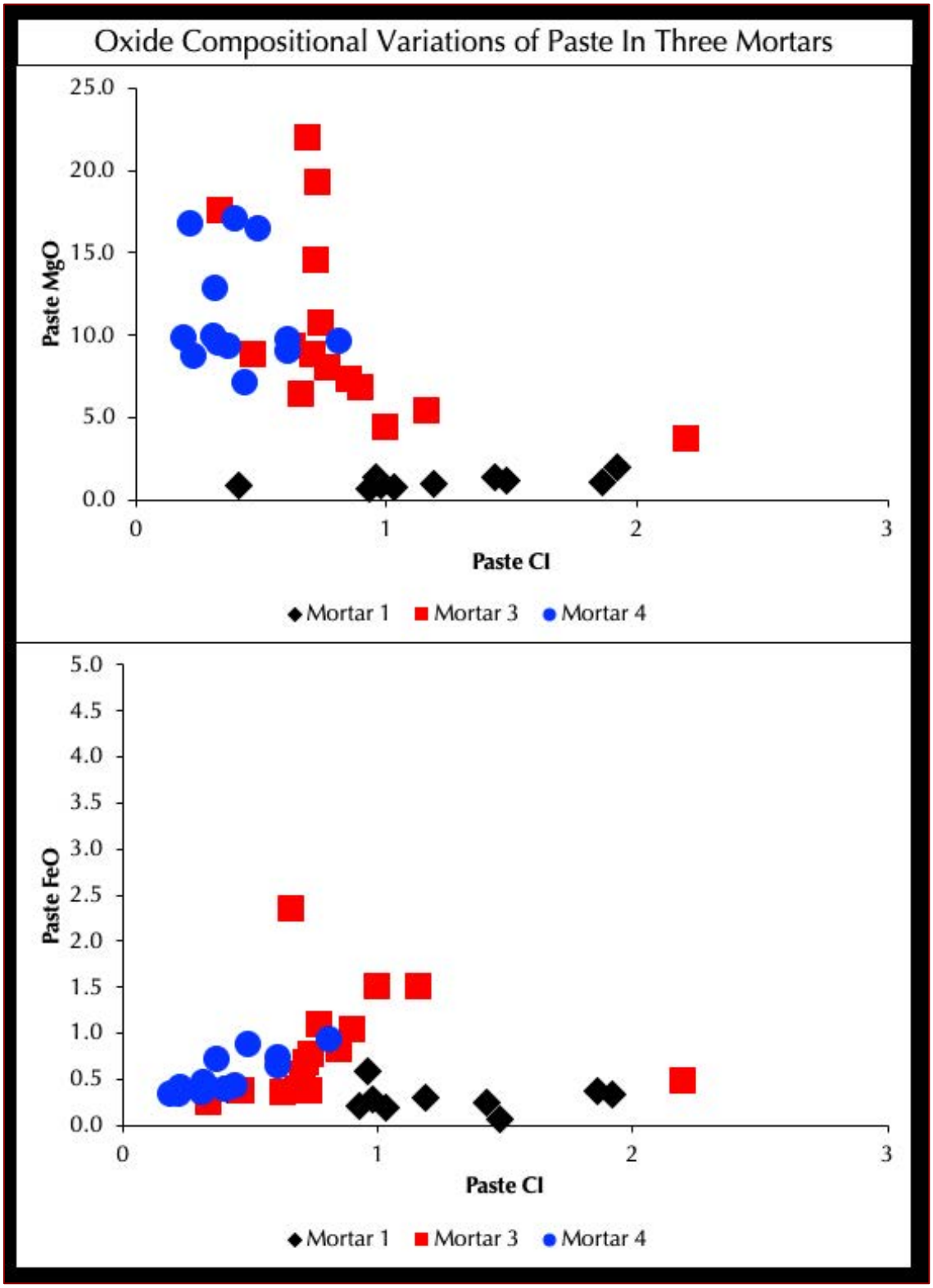

Figure 40: Oxide variation diagrams of magnesia and iron oxide contents in pastes of three mortars with paste-Cls. Both plots immediately separated paste in Mortar #1 which has very low MgO and FeO compared to noticeably higher magnesia and iron oxide found in the pastes in Mortar #3 and 4. This indicates addition of a dolomitic lime component in the binder which has introduced the excess magnesia and iron into the paste compared to the values in Mortar #1

Mineralogy of Mortar from XRD

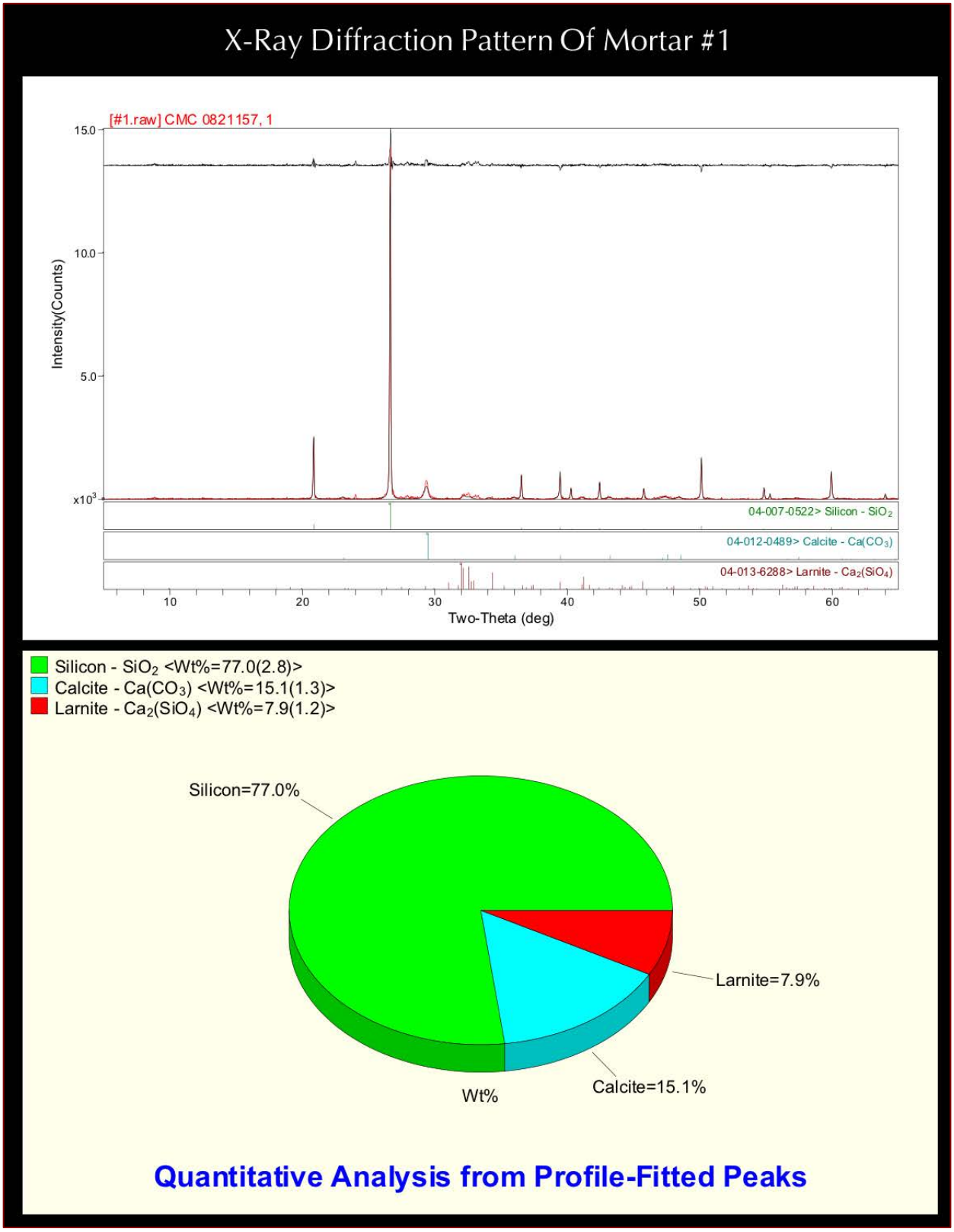

Figure 41: X-ray diffraction pattern of Mortar #1 showing the dominance of quartz from silica sand and subordinate calcite from carbonated cement paste.

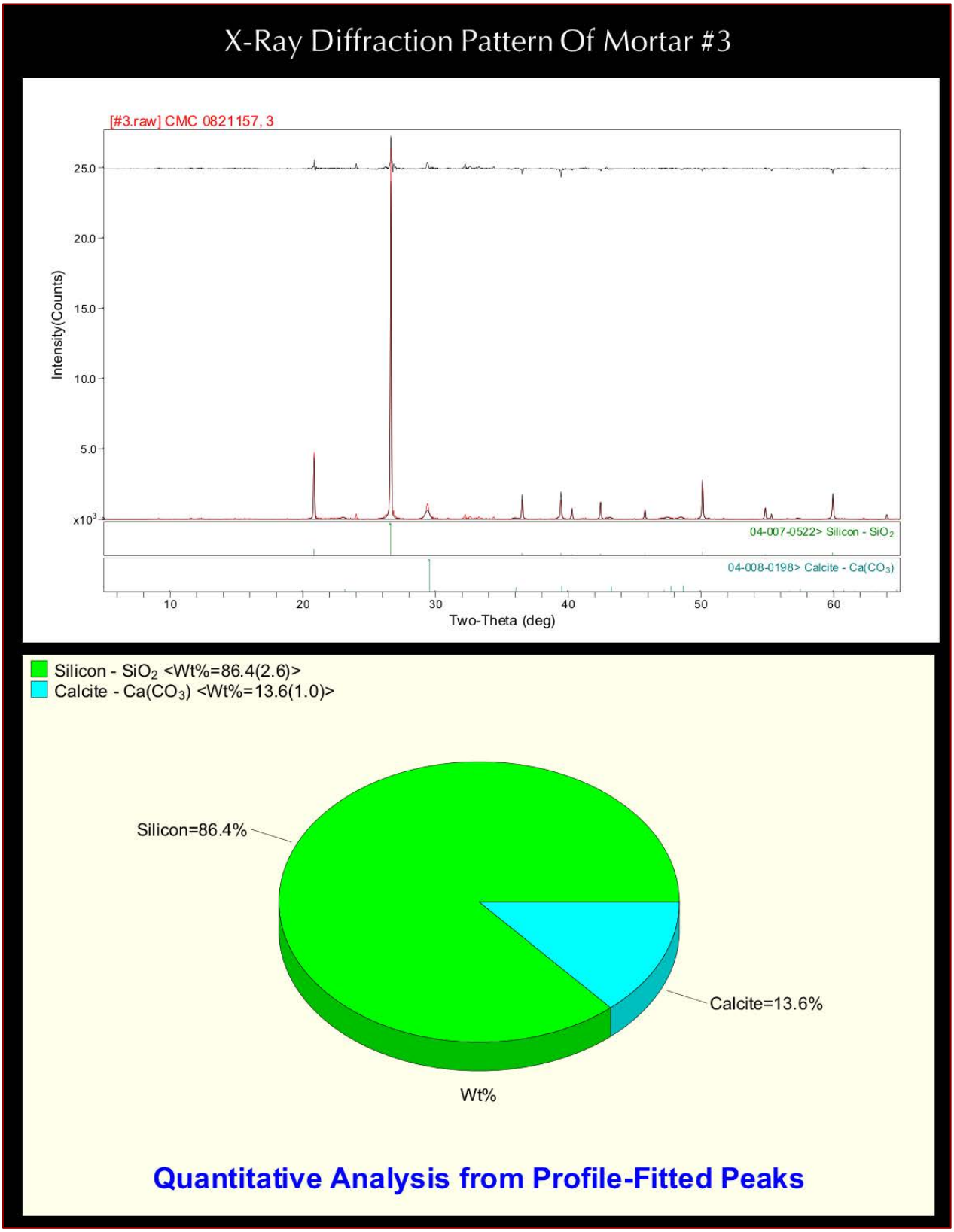

Figure 42: X-ray diffraction pattern of Mortar #3 showing the dominance of quartz from silica sand and subordinate calcite from carbonated cement paste.

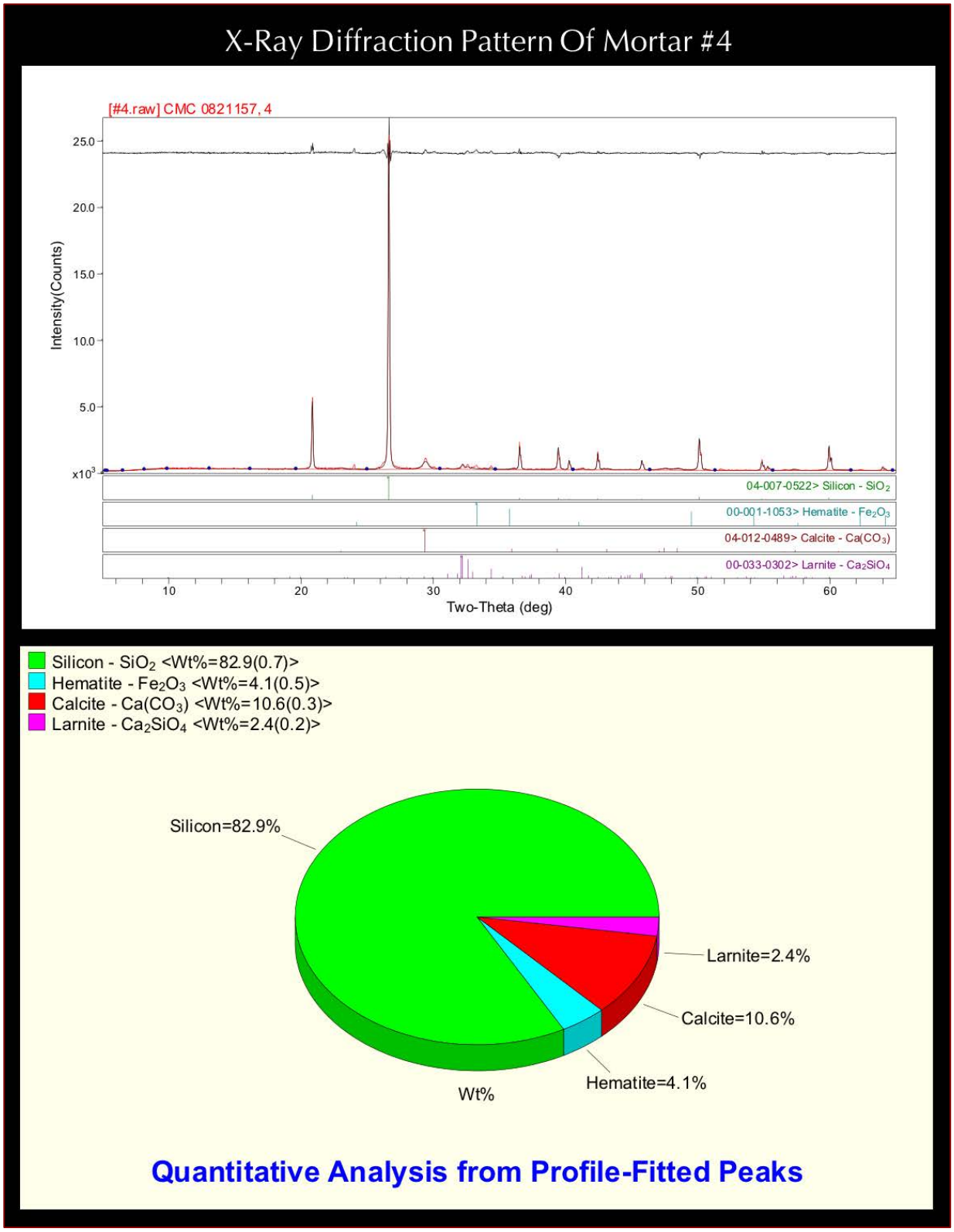

Figure 43: X-ray diffraction pattern of Mortar #4 showing the dominance of quartz from silica sand and subordinate calcite from carbonated cement paste and a minor hematite and larnite (later from residual Portland cement).

Compositions of Mortar from XRF (Major Element Oxides), Acid & Alkali Digestion (Soluble Silica), Loss on Ignition (Free Water, Combined Water, Carbonation), and Acid-Insoluble Residue Contents (Siliceous Sand Contents)

Table 1 shows oxide compositions of mortars determined from pressed pellet of pulverized (< 45 micron size) bulk mortars in XRF. Dominance of silica in mortars are a reflection of dominance of quartz in siliceous sand particles, whereas that of lime is from carbonated paste as also seen in optical microscopy and XRD analyses of the mortars.

Lime is contributed from carbonated cement paste for all mortars, and alumina, iron, and alkalis are contributed from both sand and paste. Balance includes volatiles (combined H_2O, CO_2) not measured in XRF. Higher magnesia in Mortars 3 and 4 compared to Mortar 1 in bulk samples are consistent with higher magnesia in the pastes of Mortars 3 and 4 compared to 1 as found in SEM-EDS studies.

Chemical Analyses (XRF & Gravimetric) of Mortars

Mortar Compositions	1	3	4	Methods
Silica - SiO_2	58.7	68.4	71.7	XRF
Alumina - Al_2O_3	4.19	2.29	1.82	XRF
Iron - Fe_2O_3	1.97	1.92	2.35	XRF
Lime - CaO	22.3	19.7	19.2	XRF
Magnesia - MgO	0.954	2.32	2.23	XRF
Sodium - Na_2O	0.999	ND	0.27	XRF
Potassium - K_2O	0.660	0.102	0.128	XRF
Titanium - TiO_2	0.288	0.088	0.496	XRF
Phosphorus - P_2O_5	0.095	0.0704	0.0940	XRF
Sulfate - SO_3	1.03	1.27	0.896	XRF
Balance (LOI)	8.85	3.78	0.844	XRF
Total	100	100	100	XRF
Soluble Silica in filtrates of Cold-HCl and Hot-NaOH digested mortar	6.64	5.21	4.94	Gravimetry + XRF
Acid-Insoluble Residue	59.41	66.67	66.64	Gravimetry
Loss on Ignition @ 110°C	2.10	1.90	0.90	Gravimetry
Loss on Ignition @ 550°C	4.80	3.80	2.40	Gravimetry
Loss on Ignition @ 950°C	6.80	7.90	6.70	Gravimetry

Table 1: Bulk oxide compositions and soluble silica contents of mortars from XRF, and acid-insoluble residue contents and losses on ignition from gravimetry.

Acid-insoluble residue contents are determined after digesting pulverized (<0.3 mm size) fragments of mortars in hydrochloric acid. Due to the presence of siliceous components in the sands (as determined from petrography), the determined acid-insoluble residue contents are considered representative of the siliceous sand contents of the mortars.

Losses on ignition of a separate aliquot of pulverized mortars to 110°C, 550°C, and 950°C correspond to free water, combined (hydrate) water, and degree of carbonation, respectively. The loss on ignition at 550°C corresponds to the water contents from dehydration of Portland cement paste. The loss on ignition at 950°C corresponds to degree of carbonation of carbonated paste.

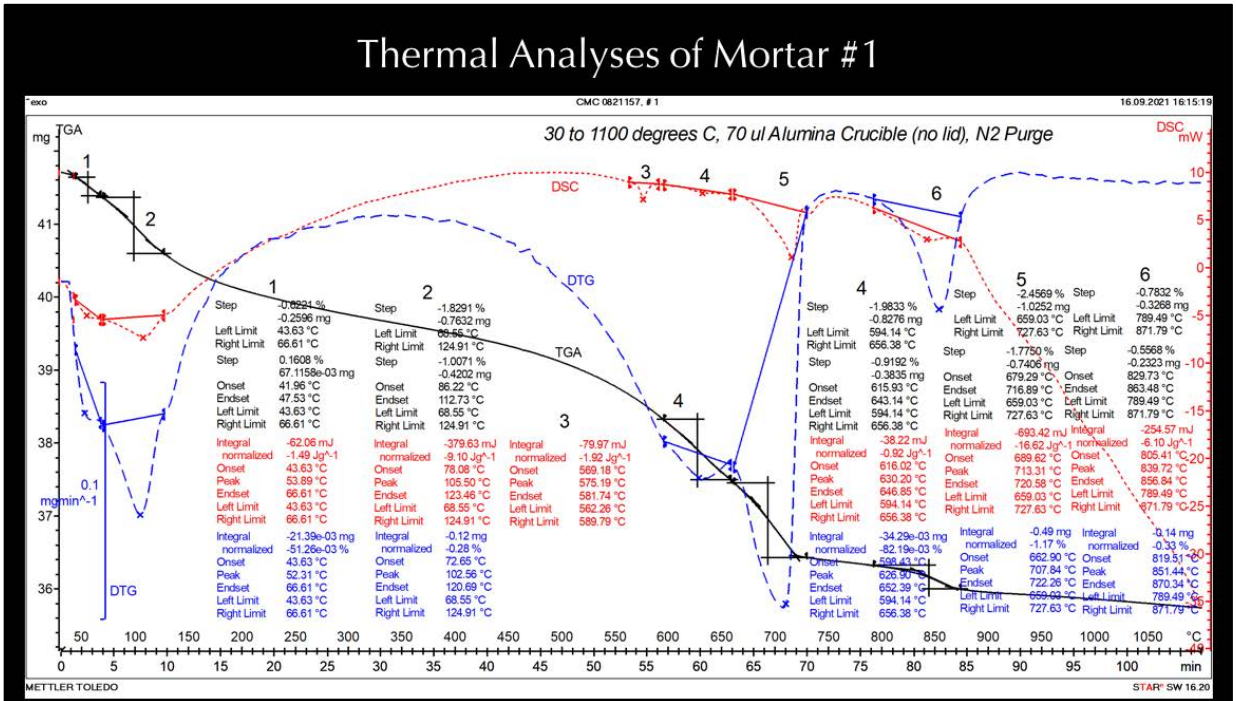

T(°C)	Up to 120°C	120°C to 200°C	200°C to 600°C	> 600°C
Phases	Hygroscopic Water	Water from Hydrated Salts	Structural Water From Hydraulic Components	CO_2 from decomposition of carbonates
Mass Loss From TGA	2.16	1.48	4.33	5.60
Mass Loss (%) From Gravimetry	2.10	-	4.80	6.80

Peaks#	Peak Position (°C)	Phase
1 (DTG)	43.6	Water
2 (DTG)	72.6	Water from Hydrated pøste
3 (DSC)	575.19	Quartz, 44.7%
4 (DTG)	626.9	Carbonated paste
5 (DTG)	707.84	Carbonated paste
6 (DTG)	851.44	Calcium silicate formation

Figure 44: TGA (in bold black), DSC (in dotted red), and DTG (in dashed blue) curves of Mortar #1 showing losses in weight due to decompositions (loss of water and carbon dioxide) of various phases during controlled heating in a Mettler-Toledo's simultaneous TGA/DSC 1 unit from 30ºC to 1100ºC in a ceramic crucible (alumina 70µl, no lid) at a heating rate of 10ºC/min in a nitrogen purge at a rate of 75 mL/min. Dehydration and decarbonation reactions are marked as endothermic peaks in the DTG curve, whereas alpha to beta-form polymorphic transition of quartz is marked at the characteristic temperature of 575ºC in the DSC curve. Similar results obtained from thermal analysis and gravimetry for mass losses from loss of free water (up to 120ºC), structural water (200 to 600ºC), and carbonation (600 to 950 ºC), respectively. Quantitative estimate of quartz is determined from the DSC results.

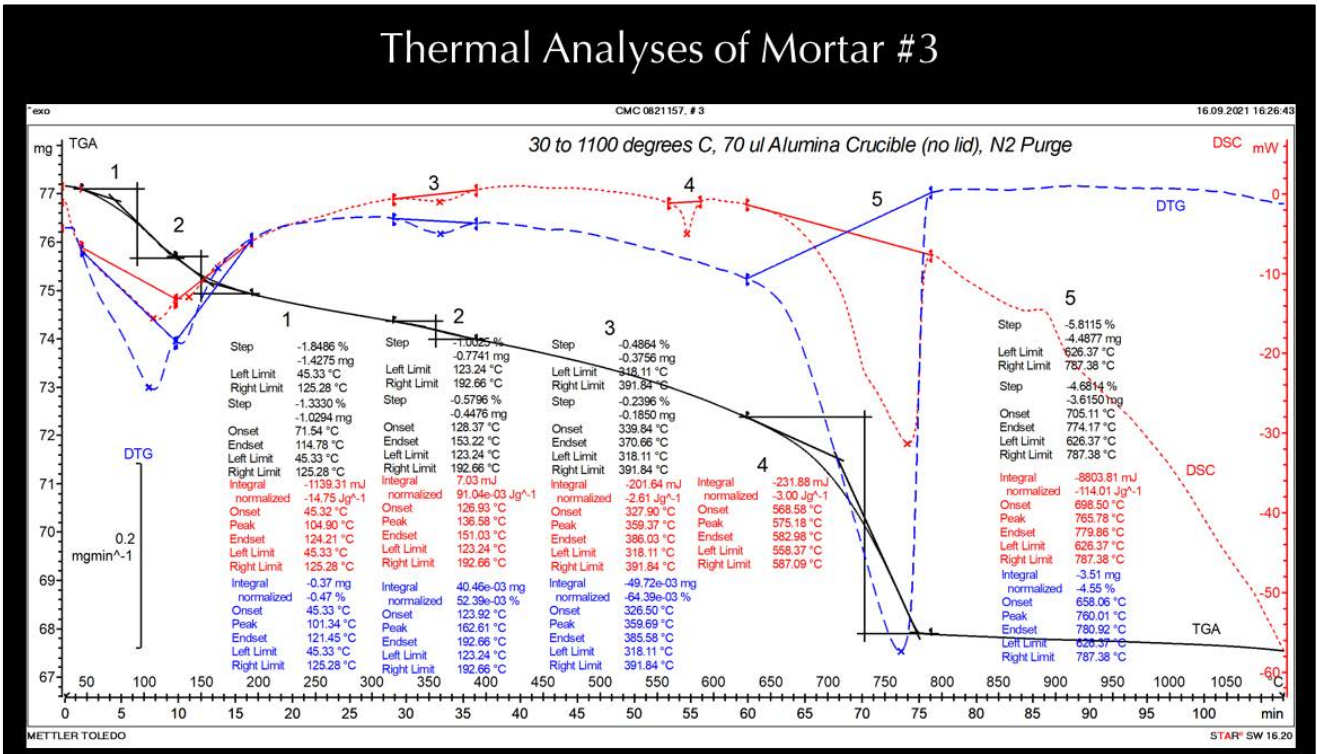

T(°C)	Up to 120°C	120°C to 200°C	200°C to 600°C	> 600°C
Phases	Hygroscopic Water	Water from Hydrated Salts	Structural Water From Hydraulic Components	CO_2 from decomposition of carbonates
Mass Loss From TGA	1.65	1.22	2.89	6.36
Mass Loss (%) From Gravimetry	1.90	-	3.80	7.90

Peaks#	Peak Position (°C)	Phase
1 (DTG)	101.3	Water from Hydrated pøste
2 (DTG)	162.6	Water from Hydrated pøste
3 (DTG)	326.5	Brucite, 0.48%
4 (DSC)	575.18	Quartz, 69.7%
5 (DTG)	760.0	Calcite

Figure 45: TGA (in bold black), DSC (in dotted red), and DTG (in dashed blue) curves of Mortar #3 showing losses in weight due to decompositions (loss of water and carbon dioxide) of various phases during controlled heating in a Mettler-Toledo's simultaneous TGA/DSC 1 unit from 30ºC to 1100ºC in a ceramic crucible (alumina 70µl, no lid) at a heating rate of 10ºC/min in a nitrogen purge at a rate of 75 mL/min. Dehydration and decarbonation reactions are marked as endothermic peaks in the DTG curve, whereas alpha to beta-form polymorphic transition of quartz is marked at the characteristic temperature of 575ºC in the DSC curve. Similar results obtained from thermal analysis and gravimetry for mass losses from loss of free water (up to 120ºC), structural water (200 to 600ºC), and carbonation (600 to 950 ºC), respectively. Quantitative estimate of quartz is determined from the DSC results.

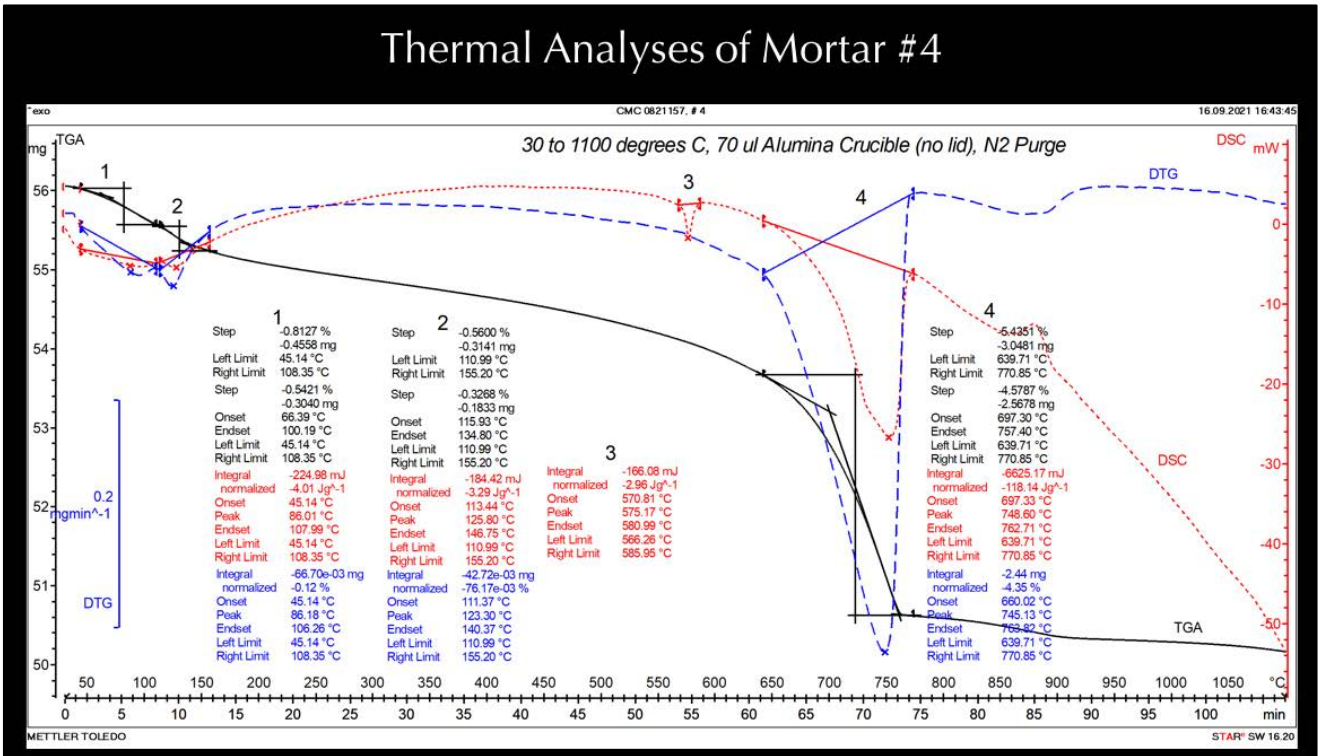

T(°C)	Up to 120°C	120°C to 200°C	200°C to 600°C	> 600°C
Phases	Hygroscopic Water	Water from Hydrated Salts	Structural Water From Hydraulic Components	CO_2 from decomposition of carbonates
Mass Loss From TGA	0.95	0.87	2.06	6.47
Mass Loss (%) From Gravimetry	0.90	-	2.40	6.70

Peaks#	Peak Position (°C)	Phase
1 (DTG)	86.20	Water
2 (DTG)	123.30	Water from Hydrated pøste
3 (DSC)	575.17	Quartz, 68.8%
5 (DTG)	745.13	Calcite

Figure 46: TGA (in bold black), DSC (in dotted red), and DTG (in dashed blue) curves of Mortar #4 showing losses in weight due to decompositions (loss of water and carbon dioxide) of various phases during controlled heating in a Mettler-Toledo's simultaneous TGA/DSC 1 unit from 30ºC to 1100ºC in a ceramic crucible (alumina 70µl, no lid) at a heating rate of 10ºC/min in a nitrogen purge at a rate of 75 mL/min. Dehydration and decarbonation reactions are marked as endothermic peaks in the DTG curve, whereas alpha to beta-form polymorphic transition of quartz is marked at the characteristic temperature of 575ºC in the DSC curve. Similar results obtained from thermal analysis and gravimetry for mass losses from loss of free water (up to 120ºC), structural water (200 to 600ºC), and carbonation (600 to 950 ºC), respectively. Quantitative estimate of quartz is determined from the DSC results.

Ion Chromatography of Water-Soluble Anions In Mortars

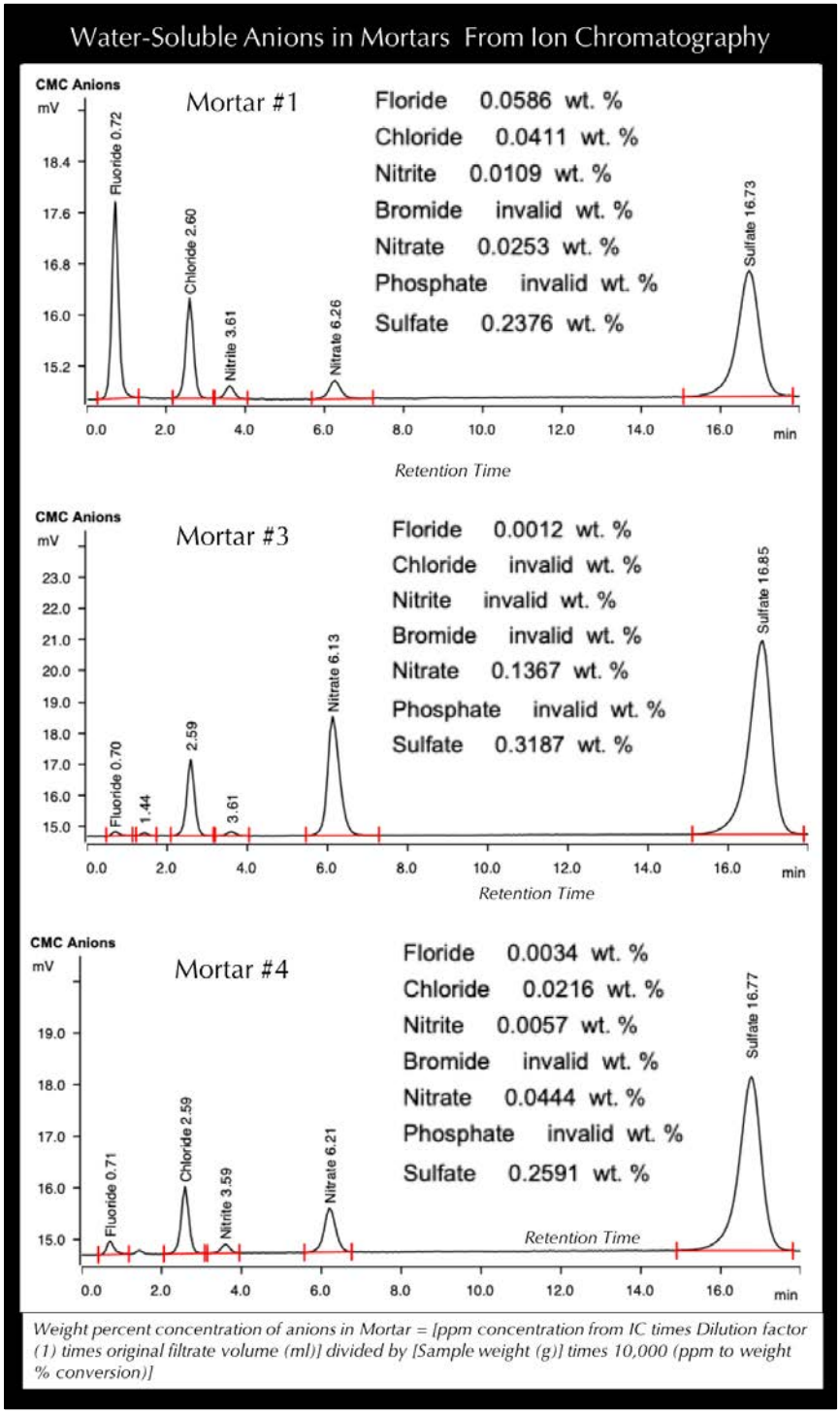

Figure 47: Ion chromatogram of water-soluble salt in mortars after digesting about a gram of pulverized mortar in deionized water for 30 minutes at a temperature below boiling, followed by continued digestion in water at the ambient laboratory condition for 24 hours. The filtrate was analyzed by ion chromatography. Results showed detectable chloride from the environment in Mortar 1 compared to Mortars 3 and 4, similar sulfate levels from the Portland cement binder, and negligible contents of other anions.

DISCUSSION

MORTAR TYPES, INGREDIENTS, AND CONDITIONS

Based on optical microscopy and SEM-EDS studies, all three mortars are determined to contain: (a) Portland cement as the major binder component, (b) variable proportions of dolomitic lime, which is mostly detected from high magnesia contents of pastes mainly in Mortars 3 and 4, and (c) siliceous sand. Overall hydraulicities of paste show higher values of cementation indices in Mortar #1 (mostly close to 1) compared to 3 (mean around 0.75), which, in turn has overall higher values than the paste in Mortar #4 (mean around 0.5) indicating a progressively higher proportion of cement in #4 to 3 to 1. Consistent with magnesian composition of paste in Mortars 3 and 4 detected in SEM-EDS studies, thermal analysis also detected brucite, but only in Mortar #3, thus confirming the dolomitic lime addition in Mortar #3. Sand showed variations in grain size, shape, angularity, and gradation to indicate their potentially different sources. Sand is noticeably finer in Mortar #1 with a fineness modulus of only 0.87 as opposed to fineness modulus of 2.09 and 2.02 in Mortars 3 and 4, respectively. Sand content is 59% in Mortar #1 compared to 66% sand detected from acid digestion in Mortars 3 and 4.

MIX CALCULATIONS OF MORTARS

Information obtained from: (a) chemical analyses to determine the soluble silica content, water contents, and insoluble residue content, and, (b) determination of use of Portland cement and progressively higher proportion of dolomitic lime from No. 1 to 3 to 4, but still at overall lower amount than Portland cement, as the binder components from microscopy, and chemical analyses are used to calculate the Portland cement, lime, and sand contents, and, eventually, the volumetric proportions of ingredients of mortars.

a. Since the sand is determined to be essentially a siliceous sand, the sand content is essentially determined from the hydrochloric acid-insoluble residue contents of mortars, which are 59.4% in Mortar 1, and 66.6% in Mortars 3 and 4.

b. Portland cement contents of 31.6%, 24.8%, and 23.5% are determined from the soluble silica contents of 6.64, 5.21, and 4.94 percent in Mortar #1, 3, and 4, respectively, assuming 21 percent soluble silica in Portland cement, and, soluble silica in mortar was contributed entirely from the Portland cement.

c. Dolomitic lime contents are determined from cement contents, assuming 63.5% lime in cement, subtracting the lime allotted to cement from the total lime content from XRF and multiplying the difference by a factor of 1.322 to be 3.04%, 5.23%, and 5.66% in Mortar #1, 3, and 4, respectively.

d. Volumetric proportions of cement to lime to sand are calculated from corresponding dry densities of 94, 40, and 80 lbs./ft^3, respectively. Volumetric proportions of cement-to-lime-to-sand are thus calculated to be, 0.336-0.076-0.742 for Mortar #1, 0.263-0.130-0.832 for Mortar #3, and 0.250-0.141-0.832 for Mortar #4.

e. Therefore, the volumetric proportions of Portland cement, lime, and silica sand are calculated to be about **1-0.22-2.20 (cement-lime-sand) for Mortar #1, 1-0.49-3.16 for Mortar #3 and 1-0.56-3.3 for Mortar #4, which are equivalent to ASTM C 270 Type M, S, and N cement-lime mortars, respectively.**

Components in Various Mortar Types	Mortar #1	Mortar #3	Mortar #4
Chemical Compositions			
Soluble Silica, SiO_2 (%) from Gravimetry	6.64	5.21	4.94
Calcium Oxide, CaO (%) from XRF	22.3	19.7	19.2
Acid-Insoluble Residue (%) from gravimetry	59.4	66.6	66.6
Assumed Compositions & Densities			
Cement – From Soluble Silica (SiO_2) (%) assuming 21% soluble silica in cement	31.6%	24.8%	23.5%
Lime – From cement content, and assuming 63.5% lime in Portland cement	3.04%	5.23%	5.66%
Bulk Density of Cement, (lbs./ft.^{3})	94	94	94
Bulk Density of Hydrated Lime, (lbs./ft.^{3})	40	40	40
Bulk Density of Sand, (lbs./ft.^{3})	80	80	80
Calculated Volumetric Proportions			
Cement-Lime-Sand	0.336-0.076-0.742	0.263-0.130-0.832	0.250-0.141-0.832
Volumetric Proportions	**1-0.22-2.20**	**1-0.49-3.16**	**1-0.56-3.3**

CONDITION

Use of Portland cement at proportions higher than that of lime has densified the microstructures of mortars at the expense of flexibility, and, as a result prevented any leaching or other effects that historic lime mortars usually undergo from prolonged exposure to a moist environment. Sands used in mortars are present in sound conditions without any deleterious reactions with the binder. Overall, despite the fragmented natures, the mortar samples are found to be present in overall sound conditions without any serious chemical or physical deterioration to interfere with long-term performance.

TUCK-POINTING MORTARS

Based on: (i) the determined binder compositions of mortars from optical microscopy; (ii) sand compositions from optical microscopy; (iii) XRF and gravimetric analyses of loss on ignition, and soluble silica contents; and (iv) XRD studies of mineralogical compositions, etc., the volumetric proportions of replacement mortars suitable for the mortars examined are judged to be ASTM C 270 Type S cement-lime mortar or Type N cement-lime mortar depending on the types of masonry units and exposure conditions. Appendix 2 discusses various common industry recommendations for tuckpointing mortars depending on the exposure conditions. Overall appearance of the final mortars would depend on a match on sand that constitutes the dominant proportion of the mortars.

Sands to be used should -

a. Be siliceous,

b. Match in color to the color of sand in the examined mortars,

c. Preferably be from similar sources,

d. Be free of any debris, unsound, clay particles, or any potentially deleterious constituents,

e. Conform to the size requirements of ASTM C 144 for masonry sand,

f. Not exceed maximum 3 times the sum of separate volumes of cement, and lime, and

g. Be durable.

As an alternate to the proposed ASTM C 270 Type N cement-lime, which is indeed a common repointing mortar used for many restoration work for original lime mortars, similar ASTM C 270 Type S or N masonry cement-sand mortar can also be tried depending on the host masonry unit and performance of the masonry wall.

REFERENCES

ASTM C 10, “Standard Specification for Natural Cement,” In Annual Book of ASTM Standards, Section Four Construction, Vol. 04.01 Cement; Lime; Gypsum; ASTM Committee C01 on Cement, 2017.

ASTM C 91, “Standard Specification for Masonry Cement,” In Annual Book of ASTM Standards, Section Four Construction, Vol. 04.01 Cement; Lime; Gypsum; ASTM Committee C01 on Cement, 2017.

ASTM C 144, “Standard Specification for Aggregate for Masonry Mortar,” In Annual Book of ASTM Standards, Section Four Construction, Vol. 04.05 Chemical-Resistant Nonmetallic Materials; Vitrified Clay Pipe; Concrete Pipe; Fiber-Reinforced Cement Products; Mortars or mortars and Grouts; Masonry; Precast Concrete; ASTM Committee C12 on Mortars or mortars for Unit Masonry, 2017.

ASTM C 1324, “Standard Test Method for Examination and Analysis of Hardened Masonry Mortar,” In Annual Book of ASTM Standards, Section Four Construction, Vol. 04.05 Chemical-Resistant Nonmetallic Materials; Vitrified Clay Pipe; Concrete Pipe; Fiber-Reinforced Cement Products; Mortars or mortars and Grouts; Masonry; Precast Concrete; ASTM Committee C12 on Mortars or mortars for Unit Masonry, 2017.

ASTM C 270, "Standard Specification for Mortar for Unit Masonry," In Annual Book of ASTM Standards, Section Four Construction, Vol. 04.05 Chemical-Resistant Nonmetallic Materials; Vitrified Clay Pipe; Concrete Pipe; Fiber-Reinforced Cement Products; Mortars or mortars and Grouts; Masonry; Precast Concrete; ASTM Committee C12 on Mortars or mortars and Grouts for Unit Masonry, 2017.

ASTM C 1713, "Standard Specification for Mortars or mortars for the Repair of Historic Masonry," In Annual Book of ASTM Standards, Section Four Construction, Vol. 04.05 Chemical-Resistant Nonmetallic Materials; Vitrified Clay Pipe; Concrete Pipe; Fiber-Reinforced Cement Products; Mortars or mortars and Grouts; Masonry; Precast Concrete; ASTM Committee C12 on Mortars or mortars and Grouts for Unit Masonry, 2017.

ASTM C 51, "Standard Terminology Relating to Lime and Limestone (as used by the Industry)'" In Annual Book of ASTM Standards, Section Four Construction, Vol. 04.01 Cement; Lime; Gypsum; ASTM Committee C07 on Lime, 2017.

ASTM C 856, "Standard Practice for Petrographic Examination of Hardened Concrete," In Annual Book of ASTM Standards, Section Four Construction, Vol. 04.02; ASTM Subcommittee C 9.65, 2017.

ASTM C 1723, "Standard Guide for Examination of Hardened Concrete Using Scanning Electron Microscopy," In Annual Book of ASTM Standards, Section Four Construction, Vol. 04.02; ASTM Subcommittee C 9.65, 2017.

ASTM C 1329, "Standard Specification for Mortar Cement," In Annual Book of ASTM Standards, Section Four Construction, Vol. 04.01; ASTM Subcommittee C01.11, 2016.

ASTM C 150, "Standard Specification for Portland Cement," In Annual Book of ASTM Standards, Section Four Construction, Vol. 04.01; ASTM Subcommittee C01.10, 2018.

ASTM C 1489, "Standard Specification for Lime Putty for Structural Purposes," In Annual Book of ASTM Standards, Section Four Construction, Vol. 04.01; ASTM Subcommittee C07.02, 2015.

ASTM C 207, "Standard Specification for Hydrated Lime for Masonry Purposes," In Annual Book of ASTM Standards, Section Four Construction, Vol. 04.01; ASTM Subcommittee C07.02, 2011.

Bartos, P. Groot, C., and Hughes, J.J. (eds.), "Historic Mortars or mortars: Characteristics and Tests", Proceedings PRO12, RILEM Publications, France, 2000.

Boynton, R., *Chemistry and Technology of Lime and Limestone, 2nd edition*, John Wiley & Sons, Inc. 1980.

Brosnan, Denis, A., Characterization of Rosendale Mortars or mortars For Fort Sumter National Monument and Degradation of Mortars or mortars by Sea Water and Frost Action, Final Report, April 19, 2012.

Callebaut, K., Elsen, J., Van Balen, K., and Viaene, W., "Nineteenth century hydraulic restoration mortars or mortars in the Saint Michael's Church (Leuven, Belgium) Natural hydraulic lime or cement?" Cement and Concrete Research, V 31, pp 397-403, 2001.

Callebaut, K., Elsen, J., Van Balen, K., and Viaene, W., Historical and scientific study of hydraulic mortars or mortars from the 19th century. In International RILEM workshop on historic mortars or mortars: Characterization and Tests; Paisley, Scotland, 12th to 14th May 1999, Edited by Barton, P., Groot, C., and Hughes, J.J., Cachan, France, RILEM Publications, 2000.

Charloa, A.E., "Mortar analysis: A comparison of European procedures." US/ICOMOS Scientific Journal: Historic Mortars or mortars & Acidic Deposition on Stone, 3 (1), pp. 2-5, 2001.

Charola, A.E., and Lazzarin, L., Deterioration of Brick Masonry Caused by Acid Rain, ACS Symposium Series, Vol. 318, pp. 250-258, 2009.

Chiari, G., Torraca, G., and Santarelli, M.L., "Recommendations for Systematic Instrumental Analysis of Ancient Mortars or mortars: The Italian Experience", *Standards for Preservation and Rehabilitation*, ASTM STP 1258, S.J. Kelley, ed., American Society for Testing and Materials, pp. 275-284, 1996.

Doebley, C.E., and Spitzer, D., "Guidelines and Standards for Testing Historic Mortars or mortars", *Standards for Preservation and Rehabilitation*, ASTM STP 1258, S.J. Kelley, ed., American Society for Testing and Materials, pp. 285-293, 1996.

Eckel, Edwin, C., *Cements, Limes, and Plasters*, John Wiley & Sons, Inc. 655pp, 1922.

Edison, M.P. (Editor), *Natural Cement*, ASTM STP 1494, American Society for Testing and Materials, 2008.

Elsen, J., "Microscopy of Historic Mortars or mortars – A Review", *Cement and Concrete Research 36*, 1416-1424, 2006.

Elsen, J., Mertens, G., and Van Balen, K., Raw materials used in ancient mortars or mortars from the Cathedral of Notre-Dame in Tournai (Belgium), Eur. J. Mineral., Vol. 23, pp. 871-882, 2011.

Elsen, J., Van Balen, K., and Mertens, G., Hydraulicity in Historic Lime Mortars or mortars: A Review, In, Valek, J, Hughes, J.J., and Groot, W.P. (Eds.), Historic Mortars or mortars Characterization, Assessment and Repair, RILEM Book series, Volume 7, pp. 125-139, Springer, 2012.

Erlin, B., and Hime, W.G., "Evaluating Mortar Deterioration", *APT Bulletin*, Vol. 19, No. 4, pp. 8-10+54, 1987.

Goins E.S., "Standard Practice for Determining the Components of Historic Cementitious Materials," National Center for Preservation Technology and Training, Materials Research Series, NCPTT 2004.

Goins, E.S., "A standard method for the characterization of historic cementitious materials." US/ICOMOS Scientific Journal: Historic Mortars or mortars & Acidic Deposition on Stone, # (1), pp. 6-7, 2001.

Groot, C., Ashall, G., and Hughes, J., Characterization of Old Mortars or mortars with Respect to their Repair, State-of-the-art Report of RILEM Technical Committee 167-COM, 2004.

Hughes, D.C., Jaglin, D., Kozlowski, R., Mayr, N., Mucha, D., and Weber, J., "Calcination of Marls to Produce Roman Cement", pp. 84-95, In, Edison, M.P. (Editor), *Natural Cement*, ASTM STP 1494, American Society for Testing and Materials, 2007.

Hughes, J.J., Cuthbert, S., and, Bartos, P., "Alteration Textures in Historic Scottish Lime Mortars or mortars and the Implications for Practical Mortar Analysis", *Proceedings of the 7th Euroseminar on Microscopy Applied to Building Materials*, Delft, pp. 417-426, 1999.

Hughes, R.E., and Bargh, B.L., The weathering of brick: Causes, Assessment and Measurement, A Report of the Joint Agreement between the U.S. Geological Survey and the Illinois State Geological Survey, 1982.

Jana, D., "Application of Petrography In Restoration of Historic Masonry Structures", In: Hughes, J.J., Lesie, A.B. and Walsh, J.A., eds. *Proceedings of 10th Euroseminar on Microscopy Applied to Building Materials*, Paisley, 2005.

Jana, D., "Sample Preparation Techniques in Petrographic Examinations of Construction Materials: A State-of-the-art Review", *Proceedings of the 28th Conference on Cement Microscopy*, International Cement Microcopy Association, Denver, Colorado, pp. 23-70, 2006.

Jedrzejewska, H., Old mortars or mortars in Poland: a new method of investigation, Studies in Conservation 5, pp. 132-138, 1960.

Leslie, A.B., and Hughes, J.J., "Binder Microstructure in Lime Mortars or mortars: Implications for the Interpretation of Analysis Results", *Quarterly Journal of Engineering Geology & Hydrogeology*, V. 35, No. 3, pp. 257-263, 2001.

Lubell, B., van Hees, Rob. P.J., and Groot, Casper J.W.P., The role of sea salts in the occurrence of different damage mechanisms and decay on brick masonry, Construction and Building Materials, Vol. 18, pp. 119-124, 2004.

Martinet, G., Quenee, B., Proposal for a useful methodology for the study of ancient mortars or mortars, Proceedings of the International RILEM workshop "Historic Mortars or mortars: Characteristics and tests," Paisley, pp. 81-91, 2000.

Mack, Robert, and Speweik, John P., *Preservation Briefs 2*, U.S. Department of the Interior, National Park Service Cultural Resources, Heritage Preservation Services, pp. 1-16, 1998.

Middendorf, B., Baronio, G., Callebaut, K, and Hughes, J.J., "Chemical-mineralogical and physical-mechanical investigation of old mortars or mortars, Proceedings of the International RILEM workshop "Historic Mortars or mortars: Characteristics and tests," Paisley, pp. 53-61, 2000.

Middendorf, B., Hughes, J.J., Callebaut, K., Baronio, G., and Papayanni, I., Mineralogical characterization of historic mortars or mortars, In. Groot, C., et al. (eds), Characterization of Old Mortars or mortars with Respect to their Repair, State-of-the-art Report of RILEM Technical Committee 167-COM, pp. 21-36, 2004a.

Middendorf, B., Hughes, J.J., Callebaut, K., Baronio, G., and Papayanni, I., Chemical characterization of historic mortars or mortars, In. Groot, C., et al. (eds), Characterization of Old Mortars or mortars with Respect to their Repair, State-of-the-art Report of RILEM Technical Committee 167-COM, pp. 37-53, 2004b.

Middendorf, B., Hughes, J.J., Callebaut, K., Baronio, G., and Papayanni, I., "Investigative Methods for the Characterization of Historic Mortars or mortars – Part 1: Mineralogical Characterization," *Materials and Structures*, Vol. 38, 2005a.

Middendorf, B., Hughes, J.J., Callebaut, K., Baronio, G., and Papayanni, I., "Investigative Methods for the Characterization of Historic Mortars or mortars – Part 2: Chemical Characterization," *Materials and Structures*, Vol. 38, pp 771-780, 2005b.

Sarkar, S.L., Aimin, Xu, and Jana, Dipayan, Scanning electron microscopy and X-ray microanalysis of Concretes, pp. 231-274, In, Ramachandran, V.S. and Beaudoin, J.J. Handbook of Analytical Techniques in Concrete Science and Technology, Noyes Publications, Park Ridge, New Jersey, 2000.

Speweik, J.P., *The History of Masonry Mortar in America 1720-1995*, 2010.

Stewart, J., and Moore, J., Chemical techniques of historic mortar analysis, Proceedings of the ICCROM Symposium "Mortars or mortars, Cements, and Grouts used in the Conservation of Historic Buildings," Rome, ICCROM, Rome, pp. 297-310, 1981.

Valek, J., Hughes, J.J., and Groot, C. (eds.), *Historic Mortars or mortars: Characterization, Assessment and Repair*, Springer, RILEM Book series Vol. 7, p. 464, 2012.

Valek, J., Hughes, J.J., and Groot, C. (eds.), Historic Mortars or mortars: Characterization, Assessment and Repair, Springer, RILEM Book series Vol. 7, 2012.

Van Balen, K., Toumbakari, E.E., Blanco, M.T., Aguilera, J., Puertas, F., Sabbioni, C., Zappia, G., Riontino, C., and Gobbi, G., "Procedures for mortar type identification: A proposal." In International RILEM workshop on historic mortars or mortars: Characteristics and Tests; Paisley, Scotland, 13- to 14- May 1999, edited by Barton, P., Groot, C., and Hughes, J.J., Cachan, France: RILEM Publications, 2000.

Vyskocilova, R., W. Schwarz, D. Mucha, D. Hughes, R. Kozlowski, and J. Weber, "Hydration processes in pastes of roman and American natural cements," *ASTM STP*, vol. 4, no. 2, 2007.

Weber, J., Gadermayr, N., Kozlowski, R., Mucha, D., Hughes, D., Jaglin, D., and Schwarz, W., Microstructure and mineral composition of Roman cements produced at defined calcination conditions, Materials Characterization, Vol. 58, pp. 1217-1228, 2007.

✪ ✪ ✪ END OF TEXT ✪ ✪ ✪

APPENDIX 1 –
LABORATORY TESTING OF MASONRY MORTARS

METHODOLOGIES[1]

Until 1970-1980, characterization of masonry mortars were mostly based on traditional wet chemical analysis (Jedrzejewska, 1960, Stewart and Moore, 1981), where interpretation of results were often difficult if not impossible without a good knowledge of the nature of different ingredients. The majority of later characterization proposed optical microscopy (Erlin and Hime 1987, Middendorf et al. 2000, Elsen 2006) as the first step in identification of different components of mortar based on which other analytical techniques including wet chemistry are performed. Many advanced instrumental analyses e.g., scanning electron microscopy and X-ray microanalysis, X-ray diffraction, X-ray fluorescence spectroscopy, atomic absorption, thermal analysis, infrared spectroscopy, etc. play significant roles in examinations of masonry mortars (Bartos et al. 2000, Elsen 2006, Callebaut et al. 2000, Erlin and Hime 1987, Goins 2001, 2004, Groot et al. 2004, Doebley and Spitzer 1996, Chiari et al. 1996, Middendorf et al. 2000, 2004, 2005, Leslie and Hughes 2001, Martinet and Quenee 2000, Valek et al., 2012, and Jana 2005, 2006). The choice of appropriate analytical technique depends mainly on the questions that have to be addressed, and, on the amount of material available.

Purposes of laboratory testing of mortar are: (a) to document a historic or modern masonry mortar by examining its sand and binder components, proportions of various ingredients, and their effects on properties and performance of the mortar, (b) evidence of any chemical or physical deterioration of mortar from unsoundness of its ingredients to effects of potentially deleterious agents from the environment (e.g., salts), (c) records of later repointing events and their beneficial or detrimental effects on the performance of the original mortar and masonry units, and finally, (d) an assessment of an appropriate restoration mortar to ensure compatibility with the existing mortar.

Currently there are two standardized procedures available that describe various laboratory techniques for analyses of masonry mortars with special emphases on historic mortars. One is ASTM C 1324 "Standard Test Method for Examination and Analysis of Hardened Masonry Mortar," which includes detailed petrographic examinations, followed by chemical analyses, along with various other analytical methods to test masonry mortars as described in various literatures, e.g., XRD, thermal analysis, and infrared spectroscopy. The second one is the RILEM method described in a series of publications from Middendorf et al. (2004, 2005).

The present mortar was tested by following these established methods of ASTM C 1324, and RILEM, which include detailed petrographic examinations, i.e., optical and scanning electron microscopy and X-ray microanalyses (SEM-EDS), followed by chemical analyses (gravimetry, acid digestion), X-ray fluorescence (XRF), X-ray diffraction (XRD), and thermal analyses (TGA, DTG, and DSC). Mortar sample was first photographed with a digital camera, scanned on a flatbed scanner, and examined in a low-power stereomicroscope for the preliminary examinations, e.g., to screen any unusual pieces having different appearances, e.g., representing contaminants from prior pointing episodes or remains of host masonry units.

Representative subset pieces of interest are then selected for: (a) optical microscopy and (b) scanning electron microscopy and X-ray microanalysis for chemical and mineralogical compositions, and microstructures of sand, paste, and overall mortar, (c) acid digestion, preferably from un-pulverized or lightly pulverized sample for extraction of siliceous sand by acid digestion for grain size distribution, (d) loss on ignition from ambient to 950°C temperatures for free and hydrate water, and carbonate contents, (e) acid digestion for determination of insoluble residue content, (f) cold acid and hot alkali digestions for determination of soluble silica content from hydraulic binder if any, after pulverizing a subset to finer than 0.3 mm size, and, (g) ultra-fine pulverization (<44-micron) of a subset for XRD, XRF, and thermal analysis. Any additional analyses, if needed, e.g., water digestion of mortar for determination of water-soluble salts by ion chromatography, or, Fourier-transform infrared spectroscopy of mortar for determining any coatings or organics added, etc. are done on the as-needed basis from the remaining set.

Information obtained from petrographic examinations is crucial to devise appropriate guidelines for subsequent chemical and other analytical methods, and, to properly interpret the results of chemical analyses. For example, detection of siliceous versus calcareous versus argillaceous components of aggregates in sample, or, the presence

[1] For details on laboratory facilities for testing of masonry mortar, visit www.cmc-concrete.com

of any pozzolan in the binder (slag, fly ash, ceramic dusts, etc.) from petrography restricts which chemical method to follow, and how to interpret the results of such analyses, e.g., acid-insoluble residue contents.

Therefore, a direct chemical analysis e.g., acid digestion of a mortar without doing a prior petrographic examination to determine the types of aggregates and binder used could lead to highly erroneous results and interpretation. Armed with petrographic and chemical data and based on assumed compositions and bulk densities of the sand and the binder(s) similar to the ones detected from petrographic examinations, volumetric proportions of sand and various binders present in the examined sample can be calculated. The estimated mix proportions from such calculations can provide only a rough guideline to use as a starting mix for mock-up mixes during formulation of a pointing mortar to match with the existing mortar.

Extraction of Siliceous Sand By Acid Digestion and Sieve Analysis

For mortars containing siliceous sand (e.g., containing quartz, quartzite, granite, sandstone, siltstone, feldspar, etc.), sand can be extracted by digesting a few representative as-received mortar fragments in (1+3) dilute hydrochloric acid to dissolve away all binder fractions and extract, wash, and dry the acid-insoluble component of mortar, which is mostly the siliceous component of sand. The mortar fragments are first gently broke down into small pieces in a porcelain mortar and pestle making sure not to reduce inherent grain-size of sand during this size-reduction process of bulk mortar. Subsequent smaller pieces are then placed in a 250-ml glass beaker completely immersed in dilute hydrochloric acid and stirred with a magnetic stirring rod over a stirrer for a period of at least 24 hours to several days depending on the binder type for complete digestion of binder fractions and settlement of siliceous sand at the bottom of beaker to be filtered out for sieve analysis.

Fig. A1: Gilson mini sieve shaker used for sieve analysis of sand extract from mortar after acid digestion.

Sand particles thus extracted are washed, oven-dried, and sieved in an automatic mini sieve shaker through various U.S. Sieves from No. 4 (4.75 mm) through 8 (2.36 mm), 16 (1.18 mm), 30 (0.6 mm), 50 (0.3 mm), 100 (0.15 mm), and 200 (0.075 mm) for determination of the size, shape, angularity, and color of sands retained on various sieves. Grain-size distribution of sand is then compared with ASTM C 144 specifications for masonry sand. Photomicrographs of sand retained on each sieve are then taken with a stereomicroscope to record the sand size, shape, and color variations. For low amount of sample, or, for sample having calcareous sand, image analysis (e.g., Image J) on stitched photomicrographs of thin sections taken from multiple areas can be done to determine the sand-size distribution (Elsen et al. 2011).

Optical Microscopy

The main purposes of optical microscopy of masonry mortar are characterization of:

a. Aggregates, e.g., type(s), chemical and mineralogical compositions, nominal maximum size, shape, angularity, grain-size distribution, soundness, alkali-aggregate reactivity, etc.;
b. Paste, e.g., compositions and microstructures to diagnose various type(s) of binder(s) used;
c. Air, e.g., presence or absence of air entrainment, air content, etc.;
d. Alterations, e.g., lime leaching, carbonation, staining, etc. due to interactions with the environmental agents during service, and effects of such alterations on properties and performance of mortar; and
e. Deteriorations, e.g., chemical and/or physical deteriorations during service, cracking from various mechanisms, salt attacks, possible reasons for the lack of bond if reported from the masonry unit, etc.

Fragments selected from preliminary examinations for microscopy are sectioned, polished, and thin-sectioned (down to 25-30 micron thickness) preferably after encapsulating and impregnating with a dyed-epoxy to improve the overall integrity of the sample during precision sectioning and grinding, and to highlight porous areas, voids, and cracks. Prepared sections are then examined in a high-power stereo-zoom microscope up to 100X magnifications having reflected and transmitted-light, and plane and crossed polarized-light facilities, and eventually in a high-power petrographic microscope (up to 600X magnifications) equipped with transmitted,

reflected, polarized, and fluorescent-light facilities. Capturing high-resolution micrographs from these microscopes via high-resolution high frame rate digital microscope cameras with appropriate image analyses software are an integral part of documentations during petrographic examinations.

Therefore, the essential steps followed during optical microscopy are:

a. Visual examination of as-received, fresh fractured, and sectioned surfaces of mortar on a flatbed scanner and in a stereo-microscope;
b. Preparation of clear epoxy-encapsulated block of mortar for subsequent sectioning and lapping for examinations of sand and binder in a stereo-microscope;
c. Preparation of a blue or fluorescent dye-mixed epoxy-impregnated large-area (50 × 75 mm) thin section of mortar of uniform thickness of 25-30 micron across the section;
d. Observation of thin section in a transmitted-light stereo-zoom microscope from 5X to 100X preferably with polarized-light facilities to observe large-scale distribution of sand and mortar microstructure in plane polarized light and sand type and carbonation of paste in crossed polarized light; and finally
e. Observation of thin section in a polarized-light (petrographic) microscope from 40X to 600X equipped with transmitted and reflected, polarized and fluorescent-light facilities for examinations of sand and binder compositions and microstructures.

For thin section preparation, representative fragments are oven-dried at 40 to 60°C to a constant mass and placed in a flexible (e.g., molded silicone) sample holder, then encapsulated with a colored dye-mixed (e.g., blue dye commonly used in sedimentary petrography, or, fluorescent dye, Elsen 2006) low-viscosity epoxy resin under vacuum to impregnate the capillary pore spaces of mortar, improve the overall integrity of sample during sectioning by the cured epoxy, highlight porous areas of mortar, alterations, cracks, voids, reaction products, etc. The epoxy-encapsulated cured solid block of sample is then de-molded, sectioned if needed, and processed through a series of coarse to fine grinding on metal and resin-bonded diamond grinding discs with water or a lubricant, eventually a perfectly flat clean ground surface is glued to a frosted large-area (50 × 75 mm) glass slide. Careful precision sectioning and precision grinding of the sample is then done in a thin-sectioning machine till the thickness is down to 50 to 60 micron. Final thinning down to 25 to 30 micron thickness is done on a glass plate with fine (5-15 micron) alumina abrasive. Thin section is eventually polished with various fine (1 micron to 0.25 micron size) diamond abrasives on polishing wheels suitable for examinations in a petrographic microscope, and eventually in SEM-EDS. Sample preparation steps are described in detail in Jana (2006).

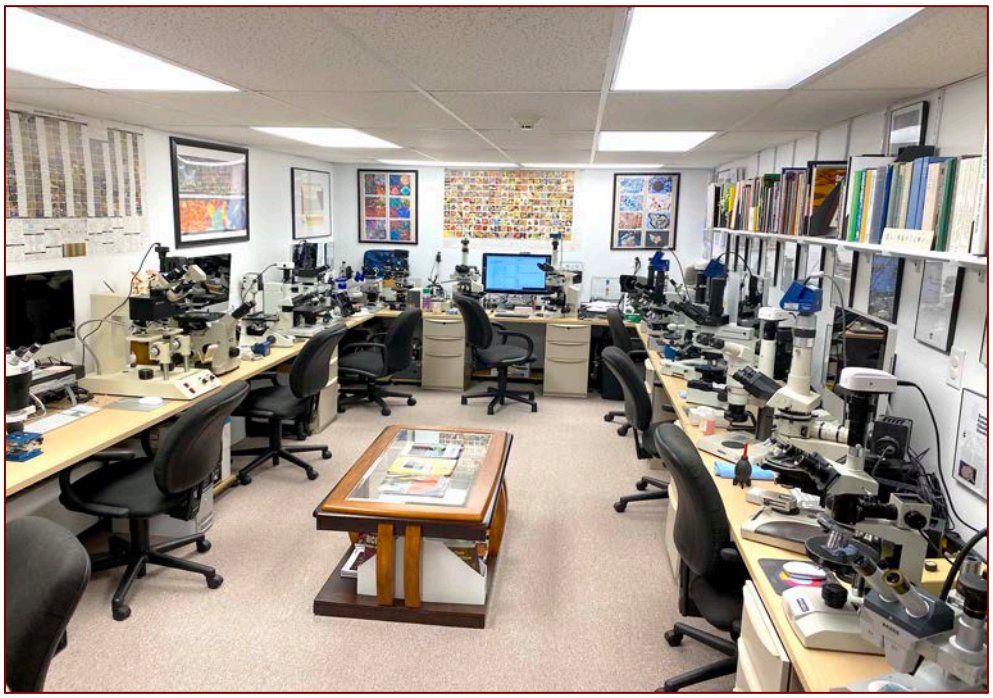

Fig. A2: CMC's optical microscopy laboratory that houses various stereomicroscopes and polarizing microscopes used for this study.

More elaborate steps followed during optical microscopy include:

a. Visual examinations of sample as-received to select fragments for detailed optical microscopy; initial digital and flatbed scanner photography of sample as-received;
b. Low-power stereo-microscopic examinations of saw-cut and freshly fractured sections of sample for evaluation of variations in color, grain-size and appearances of sand, and the nature of the paste;
c. Examinations of oil immersion mounts for special features and materials in a petrographic microscope;
d. Examinations of colored (blue or fluorescent) dye-mixed epoxy-impregnated polished thin sections in a transmitted-light stereo-zoom microscope for determination of size, shape, angularity, and distribution of sand, as well as abundance and distribution of void and pore spaces that are highlighted by the colored dye-mixed epoxy;
e. Image analyses of micrographs of thin sections for estimations of pores, voids, intergranular open spaces, and shrinkage microcracks by using Image J or other image analysis software, where multiple micrographs are collected in plane polarized light mode by using a high-resolution stereo-zoom microscope equipped with transmitted and polarizing light facilities and stitched to get an adequate representative coverage;
f. Examinations of colored (blue or fluorescent) dye-mixed epoxy-impregnated polished thin sections in a petrographic microscope for detailed compositional, mineralogical, textural, and microstructural analyses of aggregates and binders, along with diagnoses of evidence of any deleterious processes and alterations (e.g., lime leaching, precipitation of secondary deposits and alteration products, salts);
g. Examinations of polished thin or solid section in reflected-light (epi-illumination) mode of petrographic microscope after etching the surface with acids to identify various non-hydrated hydraulic phases (e.g., C_2S, C_3S, C_3A, etc., Middendorf et al., 2005);
h. Examinations of any physical or chemical deterioration or signs of improper construction practices from microstructural evidences;
i. Stereo-microscopical examinations of size, shape, and color variations of sand extracted after hydrochloric acid digestion; and finally,
j. Selection of areas of interest to be examined by scanning electron microscopy.

Scanning Electron Microscopy & Microanalysis by Energy-Dispersive X-ray Spectroscopy (SEM-EDS)

Methods followed during SEM-EDS studies include: (a) secondary electron imaging (SEI) to determine the microstructure and morphology of the examined surface of sample, (b) backscatter electron (BSE) imaging to determine compositions of various phases from various shades of darkness/grayness/brightness from average atomic numbers of phases from the darkest pore spaces to brightest iron minerals (e.g., thaumasite, periclase, ettringite, quartz, dolomite, monosulfate, gypsum, calcite, C-S-H, aluminate, calcium hydroxide, belite, alite, free lime, and ferrite having progressively increasing average atomic numbers and brightness in BSE image), (c) X-ray elemental mapping (dot mapping) of an area of interest to differentiate various phases, (d) point-mode or area (raster)-mode analysis of specific area/phase of interest on a polished thin or solid section, and (e) average compositional analysis of a specific phase or an area on a polished thin or solid section or small subset of a sample.

The main purposes of SEM-EDS examinations of masonry mortars are to:

a. Observe the morphologies and microstructures of various phases of sand and binder,
b. Characterize the typical fine-grained microstructure of hydrated, carbonated, and hydraulic components of binder that are too fine to be examined by optical microscopy and are not well crystallized to be detected by XRD;
c. Determine major element oxide compositions, and compositional variations of paste, and from that determine the type of binder(s) used, especially to differentiate non-hydraulic calcitic and dolomitic lime mortars from hydraulic lime varieties (e.g., from silica contents of paste), natural cements (e.g., from silica and magnesia contents), pozzolans, slag cements, Portland cements, etc. all from their characteristic differences in compositions and hydraulicities (e.g., cementation index of Eckel 1922);
d. Determine composition of residual hydraulic phases to assess the raw feed and calcination processes used in manufacturing of binder;
e. Assess hydration, carbonation, and alteration products of binders,
f. Investigate effects of various alterations of paste during service and its role on properties and performance of mortar,
g. Detect salts and other potentially deleterious constituents,

h. Detect pigments and fillers,
i. Examine compositional variations across multiple mortars installed, etc.; and eventually
j. Complement and confirm the results of optical microscopy.

Due to characteristic difference in compositions of pastes made using various binders, e.g., non-hydraulic lime (CaO dominates over all other oxides), variably hydraulic lime (CaO with variable SiO_2 contents depending on degree of hydraulicity), dolomitic lime (high CaO and MgO), natural cement (CaO, SiO_2, Al_2O_3, and MgO contents are high, high MgO and FeO contents are characteristic), and Portland cement (CaO and SiO_2 contents are higher than all other oxides), SEM-EDS analysis of paste is a powerful method for detection of the original binder components in the sample. Effects of chemical alterations and various chemical deteriorations of a mortar (e.g., lime leaching, secondary calcite precipitates, gypsum deposits, etc.) can also be detected by SEM-EDS.

SEM-EDS analysis is done in a CamScan Series 2 scanning electron microscope equipped with a high-resolution column 40Å tungsten, 40 kV electron optics zoom condenser 75° focusing lens operating at 20 kV, equipped with a variable geometry secondary electron detector, backscatter electron detector, EDS detector for observations of microstructures at high-resolution, compositional analysis, and quantitative determinations of major element oxides from various areas of interest, respectively. Revolution 4Pi software was used for digital storage of secondary electron and backscatter electron images, elemental mapping, and compositional analysis along a line, or on a point or an area of interest. Portion(s) of interest on the polished 50 mm × 75 mm size thin section used for optical microscopy were subsequently coated with carbon or gold-palladium film and placed on a custom-made aluminum sample holder to fit inside the large multiported chamber of CamScan SEM equipped with the eucentric 50 × 100 mm motorized stage. Usually, features of interest from optical microscopy are marked on the thin section with a fine-tipped conductive marker pen for further observations in SEM. Alternately, solid polished section or grain mount from phases or areas of interest can also be examined. Procedures for SEM examinations are described in ASTM C 1723 and Sarkar, Amin, and Jana (2000).

Fig. A3: Camscan SEM equipped with Ametek EDAX silicon drift detector for elemental analyses, secondary electron detector for morphological analyses and high-resolution YAG backscatter electron detector for microstructural analyses, and 4Pi revolution module for data collection and analyses.

Chemical Analysis (Gravimetry and Instrumental Analysis)

Following petrographic examinations, chemical analyses of the mortar are done to determine the:

a. Hydrochloric acid-insoluble residue content to determine the siliceous sand content;
b. Losses on ignition due to release of free water, hydrate water, and CO_2;
c. Soluble silica contents contributed from hydraulic binders; and,
d. Bulk oxide contents, e.g., lime, silica, alumina, magnesia, alkalis, and others.

Chemical analyses are done by using various methods outlined in ASTM C 1324 and Middendorf et al. 2005a, e.g., by wet chemistry (gravimetry) and various instrumental techniques, e.g., atomic absorption spectroscopy (AAS),

inductively-coupled plasma atomic emission spectroscopy (ICP-AES), and X-ray fluorescence spectroscopy (XRF). Steps followed during chemical analyses of mortars are summarized in Fig. A4.

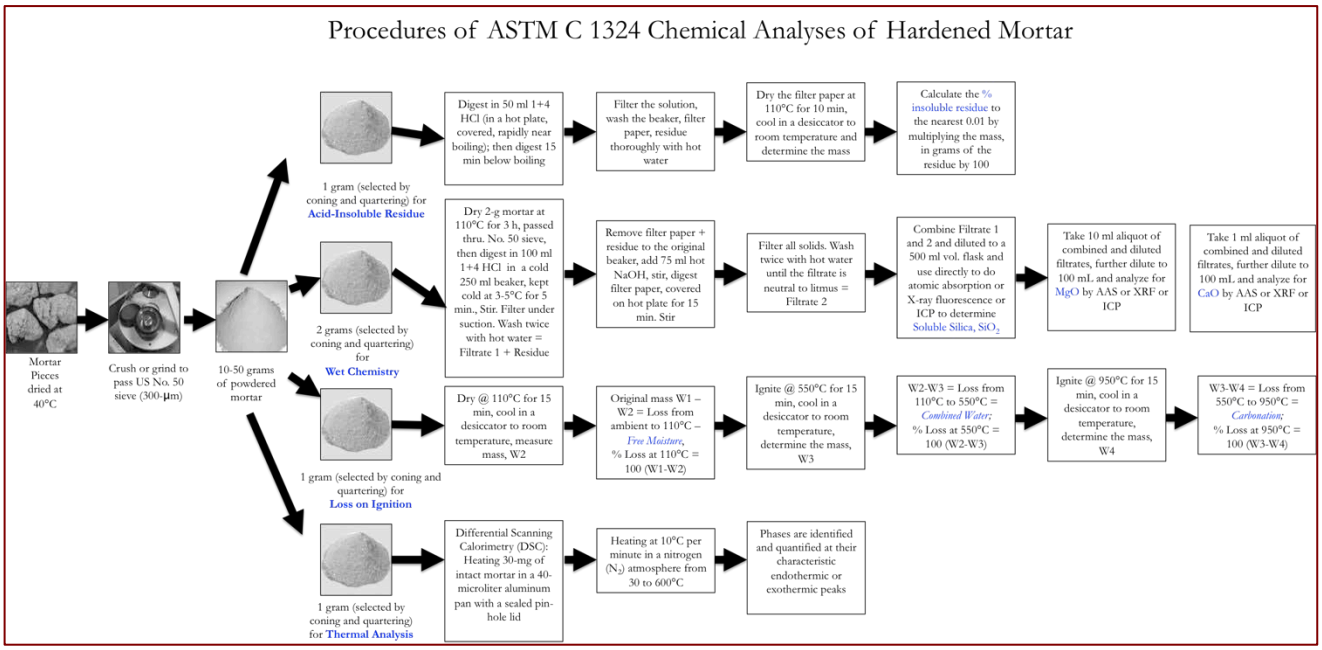

Fig. A4: Steps followed during various chemical analyses of mortars according to ASTM C 1324.

Acid Digestion

Acid digestion is perhaps the most commonly used test of masonry mortar, which is done to: (a) extract sand from sample by dissolving out the binder fractions so that grain-size distribution of sand can be done by sieve analysis, and (b) assess insoluble sand content in the sample. Sand content after acid digestion is determined both from: (a) 1.00 gram of pulverized sample (finer than 0.3 mm size) digested in 50-ml dilute (1+3) HCl (heated rapidly but below boiling), and, (b) from digesting a representative bulk sample *per se* (for harder mortars or mortars perhaps with light pulverization) in multiple fresh batches of (1+3) HCl at ambient temperature. The former usually gives better result due to small amount, pulverization to easily remove the binder fraction for digestion, and use of rapidly heated acid, whereas latter method requires multiple episodes of digestion in fresh acid and is time-consuming. Acid digestion is also done as the first step to determine soluble silica content in a sample as described below, which is contributed from the hydraulic components in binder.

All these goals of acid digestion depend on the assumptions that: (i) sand is siliceous in composition and does not contain any acid-soluble constituents (e.g., carbonates), and, (ii) binder entirely dissolves in acid and does not contain any acid-insoluble constituents (gypsum, clay, etc.). Applicability of acid digestion to assess these tasks should therefore be first verified by optical microscopy to confirm the siliceous nature of sand without any appreciable acid-soluble constituents, and calcareous nature of binder, and none without any appreciable argillaceous (clay) constituents.

For grain-size distribution of sand (for sample found from optical microscopy to contain siliceous sand), a few representative fragments of (preferably not pulverized or lightly pulverized in a porcelain mortar and pestle for harder mortars to break down to smaller size fraction without crushing the sand to retain the original sand size) are selected for digestion in multiple fresh batches of (1+3) dilute hydrochloric acid to dissolve away all binder fractions and extract, wash, and oven-dry the acid-insoluble component of aggregate. Usually multiple episodes of acid digestion in fresh batches of acid and filtration of residues are needed to entirely remove the binder fractions without losing the finer fractions of sand.

Soluble Silica From Cold Acid & Hot Alkali Digestion

Digestion of a pulverized sample of mortar in a cold acid followed by further digestion of residue in a hot alkali hydroxide solution are done to determine the soluble silica content contributed from the hydraulic component of binder, where cold acid digestion usually dissolves most of the binder without affecting the sand, followed by hot alkali hydroxide digestion to dissolve remaining soluble silica from calcium silicate hydrate component of paste or in mortars containing hydraulic binders. The soluble silica content corresponds to the silica mostly contributed from the hydraulic binder components (and a minor amount from any soluble silica component in the aggregates).

For determination of soluble silica content (modified from ASTM C 1324), 5.00 grams of pulverized sample (finer than 0.3 mm size, without excessive fines) is first digested in 100-mL cold (at 3 to 5°C) HCl and filtered through two 2.5-micron filter papers (filtrate #1). The residue with filter papers is then digested again in hot (below boiling) 75-ml NaOH, and filtered through two 2.5-micron filter papers (filtrate# 2). The two filtrates from acid and alkali digestions are then combined, re-filtered twice with 2.5-micron and then through 0.45-micron filter paper to remove any suspended silica fines, brought to 250 ml volume with deionized water, and then used for soluble silica determination by an analytical method, such as atomic absorption spectroscopy (AAS), inductive coupled plasma optical emission spectroscopy (ICP-OES), or X-ray fluorescence spectroscopy (XRF). Multiple steps of filtrations from 2.5-micron to submicron filter papers are necessary to remove any suspended silica from sand that can skew the result. Instrument to be used for such determination must be calibrated with several silica standards in matrices similar to the one used in mortar analysis. An XRF unit calibrated with filtrates from acid-and-alkali-digested series of laboratory-prepared standards of Portland cement and silica sand mortars (moist cured at *w/c* of 0.50 for 30 days) having various proportions of Portland cements (SiO_2 contents of standards ranging from 1 to 10%) were used for determining SiO_2 Kα X-ray intensities from known stoichiometric silica (cement) contents of standards (using exact 5.00 grams as samples) prepared by the same procedure of cold HCl-digestion/filtration/hot NaOH-digestion/2nd filtration/combination of two filtrates/re-filtration steps as followed for mortars.

Hydraulic binder content is calculated as: [(soluble SiO_2, weight percent in sample as calculated) divided by assumed soluble SiO_2 content in binder] ×100, where assumed SiO_2 contents of binders varies with binder types, e.g., 21% in Portland cement, 20% in natural cement, 27% in slag cement, 7 to 10% in hydraulic lime, etc., or, more preferably, from the average paste-SiO_2 content determined from SEM-EDS.

Weight Losses on Ignition

Losses in weight of a mortar on step-wise heating from ambient to 110°C, 550°C, and 950°C temperatures liberate free water from capillary pore spaces by 110°C, combined water from dehydroxylation of various hydrous phases (calcium silicate hydrate, calcium hydroxide, etc.) by 550°C, and liberation of carbon dioxide from decomposition of carbonated paste and carbonate minerals by 950°C. Such losses in weight are measured by following the procedures of ASTM C 1324 by heating 1.00 gram of pulverized mortar (finer than 0.3 mm) in an alumina crucible in a muffle furnace in a controlled step-wise heating at a heating rate of 10ºC/min. Mortars having hydraulic binders and hydration products of such provide measurable combined water contents after calcination to 550°C, whereas those having high calcareous components (high-calcium lime mortar or mortar having calcareous sand) produce higher weight losses during ignition to 950°C. Usually, a good correlation is found between weight losses at 550°C from dehydration of combined water, and, soluble silica contents contributed from hydraulic binders amongst series of mortars containing variable amounts of hydraulic phases.

X-ray Diffraction (XRD)

X-ray diffraction is a powerful laboratory technique used during investigation of masonry mortars, for reasons, such as:

a. Determination of bulk mineralogical composition of mortar, including its aggregate and binder mineralogies; e.g., quartz in sand from major diffraction peaks at 26.65º, 20.85º, 50.14º 2θ, or calcite in sand or carbonated lime binder

from major peaks at 29.41º, 39.40º, 43.15º 2θ, or Portlandite in binder from major peaks at 34.09º, 18.09º, 47.12º 2θ;

b. Individual mineralogy and alteration products of aggregate at various size fractions, and binder phases;
c. Detection of dolomitic lime binder from brucite in the mortar from major peaks at 38.02º, 18.59º, 50.86º 2θ;
d. Detection of lime (Portlandite), gypsum (11.59º, 20.72º, 29.11º 2θ), or cement binders;
e. Detection of any potentially deleterious constituents, e.g., deleterious salts, or efflorescence deposits;
f. Detection of a mineral oxide-based pigmenting component; and,
g. Detection of components, which are difficult to detect by microscopical methods.

X-ray diffraction can be done on: (i) pulverized (to finer than 45 micron size) portion of bulk sample, or (ii) on the sand extracted from mortar by acid digestion, if sand has complex mineralogy, or also (iii) on the binder-fraction by separating sand from the binder from a carefully ground sample (in a mortar and pestle) and passing the ground mass through US 200 sieve (75 micron) to collect the fraction rich in binder. XRD pattern of a sample containing silica sand typically shows quartz as the dominant phase that surpasses peaks for all other phases (e.g., calcite, dolomite, clay, secondary deposits); hence binder separation is sometimes useful to detect minor minerals of interest (e.g., salts or pigments). For mortars containing marine shell fragments as sand, aragonite appears with calcite as two calcium carbonate phases from the shell fragments and paste. For binder mineralogy, sample is first dried at 40°C to a constant mass, then carefully crushed without pulverizing the sand, and sieved through a 75-micron opening screen to retain sand-rich fraction on the sieve and obtain the finer binder-rich fraction for further pulverization down to finer than 45 micron. Salts and other soft components can be analyzed from binder fraction. Efflorescence salts on masonry walls are also analyzed routinely in XRD.

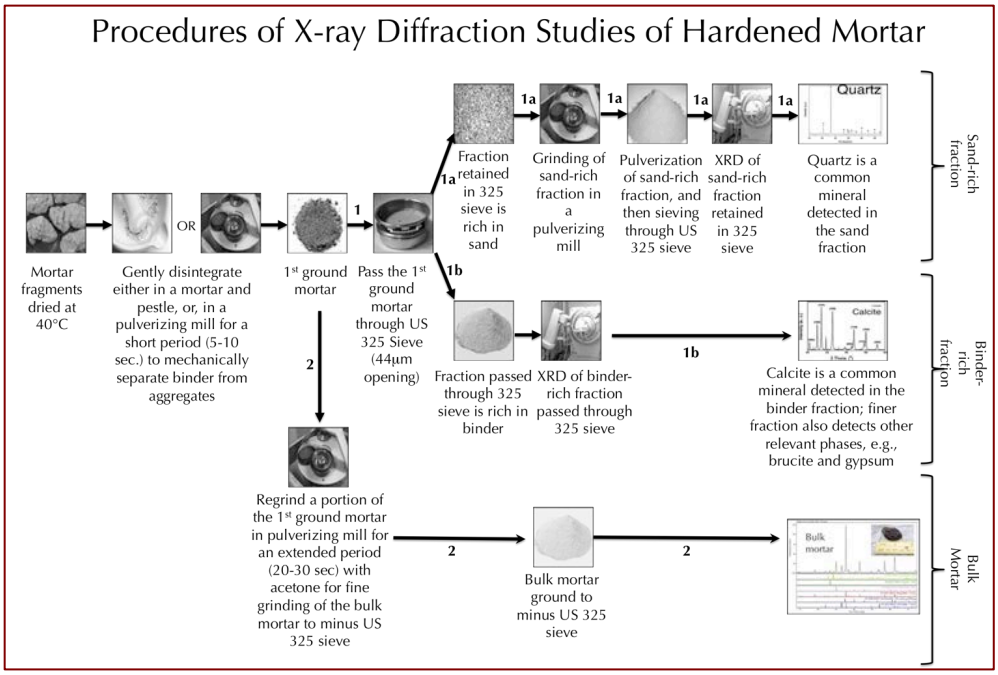

Fig. A5: Steps followed during XRD studies.

For sample preparation, a Rocklab (Sepor Mini-Thor Ring) pulverizer is used to grind sample down to finer than 100 microns. Usually, a few drops of anhydrous alcohol are added to reduce decomposition of hydrous phases from the heat generated from grinding. Approximately 10 grams of sample is ground first in the pulverizer, from which about 8.0 grams of sample is selected, mixed with an appropriate binder (e.g., three Herzog grinding aid pellets from Oxford Instruments having a total binder weight of 0.6 gram for 8 grams of sample for a fixed binder proportion of 7.5 percent); the mixture is then further ground in Rocklab pulverizer and in a McCrone micronizing mill with anhydrous alcohol down to finer than 44 micron size. Approximately 7.0 grams of binder-mixed pulverized sample thus prepared is weighed into an aluminum sample cup and inserted in a stainless steel die press to prepare the sample pellet. A 25-ton Spex X-press is used to prepare 32 mm diameter pellet from the pulverized sample. The pressed pellet is then placed in a custom-made circular sample holder for XRD and excited with the copper radiation of 1.54 angstroms. Sample holders made with quartz or silicon are best for working with very small quantities of sample because these holders create no diffraction peaks between 2° and 90° 2θ (Middendorf et al. 2005).

XRD is carried out either: (a) in a Bruker D2 Phaser benchtop powder diffractometer equipped with a Lynxeye 1D detector, a θ-θ goniometer, a Cu X-ray tube (Cu k-alpha radiation of 1.54 angstroms), a primary slit of 1 mm, a receiving slit of 3 mm, a position sensitive 1D Lynxeye XE-T detector, generator settings used are 30 kV and 10mA (300 watt, scanned at 2θ from 8° to 64° with a step of 0.05° 2θ integrated at 0.05 sec. step^{-1} dwell time, or, (b) in a floor-standing Siemens D5000 Powder diffractometer (θ-2θ goniometer) employing a long line focus Cu X-ray tube, divergent and anti-scatter slits fixed at 1 mm, a receiving slit (0.6 mm), diffracted and incident beam Soller slits (0.04 rad), a curved graphite diffracted beam monochromator, and a sealed proportional counter. Siemens D5000 is equipped with (a) a horizontal stage (fixed), (b) an X-ray generator with CuKα, fine focus sealed tube source, (c) large diameter goniometer (600 mm), low divergence collimator, and Soller slits, (d) fixed detector slits 0.05, 0.2, 0.6, 1.0, 2.0, and 6.0, and (e) Scintillation detector. Generator settings used are 40 kV and 30 mA. Tests are usually run at 2θ from 4° to 64° with a step scan of 0.02° and a dwell time of one second. The resulting diffraction patterns are collected by DataScan 4 software of Materials Data, Inc. (MDI) for Siemens D5000 or Bruker Diffrac.Suite software for D2 Phaser, and analyzed by Jade software of MDI with ICDD PDF-4 database of diffraction data for the Siemens D5000 unit, or Bruker Diffrac.Eva software with COD (Crystallographic Open Database) for the D2 Phaser. Phase identification, and quantitative analyses were carried out with MDI's Search/Match with Easy Quant, or Bruker's Diffrac.Eva, and both with Rietveld modules, respectively. A third-party Match! software is also used for transferring raw data from both equipment and processing for phase identification and Rietveld analyses using search/match with the inherent COD database.

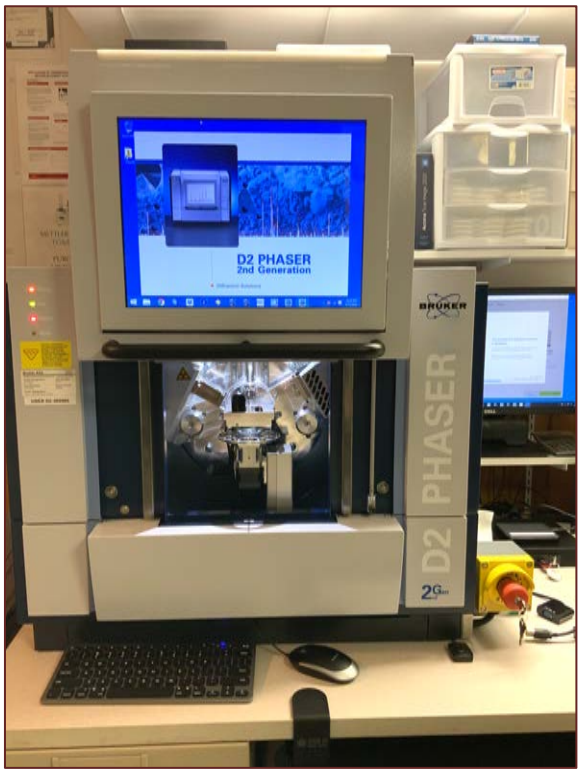

Fig. A6: Bruker D2 Phaser with automated six-sample stage.

Fig. A7: Siemens D5000 X-ray diffractometer and MDI Jade search/match software used for determination of mineralogical composition of mortar. Left to right: Rocklab pulverizer for initial grinding of sample with anhydrous alcohol; McCrone micronizing mill for final grinding; Spex 25-ton press for pellet preparation; Siemens D5000 X-ray diffractometer; and custom-made sample holder to place a 32-mm diameter pellet on sample stage.

X-ray Fluorescence (XRF)

X-ray fluorescence (XRF) is used for determining: (a) major element oxide composition of sample, and, (b) soluble silica content of filtrate after digestion of sample in cold-HCl and hot-NaOH. Major element oxide compositions provide clues about the siliceous sand content of mortar from silica content, type of binder used (e.g., a dolomitic lime or natural cement based binder gives a characteristically higher magnesia than a calcitic lime or Portland cement based binder), calculation of lime content in a cement-lime mortar from bulk CaO content from XRF, effect of alterations and deteriorations (e.g., salt ingress in a mortar from marine environment can be diagnosed from excessive sodium, sulfate, and chlorine, etc.), etc. A series of standards from Portland cements, lime, gypsum, to various rocks, and masonry cements of certified compositions (e.g., from USGS, GSA, NIST, CCRL, Brammer, or measured by ICP) are used to calibrate the instrument for various oxides, and empirical calculations are done from such calibrations to determine oxide compositions of mortars. For mortars with highly unusual compositions (e.g. severely salt-contaminated or a gypsum-based mortar) a standard-less FP calculation is done to determine the best possible composition.

Fig. A8: Rigaku NEX-CG in CMC, which can perform analyses of 9 pressed pellet or fused bead of sample. Samples are prepared either as pressed pellet (usually the one already prepared for XRD) or can also accommodate fused bead with proper calibration of standard beads

An energy-dispersive bench-top X-ray fluorescence unit from Rigaku Americas Corporation (NEX-CG) is used. Rigaku NEX-CG delivers rapid qualitative and quantitative determination of major and minor atomic elements in a wide variety of sample types with minimal standards. Unlike conventional EDXRF analyzers, the NEX-CG was engineered with a unique close-coupled Cartesian Geometry (CG) optical kernel that dramatically increases signal-to-noise. By using monochromatic secondary target excitation, instead of conventional direct excitation, sensitivity is further improved. The resulting dramatic reduction in background noise, and simultaneous increase in element peaks result in a spectrometer capable of routine trace element analysis even in difficult sample types. The instrument is calibrated by using various certified (CCRL, NIST, GSA, and Brammer) reference standards of cements and rocks. The same pressed pellet used for XRD for mineralogical compositions is used for XRF to determine the chemical composition.

Thermal Analyses (TGA, DTG, and DSC)

Thermal analyses encompasses: (1) thermogravimetric analysis (TGA), which measures the weight loss in a sample as it is heated, where weight loss can be related to specific physical decomposition of a phase of interest at a specific temperature that is characteristic of the phase from which both the phase composition and the abundance can be determined; (2) differential thermal analysis (DTA, or first derivative of TGA i.e. DTG) measuring temperature difference between the sample and an inert standard (Al_2O_3) both are heated at the same rate and time where endothermic peaks are recorded when the standard continues to increase in temperature during heating but the sample does not due to decompositions (e.g., dehydration of hydrous or decarbonation of carbonate phases); the endothermic or exothermic transitions are characteristic of particular phase, which can be identified and quantified using DTA (or DTG); and (3) differential scanning calorimetry (DSC), which follows the same basic principle as DTA, whereas temperature differences are measured in DTA, during heating using DSC energy is added to maintain the sample and the reference material (Al_2O_3) at the same temperature; this energy use is recorded and used as a

measure of the calorific value of the thermal transitions that the sample experiences; this is useful for detection of quartz that undergoes polymorphic (α to β form) transitions and no weight loss.

Thermal analyses are done to determine the presence and quantitative amounts of: (a) hydrates (e.g., combined water liberated from paste dehydration during decomposition of calcium-silicate-hydrate component in paste at 180-190ºC); (b) sulfates (gypsum from decompositions at 125ºC, and 185-200ºC, ettringite at 120-130ºC, thaumasite at 150ºC); (c) brucite from its dehydroxylation at 300-400ºC to confirm the presence of dolomitic lime; (d) hydrate water from decomposition of Portlandite component of paste at 400-600ºC; (e) quartz from polymorphic transformation (α to β form) at 573ºC; (f) cryptocrystalline calcite in the carbonated lime matrix from decomposition at 620-690ºC, or magnesite at 450-520ºC, or (g) coarsely crystalline calcite e.g., in limestone by decomposition at 680-800ºC or (h) dolomite at 740-800ºC and 925ºC, and (i) phase transition of belite (C_2S) at 693ºC, etc. Phases are determined from their characteristic decomposition temperatures occurring mostly as endothermic peaks or polymorphic transition temperatures as for quartz.

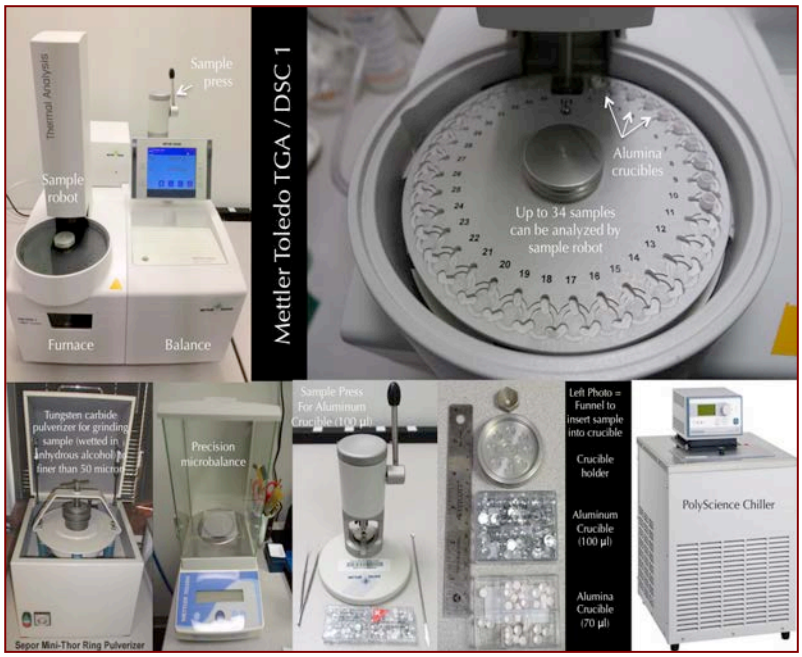

Fig. A9: Mettler-Toledo simultaneous TGA/DSC1 unit in CMC that can accommodate 32 samples. The top left photo shows the TGA/DSC1 unit with sample robot for automation as well as the sample holder for pressing aluminum sample holders. Sample is pulverized in a ring pulverizer shown in the bottom left, then a small amount (usually 30-70 mg) is weighed in a precision balance (shown 2nd from left in bottom row) and taken in an alumina sample holder (without lid). For DSC measurements up to 600°C, sometimes sample is taken in an aluminum holder and pressed in sample press (3rd from left in bottom row) and pierced with a needle for release of volatiles from decomposition. A PolyScience chiller (rightmost one in the bottom row) is used to cool the furnace. An ultrapure nitrogen gas is purged through the system during analyses.

a. 120-150°C = Ettringite decomposition from cement paste (thaumasite at 150ºC) and water release (endotherm);

b. 120, 180-200°C = Gypsum decomposition and water release (endotherm);

c. 100-200ºC = Hydrate water from decomposition of calcium silicate hydrate (CSH);

d. 300-400°C = Brucite decomposition from dolomitic lime mortar (or from soluble magnesium salts in the paste from the use of natural cement) and water release (endotherm);

e. 400-600°C = Portlandite decomposition from Portland cement paste and water release (endotherm);

f. 500-680°C = Magnesite decomposition for dolomitic lime mortar (endotherm);

g. 573°C = Alpha-to-beta polymorphic transformation of quartz the main component of silica sand in mortar;

h. 620-690°C = Calcite decomposition for cryptocrystalline calcite formed during carbonation of lime in mortar;

i. 680-800°C= Calcite decomposition for coarsely crystalline calcite in limestone or marine shells (endotherm);

j. 740-800ºC = Dolomite decomposition (endotherm);

k. >950°C = Slight exotherm from initial surface reaction of lime and silica, followed by larger endotherm from melting.

Simultaneous TGA and DSC analyses are done in a Mettler Toledo TGA/DSC 1 unit on 30-70 mg of finely ground (<0.6 mm) sample in alumina crucible (70 µl, no lid) from 30°C to 1000°C at a heating rate of 10°C/min with high purity nitrogen as purge gas at a flow rate of 75.0 ml/min. TGA/DSC 1 simultaneously measures heat flow in addition to weight change. The instrument offers high resolution (ultra-microgram resolution over the whole measurement range), efficient automation (with a reliable sample robot for high sample throughput), wide measurement range (measure small and large sample masses and volumes) broad temperature scale (analyze samples from ambient to 1100°C), superior ultra-micro balance, simultaneous DSC heat flow measurement (for simultaneous detection of thermal events, e.g., polymorphic alpha-to-beta transition of quartz and quartz content), and a gastight cell (ensures a properly defined measurement environment).

Fourier Transform Infra-red Spectroscopy (FT-IR)

Fourier-transform infrared spectroscopy (FT-IR) measures interaction between applied infrared radiation and the molecules in the compounds of interest (Middendorf et al. 2005). FT-IR is particularly useful for detection of admixture, additives, and polymer resins, mainly to identify various organic components (functional groups) in mortar (e.g., methyl CH_3, organic acids CO-OH, carbonates CO_3) from their characteristic spectral fingerprints in FT-IR spectrum. FT-IR can also be used for detection of main mineral phases in a hydraulic binder, CSH, carbonates, gypsum, and clays (Middendorf et al. 2005). Organic compounds such as synthetic (e.g., acrylics, polyesters) and natural resins, carbohydrates, colorants, oils and fats, proteins, waxes as well as inorganic compounds, e.g., corrosion products, minerals, pigments, paints, fillers, stone, glass, and ceramics can be detected by this technique.

Fig. A10: Perkin Elmer Spectrum 100 FT-IR unit with Universal ATR attachment for examinations of coatings on mortars.

FT-IR measurements are done in a Perkin Elmer Spectrum 100 FT-IR spectrophotometer running with Spectrum 10 software. Sample is measured using attenuated total reflection (ATR) on a single bounce diamond/ZnSe ATR crystal between a frequency range of 4000 to 650 cm^{-1}. Each run is collected at 4 cm^{-1} resolution with Strong Beer-Norton apodization. Data are collected with a temperature-stabilized deuterated triglycine sulfate (DTGS) detector by placing the sample in contact with the ATR crystal and by applying force from the pressure applicator supplied with the ATR accessory. The application of pressure enable the sample to be in intimate contact with the ATR crystal, ensuring achievement of a high-quality spectrum. Additionally, more conventional KBr pellet is also sometimes used for samples on as-needed basis.

Ion Chromatography

Salts can cause various deteriorations from: (a) mere aesthetic issues of surface efflorescence by precipitation from evaporation of leachates on the surfaces followed by atmospheric carbonation of the precipitates where salts deposit as individual crystals or as crust to (b) more serious internal distress in mortar from crystallization inside the pores (sub-fluorescence or crypto-fluorescence) from expansive forces associated with crystallization of salt from supersaturated solutions. Some common salts are calcium carbonates (e.g., calcite, vaterite), magnesium carbonate (magnesite), sodium carbonate hydrate and bicarbonate (thermonatrite, trona, nahcolite), sulphates (gypsum, thenardite, epsomite, melanterite, mirabilite, glauberite, or ettringite and thaumasite from oxidation of sulfides or cement hydrates), and chlorides (halite, sylvite, calcium

Fig. A11: Water-soluble anions in mortars are determined from Metrohm 861 ion Chromatography unit with attached 788 Sample Processor, or Metrohm 881 ion chromatography unit with attached 858 automated sample processor.

oxychloride from deicing salts, salt-bearing aggregates, ground water). X-ray diffraction and SEM-EDS can determine many of these salts as long as they are present in detectable amounts. Ion chromatography is an established technique used for analyses of various water-soluble anions and cations in salts (e.g., chloride, sulfate, and nitrate anions, and magnesium, calcium, alkali, ammonium cations) to assess magnitude of environmental impacts on masonry units and mortars, and subsequent effects of such salt ingress. Samples are pulverized, digested in deionized water to remove all water-soluble salts, then solid residues are filtered out and the water-digested filtrates are analyzed by an ion chromatograph.

Ion chromatography methods are described in ASTM D 4327 "Standard Test Method for Anions in Water by Chemically Suppressed Ion Chromatography." Briefly, an aliquot of 1 gram of pulverized sample (passing No. 50 sieve) is digested in 50 ml deionized water for 6 to 8 hours on a magnetic stirrer at a temperature below boiling point of water; then the digested sample is filtered through two 2.5-micron filter papers using vacuum, followed by a second filtration through micro-filter (0.45 micron) paper, then the filtrate is either used directly or diluted to 100 to 250 ml with deionized water depending on the concentration of anions, and used for analysis to get ppm-level fluoride, chloride, nitrite, bromide, nitrate, phosphate, and sulfate in the water-digested sample in Metrohm 861 Advanced Compact IC. The instrument is calibrated against ten different custom-made Metrohm anion standard solutions having all these anions from 10-ppm to 100-ppm levels. To check the accuracy of the instrument, a solution of know concentration is run first prior to the analyses of samples. Weight percent concentrations are obtained from (ppm-results times original filtrate volume times dilution factor) divided by sample weight.

Steps Followed During Laboratory Testing

Figure A12 shows the four main steps followed during laboratory investigation of masonry mortars, e.g.,

a. From preliminary visual examinations to petrographic examinations of mortars to determine the types of aggregates used and the binders present, based on which
b. Subsequent chemical analyses were done to determine the chemical compositions of binders and proportions of sand, water, and degree of carbonation. Information obtained from petrographic examinations is useful and form the very guidelines to devise the appropriate chemical methods to follow, and to properly interpret the results of chemical analyses.
c. For example, detection of siliceous versus calcareous versus argillaceous natures of aggregates in mortar, or the presence of any pozzolan in the binder (slag, fly ash, ceramic dusts, etc.) from petrography restricts which chemical method to follow, and how to interpret the results of such analyses, e.g., acid-insoluble residue contents.
d. Therefore, a direct chemical analysis e.g., acid digestion of a mortar without doing a prior petrographic examination to determine the types of aggregates and binder used could lead to highly erroneous results and interpretation.
e. Armed with petrographic and chemical data and based on assumed compositions and bulk densities of the sand and the binder(s) similar to the ones detected from petrographic examinations volumetric proportions of sand and various binders present in the examined mortar can be calculated.
f. The estimated mix proportions from such calculations can provide at least a rough guideline to use as a starting mix during formulation of mock-up tuck pointing mixes to match with the existing mortar.

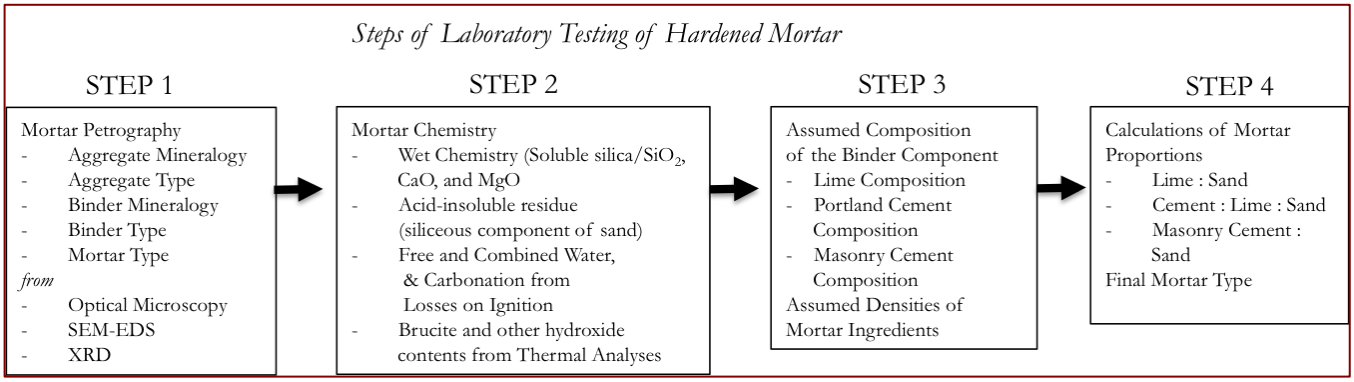

Fig. A12: Steps followed during laboratory investigation of mortar.

Laboratory Analyses of Masonry Mortars

Initial Mortar (50 to 100 grams) [Photographed with digital camera & flat-bed scanner, As-received condition, total weight, and dimensions of largest piece are documented]

Intact Pieces (20+ g)

1. *Optical Microscopy*

I. Perform visual examination of mortar as received, then saw-cut and fractured surfaces and with a low-power stereomicroscope,
II. Take digital and flat bed scanner photos of intact piece(s),
III. Encapsulate the piece for thin section microscopy in a flexible mold with a low-viscosity colored or fluorescent dye-mixed epoxy to highlight voids, pores, cracks, etc.,
IV. Prepare thin section (< 30 micron thickness) and polish the thin section for optical and SEM-EDS analyses,
V. Scan the thin section on a flat-bed scanner with the thin section residue,
VI. Take transmitted light high-power stereo-zoom photomicrographs of thin sections from different areas to be stitched to determine volumes and size distributions of pore spaces and sand grains by Image J,
VII. Take plane and crossed polarized-light photomicrographs of sand and binder fractions in thin section from a petrographic microscope and determine areas for further studies by SEM-EDS,
VIII. Do detailed petrographic examinations to determine the sand and binder compositions, sand mineralogy and texture, binder phases, residual binders, alterations, and products of any deleterious reactions, immersion mounts of specific areas of interest, etc.

2. *SEM-EDS*

I. Put conductive coating only on the portion of polished thin section intended for SEM-EDS studies from optical microscopy,
II. Take backscatter and/or secondary electron images, and if needed X-ray elemental maps,
III. Select multiple areas on paste to determine oxide compositions and Eckel's cementation indices,
IV. Tabulate the paste composition variations across the backscatter/secondary electron image.
V. Determine chemical compositions of resides left from the original components of the binders, as well as the hydration and carbonation and other alteration products

Lightly hand-ground in a Mortar & Pestle (30+ g)

3. *Acid Digestion - Sand Color & Sand Size Distribution* (10 g)

I. Take 10 g. of mortar lightly ground in mortar & pestle and digest in HCl (1+3) in a 250 ml beaker on a magnetic stirrer until all sand separates and settles at the bottom of beaker,
II. Filter all through two 2.5 micron filter paper, wash the beaker, filter paper, and all sand residue with dist. water,
III. Dry the residue at 110°C in an oven for 10 min., gently brush out from the filter paper and collect, then sieve the entire sand residue through No. 4 through 200 sieves in a mini sieve shaker (e.g., from Gilson),
IV. Determine the mass retained on each sieve, and on the pan (finer than No. 200 sieve),
V. Take photomicrographs of sand particles retained on each sieve for sand color variations in a stereomicroscope.

4. *Acid & Alkali Digestion – Soluble Silica for Hydraulic Binder* (5 g)

I. Grind 5-6 g of lightly ground fraction from mortar & pestle in a WC pulverizer for 30 sec.
II. Sieve thru. No. 50 sieve, collect the fraction passing the sieve,
III. Re-grind the residue retained on sieve for 15 sec. and mix thoroughly with the previous fraction;
IV. Use 5.000 g of thus prepared powder (passing No. 50 sieve) for digestion in 100 ml cold (3-5°C/38-41°F) HCl (1+4) in a 250 ml beaker for 15 min. on a magnetic stirrer,
V. Filter thru. two 2.5 micron filter paper and keep the filtrate# 1,
VI. Digest the residue with filter paper in 75 ml hot NaOH (below boiling) on hot plate for 15 min. on magnetic stirrer,
VII. Cool down to room temp. and filter thru. two 2.5 micron filter paper and collect filtrate# 2,
VIII. Combine these two filtrates, filter the combined filtrates thru. two 2.5 micron filter paper to remove any suspended silica (especially for sand-rich mortars, or if mortar is grounded too long); then dilute to 250 ml in a volumetric flask with dist. water, an aliquot (about 10 ml) is then used for XRF for soluble silica determination against the calibrations with standard PC mortars of known soluble silica contents prepared in the same way.

5. *Acid Digestion – Acid-Insoluble Residue Content for Siliceous Sand Content* (2 g)

I. Take 1-2 g of prepared mortar powder from Step 4 iii (passing No. 50 sieve) and digest in 50 ml HCl (1+3) in a 250 ml beaker (covered) on a hot pate rapidly near boiling, then 15 min. at a temp. below boiling, then cool down to room temperatures,
II. Filter thru. two pre-weighed 2.5 micron filter papers, washing the beaker, paper, and residue thoroughly with hot water,
III. Dry the filter paper at 110C for 10 min, cool in a desiccator to room temp. and measure the weight.
IV. Subtract from mass of dry filter paper to determine acid-insoluble residue content.

6. *Chemical Analysis – Loss On Ignition for Free and Combined Water Content, and Carbonate plus Carbonation* (2 g)

I. Take 1-2 g (W_1) of prepared mortar powder from Step 3 iii (passing No. 50 sieve) in a tarred porcelain crucible (keep a record of mass of the empty crucible),
II. Dry at 110°C for 15 min in a muffle furnace pre-set to 110°C, cool in a desiccator to room temp. and measure the mass (W_2) by subtracting the empty crucible mass from the total mass,
III. Ignite at 550°C for 15 min. in the muffle furnace pre-set to 550°C, cool in a desiccator to room temp. and measure the mass (W_3) by subtracting the empty crucible mass from the total mass,
IV. Ignite at 950°C for 15 min. in the muffle furnace pre-set to 950°C, cool in a desiccator to room temp. and measure the mass (W_4) by subtracting the empty crucible mass from the total mass,
V. Calculate the losses on ignition at 110°C, 550°C, and 950°C for free water, combined water, and carbonate plus degree of carbonation, respectively.

7. *Mineralogy of Bulk Mortar, Extracted Sand, Extracted Binder, or Salt from XRD* (at least 8 g)

I. Weigh 8.00 g of mortar (or extracted sand or binder as needed) lightly ground in a mortar & pestle, add three grinding/pelletizing aid tablets (e.g., from Oxford Instruments) and pulverize in a suitable mill to minimize contamination (e.g., Rocklab pulverizer with WC bowl or McCrone Micronizing Mill with agate) for 3 min. with anhydrous alcohol to get <45 micron size particles passing U.S. No. 325 sieve,
II. Take 6.8 to 7.0 g. of ground <45 micron prepared mass in an aluminum sample holder inside a stainless steel die to prepare a 32 mm pellet with 25 ton pressure for 1 min,
III. Use the prepared pellet for XRD and then use the same pellet for XRF.
IV. Do XRD on the binder-rich fraction, or salt either on a shallow-depth sample holder or preferably on a zero background quartz plate for small volume of sample.

8. *Bulk Mortar's Composition from X-Ray Fluorescence (XRF)* (same pellet used in XRD)

I. Use the same pellet prepared for XRD in the XRF, or, use a fused bead if sample volume is low to prepare a pellet. In either method, have calibrations of measured oxides with adequate standard.
II. XRF can also be used with proper calibrations for soluble silica determination on the filtrates after acid and alkali digestions, as described in Section 4.

9. *Thermal Analyses* (0.1 g), TGA, DTG, DSC, DTA, for quantitative analysis of various hydrous, sulfate, and carbonate phases in mortar, content of dolomitic lime added from the brucite content in mortar as determined from TGA or DSC, etc.

I. Simultaneous TGA and DSC analyses can be done on 30-70 mg of finely ground (<0.6 mm) mortar in alumina crucible (70 µl, no lid) from 30°C to 1000°C at a heating rate of 10°C/min with high purity nitrogen as purge gas at a flow rate of 75.0 ml/min .

10. *Infrared Spectroscopy,* for determination of various organic additives, paint, and clays in mortar

I. Take an aliquot of powder prepared for thermal analysis, or peel a paint and use that in Universal ATR of FTIR.
II. Alternately, digest a pulverized mortar in acetone to extract the organic additive and analyze the liquid in FTIR for characteristic functional groups.

11. *Ion Chromatography of Water-Soluble Salts* (1 g)

I. Take an aliquot of 1.00 gram powder prepared for chemical analysis (i.e. passing U.S. No. 50 sieve), digest in hot (below boiling) 50 ml distilled or deionized water for at least 6 hours in a beaker on a magnetic stirrer covered with watch glass, filter the solid residues out to collect the filtrate and analyze the final 100 ml of filtrate for soluble salts (chloride, sulfate, nitrate, nitrite, phosphate, etc.) by ion chromatography.

Fig. A13: Outlines of step-by-step procedures of various laboratory analytical methods for examination of a masonry mortar.

Which Technique(s) to Use?

The following Table summarizes various properties of mortars obtainable by different laboratory techniques, including relative merits of these techniques for specific information.

Information	Optical Microscopy	SEM-EDS	XRD	XRF	Chemical (Gravimetry)	Chemical (Titration & IC)	Sieve Analyses of Sand	Thermal	FTIR
Mortar Sand Type	X	X	X	X		X			
Sand Composition	X	X	X	X					
Sand Mineralogy	X	X	X						
Sand Soundness	X	X							
Sand Fineness	X						X		
Sand Grading & Color	X						X		
Mortar Binder Type(s)	X	X	X					X	
Binder Composition	X	X	X					X	
Binder Microstructure	X	X							
Portland Cement	X	X	X	X				X	
Hydrated Calcitic Lime	X	X						X	
Dolomitic Lime	X	X	X					X	
Hydraulic Lime	X	X							
Masonry Cement	X	X							
Natural Cement	X	X							
Carbonation	X	X	X					X	X
Carbonated Paste vs. Carbonate Sand	X							X	
Fillers	X	X						X	
Organic Components		X						X	X
Surface Treatments	X	X							X
Clay Contaminants	X		X					X	X
Mortar Type	X	X			X				
Masonry Discoloration	X	X	X	X				X	
Masonry Cracking	X	X	X						
Mortar Softening	X	X			X				
Mortar Crumbling	X	X	X		X				
Mortar Cracking	X	X	X	X			X	X	
Mortar Discoloration	X	X	X	X					
Mortar Shrinkage, Stiffening	X	X							
Bond to Masonry	X	X							
Masonry efflorescence	X	X	X	X					
Salt Attack	X	X	X			X		X	
Polymer								X	X
Mix Proportion	X	X	X	X	X				
Tuckpointing Mortar Suggestions	X	X	X	X	X		X	X	X
Miscellaneous Failure Analysis	X	X	X	X	X			X	X

Techniques: Optical microscope = Low power stereomicroscope, petrographic microscope having reflected and transmitted-light facilities. SEM-EDS = Scanning electron microscopy and energy-dispersive X-ray microanalysis. XRD = X-ray diffraction. XRF = X-ray fluorescence. Gravimetry = Loss on ignition, acid-insoluble residue, and soluble silica. Titration = Potentiometric titration for chloride. IC = Ion chromatography for chloride, sulfate, and nitrate anions. Sieve Analysis = Grain size distribution of sand extracted from mortar. Thermal = Thermogravimetric analysis (TGA) i.e. weight loss under controlled heating, and differential scanning calorimetry (DSC) i.e. measurement of differential heat flow during heating. FTIR = Fourier Transform Infrared Spectroscopy.

APPENDIX 2 –
SUGGESTIONS FOR TUCK-POINTING MORTAR

SUGGESTIONS ON FORMULATION OF TUCK-POINTING MORTARS

The following two Tables provide various tuck pointing mortar formulations, many of which are commonly suggested for historic as well as modern masonry renovation projects, where the choice depends on: (a) the type of the masonry units present, (b) the exposure condition during service, and (c) the type of the original mortar present. The following suggestions from various references are for general guideline purposes only and provide no guarantee to the overall match in appearance and properties to the existing mortars, which must be determined by trial and error by the project architect/engineer.

Masonry Units	Mortar Type		
	Sheltered	Moderate	Severe
Very hard and durable (e.g., granite, hard-cored brick, etc.)	Type O (1-2-9), or, 1-part NHL 3.5 to 2-part sand	Type N (1-1-6), or, 1-part NHL 3.5 to 5 to 2-part sand	Type S (1-0.5-4.5) or, 1-part NHL 3.5 to 5 to 2-part sand
Moderately hard and durable (e.g., limestone, durable stone, molded brick)	Type K (1-3-11), or, 1-part NHL 2 to 3.5 to 2-part sand	Type O (1-2-9), or, 1-part NHL 3.5 to 2-part sand	Type N (1-1-6), or, 1-part NHL 3.5 to 5 to 2-part sand
Minimally durable, soft (soft hand-made brick)	Type L (0-1-3), or, 1-part NHL 2 to 2-part sand	Type K (1-3-11), or, 1-part NHL 2 to 3.5 to 2-part sand	Type O (1-2-9), or, 1-part NHL 3.5 to 2-part sand

Table A2-1: Various possibilities of tuck pointing mortars made using cement, lime, and sand for various masonry units and exposure conditions (Mack and Speweik, 1998), where the mix proportions by volume within parentheses indicate cement-to-lime-to-sand proportions for various formulations. Type 'L' is a straight lime mortar containing no cement. For restoration of historic structures containing lime mortars, natural hydraulic lime (NHL) mortars, or, natural cement – lime mortars are more preferable than modern ASTM C 270 Portland cement-based mortars.

Location	Mortar Type	
	Recommended	Alternative
Interior	Type O, or, 1-part NHL 3.5 to 2-part sand	Type K or Type N
Exterior - Above Grade, Exposed on one side, unlikely to be frozen when saturated, not subject to high wind or other significant lateral load	Type O, or 1-part NHL 3.5 to 2-part sand	Type N or Type K
Exterior – Other than above	Type N, or 1-part NHL 3.5 to 5 to 2-part sand	Type O

Table A2-2: ASTM C 270 Guide for selection of tuck-pointing mortar. Mix formulations for different suggestions are as follows: Type K: 1-part Portland cement and $2^1/_2$ to 4 parts hydrated lime; Type O: 1-part Portland cement and $2^1/_2$ parts hydrated lime or lime putty; Type N: 1-part Portland cement to over $1^1/_4$ to $2^1/_2$ parts hydrated lime or lime putty. Aggregate ratio of $2^1/_4$ to 3 times sum of volume of cement and lime for all formulations.

Finally, the following section provides some additional information to consider during selection of an appropriate tuck-pointing mortar for a renovation project:

a) It is more important for a tuck pointing mortar to be as close in physical, chemical, and mechanical properties to the existing mortar as possible than to conform to the ASTM C 270 specification for cement-lime or masonry/mortar cement mortars for unit masonry, which are for modern mortars to use for modern structural applications, and not necessarily applicable to renovation of historic lime mortars. As a general rule, tuck-pointing mortar should be of same strength or softer than the original mortar.

b) Aggregate to use in the tuck-pointing mortar should be similar in color, gradation, appearance, mineralogy, and composition to the sand used in the existing mortar as long as sand to be used does not contain any potentially unsound constituents if detected in the original sand. Sand should be clean, free of any debris,

unsound, or clay particles. Masonry sands should conform to the grading requirements of ASTM C 144. Avoid using sand that contains appreciable amounts of potentially alkali-silica reactive particles (e.g., strained quartz, quartzite, chert). Many historic mortars contain fine sand having fineness modulus noticeably lower than modern ASTM C 144 sand, use of excessive fines in sand would increase the water requirement of mortar mix and hence should be substituted with masonry sand in conformance to the grading requirements of ASTM C 144. Carbonate sands, if detected from petrographic examinations (crushed marble, seashell, etc.) should be substituted with similar sands. Clay fractions and micaceous minerals should be avoided since those constituents can absorb moisture and bring undesirable expansions. Brick chips in sand, if detected, are known to develop good mechanical bond to paste and hence should be used from similar sources.

c) Binder for tuck-pointing mortar should be as close to the binder of the existing mortar in composition and properties as possible. For historic lime mortars, possible choices of binders are many:

   (i) Non-hydraulic high-calcium lime, or magnesian lime, or dolomitic lime (ASTM C 51) either in dry hydrate (hydrated lime) form, or in slurry or putty form;

   (ii) Hydraulic lime of various types produced from calcination of impure limestone or dolomite; e.g.,

   (iii) Natural hydraulic lime (i.e., NHL 2, NHL 3.5, and NHL 5 with increasing strengths, e.g., for respective applications on stuccos, or brick/stone masonry units, or load-bearing applications; feebly, moderately, and eminently hydraulic natural hydraulic limes with increasing hydraulicity and 28-day compressive strengths from >2 to <7 MPa, to >3.5 to <10 MPa, to >5 to <15 MPa, respectively, produced from calcination of impure limestones having up to 10% clay, 11-20% clay, and 21-30% clay, respectively);

   (iv) Natural cements conforming to specifications of ASTM C 10;

   (v) A combination of above-mentioned binders, e.g., natural cement and lime binders

   (vi) With or without a pozzolan (e.g., fly ash, slag, etc. with lime if added strength and durability are needed);

   (vii) Portland or masonry cement, if used must be added at appropriate proportions to lime depending on the applications, having cement-lime proportions tested to find the best match in properties to the existing mortar.

   (viii) For breathability of the masonry wall, least stress to the exiting mortar, accommodation of building movements, and good bond to masonry units, the binder of choice should be durable and similar in properties and performance to the existing binder having a good service record.

d) During applications of modern masonry mortars: (i) a job-mixed cement-lime mortar is commonly preferred by the architects than a masonry cement mortar, due to the better quality control of the former mortar; (ii) a masonry cement mortar is characteristically air-entrained, which may interfere with the bond to the adjacent masonry units, whereas, a non-air-entrained cement-lime mortar provides a better bond to the adjacent masonry units than an air-entrained masonry cement mortar, (iii) air entrainment usually provides better workability and freeze-thaw durability to a mortar, however, as mentioned, it reduces the bond to the adjacent masonry units (depending on air content); (iv) for Portland cement-lime mortars, a Type M or S mortar (i.e. having a higher cement content than lime and hence a higher strength) is preferred for load-bearing applications than a Type N mortar (having a higher lime content than cement, hence provides better workability and water retention than a Type S or M mortar); (v) Portland cement to use in a mortar should conform to the specification of ASTM C 150; hydrated lime should conform to ASTM C 207; masonry/mortar cement, if used, should conform to ASTM C 91/C 1329; blended hydraulic cement, if used, should conform to ASTM C 595; (vi) relative proportions of Portland cement and lime will control the overall strength, workability, and bond properties of the repointing mortar.

e) Mineral oxides or carbon-based pigments, if used and positively detected in an examined mortar, should be carefully replicated in the tuck pointing process to reproduce the color, texture, and appearance similar to the existing mortar (including the effects of atmospheric weathering on pigments). Dosage of pigment in the tuck-pointing mortars should be estimated from trial mixes of various dosages.

f) If the original mortar contains a polymer component as suspected from microscopy, characterization of polymer should be done by FTIR-spectroscopy.

g) A mortar strong in compressive strength might be desirable for a hard stone (such as granite), whereas a softer, more permeable lime mortar would be preferable for a historic wall of soft brick. Masonry deterioration caused by salt deposition results when the mortar is less permeable than the masonry unit. A strong mortar is still more permeable than hard, dense stone. However, in a wall constructed of soft bricks where the masonry unit itself has a relatively high permeability or vapor transmission rate, a soft, high lime mortar is necessary to retain sufficient permeability; using a strong mortar with a soft brick will result in spalling of bricks.

h) To have an optimum bond of a mortar to the adjacent masonry unit, relative proportions of cementitious materials and lime contents in the mortar should be carefully controlled. Lime provides the necessary workability and water retention, which are important in a mortar when used with a masonry unit of high suction). Therefore, the initial rate of absorption (or suction property) of the adjacent masonry units should also be carefully determined to match with the appropriate lime content in the mortar.

i) The final tuck pointing mortar should match in color and appearance to the existing mortars; the closest match should be determined by trial and error on small test areas of the masonry wall to be tuck-pointed with mock-up mixes.

END OF REPORT[2]

[2] The CMC logo is made using a lapped polished section of a 1930's concrete from an underground tunnel in the U.S. Capitol.